Active Fault Mapping and Fault Avoidance Zones for Wellington City

R Morgenstern RJ Van Dissen

GNS Science Consultancy Report 2020/57
May 2021

DISCLAIMER

This report has been prepared by the Institute of Geological and Nuclear Sciences Limited (GNS Science) exclusively for and under contract to Wellington City Council. Unless otherwise agreed in writing by GNS Science, GNS Science accepts no responsibility for any use of or reliance on any contents of this report by any person other than Wellington City Council and shall not be liable to any person other than Wellington City Council, on any ground, for any loss, damage or expense arising from such use or reliance.

Use of Data:

Date that GNS Science can use associated data: July 2020

BIBLIOGRAPHIC REFERENCE

Morgenstern R, Van Dissen RJ. 2021. Active fault mapping and fault avoidance zones for Wellington City. Lower Hutt (NZ): GNS Science. 94 p. Consultancy Report 2020/57.

CONTENTS

FIGURES

TABLES

APPENDICES

APPENDIX FIGURES

APPENDIX TABLES

EXECUTIVE SUMMARY

The area administered by Wellington City Council (WCC) is known to be traversed by seven active faults (from most active to least): the Wellington, Ohariu, Aotea, Shepherds Gully, Evans Bay, Moonshine and Terawhiti faults. WCC commissioned GNS Science for a reassessment and update of the WCC active fault traces.

A review was undertaken of all existing data (e.g. New Zealand Active Faults Database, QMAP, published papers and maps, unpublished GNS Science consultancy and science reports and detailed survey maps). Fault features were re-mapped using 2013 high-resolution Light Detection And Ranging (LiDAR) data and colour aerial photographs captured in 2017.

The faults were then assessed, where appropriate, following the guidelines issued by the Ministry for the Environment (MfE) on planning for development of land on, or near, active faults. The aim of the MfE Active Fault Guidelines is to assist resource management planners tasked with developing land-use policy and making decisions about development of land on, or near, active faults. The MfE Active Fault Guidelines promote a risk-based approach when dealing with development in areas subject to fault rupture hazard. The surface rupture hazard of an active fault in the MfE Active Fault Guidelines is characterised by two parameters: (1) location/complexity of surface rupture of the fault; and (2) activity of the fault, as measured by its average recurrence interval of surface rupture.

Fault Avoidance Zones (i.e. point 1 in the preceding paragraph) have been defined around all of the Wellington, Ohariu, Shepherds Gully, Moonshine and Terawhiti faults based on the fault's location and complexity. Fault Avoidance Zones are attributed as *well-defined*, *well-defined extended*, *distributed*, *uncertain constrained*, or *uncertain poorly constrained*. The zones range in width from several tens of metres to several hundred metres. Due to significant locational uncertainties, Fault Avoidance Zones were not established for the Aotea and Evans Bay faults.

Each active fault has been placed into a specific Recurrence Interval Class (i.e. point 2) based on existing data relevant to its recurrence interval:

- Wellington Fault – Recurrence Interval Class I (≤2000 years)
- Ohariu Fault – Recurrence Interval Class II (>2000 to ≤3500 years)
- Aotea Fault – Recurrence Interval Class III (>3500 to ≤5000 years)
- Shepherds Gully Fault – Recurrence Interval Class III (>3500 to ≤5000 years)
- Moonshine Fault – Recurrence Interval Class IV (>5000 to ≤10,000 years)
- Evans Bay Fault – Recurrence Interval Class IV (>5000 to ≤10,000 years)
- Terawhiti Fault – Recurrence Interval Class IV (>5000 to ≤10,000 years).

The risk from fault rupture at a site is a function not only of the location (point 1) and activity of a fault (point 2) but also on the type of structure/building that may be impacted by rupture of the fault. Building Importance Category is used here (and in the MfE Active Fault Guidelines) to characterise building type/importance with respect to life safety. By combining Building Importance Category with fault rupture hazard parameters and development status of a site (i.e. a previously developed site or an undeveloped 'greenfield' site), it is possible to formulate appropriate risk-based planning measures to mitigate the adverse and potentially life-threatening effects of fault rupture.

This page left intentionally blank.

1.0 INTRODUCTION

1.1 Background and Context

New Zealand lies within the deforming boundary zone between the Australian and Pacific tectonic plates. The area administrated by Wellington City Council (WCC) lies within one of the more active parts of this boundary zone. Wellington City is underlain at depth by the subducting Pacific Plate, and the district is traversed by a number of significant active faults that break and rupture the ground surface (or seabed); these are the Evans Bay, Aotea, Wellington, Moonshine, Ohariu, Shepherds Gully and Terawhiti faults (listed from east to west; Figure 1.1). Data collected from these faults indicate that they are capable of generating large (i.e. metre-scale) single-event surface rupture displacements. Surface rupture along these active faults will result in a zone of intense ground deformation as opposite sides of the fault move past each other during an earthquake (Appendix 1). Property damage can be expected and loss of life may occur where buildings, and other structures, have been constructed across the rupturing fault (Appendix 2).

At a regional scale, the active faults in Wellington City have been most recently mapped by Begg and Mazengarb (1996; 1:50,000-scale geological map) and Begg and Johnston (2000; 1:250,000-scale geological map). However, the scale of this mapping is not refined enough to permit its use in site-specific land-use planning. Fault features have been studied at various levels of detail along the Ohariu (Williams 1975; Ota et al. 1981; Van Dissen and Berryman 1996; Heron et al. 1998; Litchfield et al. 2004, 2006, 2010), Shepherds Gully and Terawhiti faults (Ota et al. 1981), along the Wellington Fault (Ota et al. 1981; Perrin and Wood 2003a, b; Little et al. 2010; Langridge et al. 2011; Rhoades et al. 2011; Ninis et al. 2013; Berryman 2019) and offshore along the Aotea and Evans Bay faults (Barnes et al. 2019). These have allowed earthquake hazard parameters (e.g. fault location, earthquake size and recurrence interval) for these faults to be defined to a greater or lesser extent. The Moonshine and Terawhiti faults, by comparison, have received very little study. The general activity (Recurrence Interval Class) for these faults is shown in Figure 1.2 and is discussed in more detail in Section 3.

In the report that follows, we first outline the background, objectives and scope of the study (Section 1) and then discuss in some detail the methodology used to achieve the study's objectives (Section 2). Following this, we present the results of the study (Section 3) whereby, on a fault-by-fault basis, we define Fault Avoidance Zones based on fault rupture location and complexity and Recurrence Interval Class based on the fault's average recurrence interval of surface rupture. The report ends with a number of conclusions and recommendations (Section 4), including brief comment on how Fault Avoidance Zones, when combined with information on Building Importance Category (i.e. building type) and development status (i.e. previously developed or 'greenfield' sites), can be used to formulate appropriate risk-based planning measures to mitigate the adverse and potentially life-threatening effects of fault rupture.

This report is also supported and supplemented by three appendices. The first covers aspects related to active fault definition and movement style. The second appendix presents a comprehensive compilation of the impacts that surface fault rupture has had on residential structures in recent New Zealand earthquakes and the implications of these observations for the mitigation of surface fault rupture hazard. Appendix 3 presents examples of resource consent categories applicable for various combinations of proposed building type, fault activity, fault locational certainty/uncertainty and site development status.

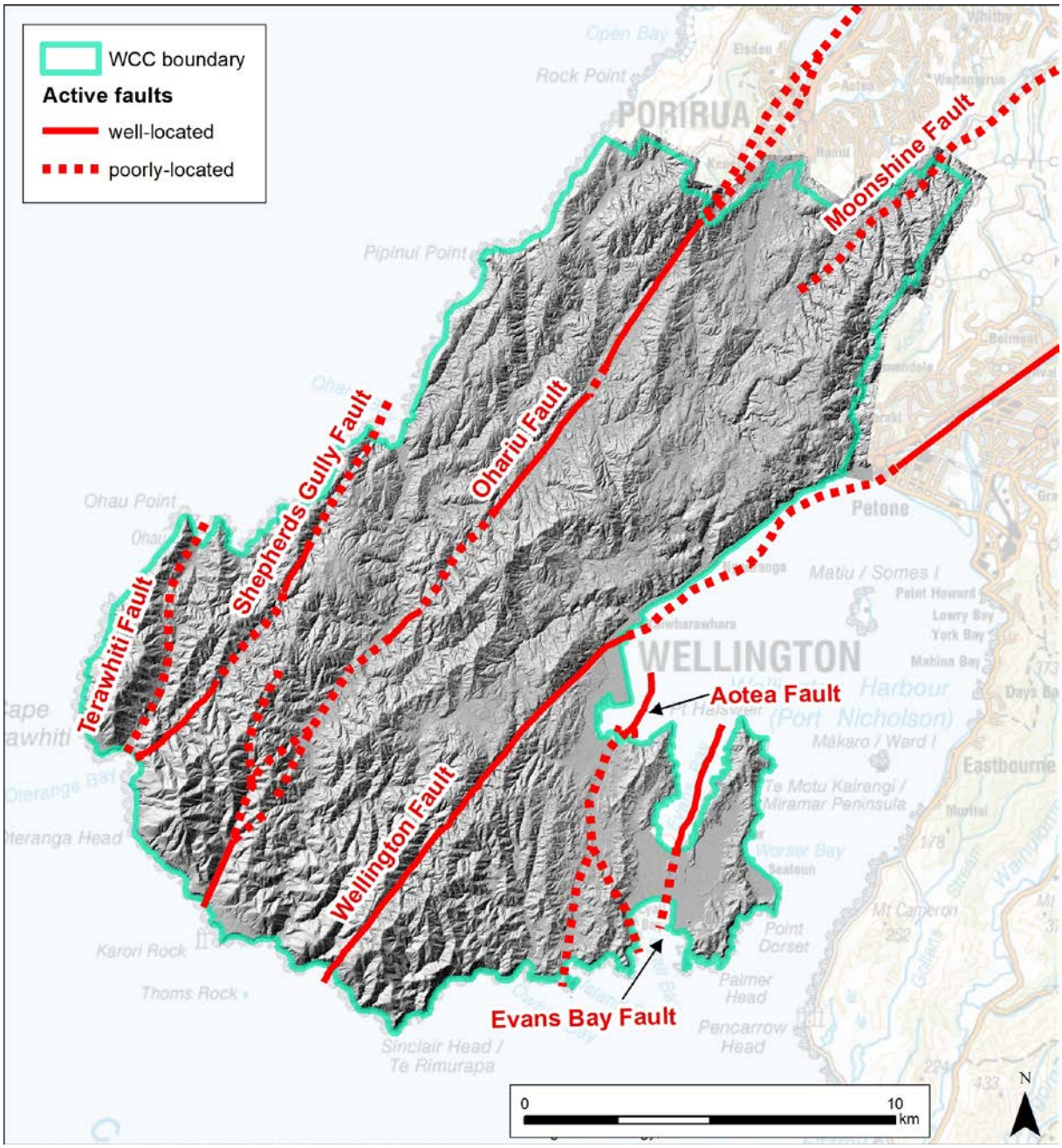

Figure 1.1 Active faults in Wellington City (classified by locational accuracy) compiled during this study from: (1) new fault trace mapping (this study) using LiDAR data, (2) the high-resolution version of the New Zealand Active Faults Database (as mapped prior to this study) and (3) interpretation by Barnes et al. (2019) of the Aotea and Evans Bay faults. WCC = Wellington City Council.

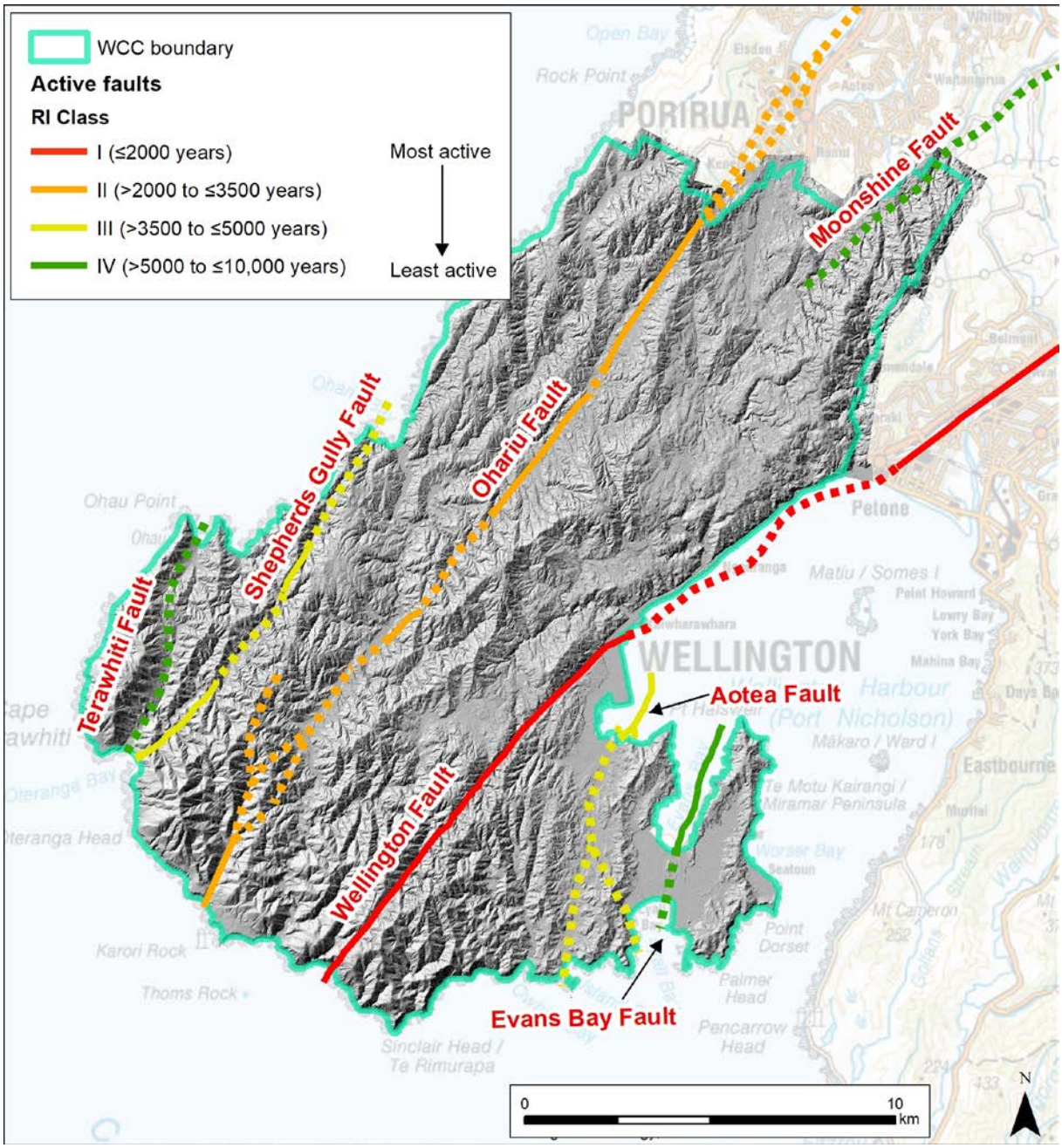

Figure 1.2 Active faults in Wellington City colour-coded by rate of activity (as defined by Recurrence Interval (RI) Class – see Section 3 for more detail). RI Class I faults are more active than RI Class II faults, which, in turn, are more active than RI Class III faults, and so on. Solid lines have good locational accuracy, dashed lines have poor locational accuracy. Compilation of this figure is based on: (1) new fault trace mapping (this study) using LiDAR data, (2) the high-resolution version of the New Zealand Active Faults Database (as mapped prior to this study) and (3) interpretation by Barnes et al. (2019) of the Aotea and Evans Bay faults. WCC = Wellington City Council.

1.2 Framework of the Ministry for the Environment Active Fault Guidelines

The New Zealand Ministry for the Environment's active fault guidelines titled 'Planning for development of land on or close to active faults: A guideline to assist resource management planners in New Zealand' (Kerr et al. 2003; see also King et al. 2003; Van Dissen et al. 2006) is the primary document providing guidance with regard to the mitigation of ground-surface fault rupture hazard. The aim of the Ministry for the Environment guidelines[1] (hereafter referred to as the MfE Active Fault Guidelines) is to assist resource management planners tasked with developing land-use policy and making decisions about development of land on, or near, active faults. The guidelines provide information about active faults, specifically fault rupture hazard, and promote a risk-based approach when dealing with development in areas subject to fault rupture hazard. In the MfE Active Fault Guidelines, the surface rupture hazard of an active fault at a specific site is characterised by two parameters:

- location/complexity of surface rupture of the fault; and
- activity of the fault, as measured by its average recurrence interval of surface rupture.

The MfE Active Fault Guidelines also advance a hierarchical relationship between fault recurrence interval and building importance, such that the greater the importance of a structure, with respect to life safety, the longer the avoidance recurrence interval. For example, only low-occupancy structures, such as farm sheds and fences (i.e. Building Importance Category [BIC] 1 structures), are allowed to be built across active faults with average recurrence intervals of surface rupture less than 2000 years. In contrast, in a 'greenfield' (i.e. undeveloped) setting, more significant structures, such as schools, airport terminals and large hotels (i.e. BIC 3 structures), should not be sited across faults with average recurrence intervals shorter than 10,000 years.

In order for WCC to mitigate and manage the hazard and risk posed by ground surface fault rupture, and to do this in a fashion consistent with neighbouring councils, there was a need to:

1. assess the suitability of the existing active fault information to support decision making and inform statutory (and non-statutory) documentation; and
2. update and better constrain that information (i.e. fault location and recurrence interval characterisation), when warranted, so it is compatible with application of the MfE Active Fault Guidelines.

1.3 Project Objective

The objective of this project was to summarise the current available fault mapping information available to the Council, update that data (where efficiently possible), and advise on the soundness and limitations of this data. Where possible, we cast that updated fault location and fault activity data in a manner that facilitates application of the MfE Active Fault Guidelines, and, when necessary, we outline possible steps to further improve this information to further enhance the Council's decision-making capabilities and review of the District Plan largely, we suggest, through the lens of the MfE Active Fault Guidelines.

1 The Ministry for the Environment's guidelines 'Planning for Development of Land on or Close to Active Faults' is available from the Ministry for the Environment website (https://environment.govt.nz/publications/planning-for-development-of-land-on-or-close-to-active-faults-a-guideline-to-assist-resource-management-planners-in-new-zealand/).

1.4 Project Scope

The key tasks of this project as outlined in the job brief dated 6 November 2019 between WCC and GNS Science were:

1. Review and modification of existing and available fault mapping data.
2. Establish Fault Avoidance Zones for the on-land portions of the Wellington, Ohariu, Shepherds Gully and Terawhiti faults (see Sections 3.1, 3.2, 3.3 and 3.6).
3. Establish Recurrence Interval Classes for all active faults in Wellington City (see Section 3).
4. Provide comment on other faults; in particular, Aotea, Evans Bay and Moonshine faults (see Sections 3.4, 3.5 and 3.7).
5. Comment on engineering mitigation options (see Section 4.2.5 and Appendix 2).
6. Presentation of results.

2.0 METHODOLOGY

The methodology outlined in the MfE Active Fault Guidelines was used in this project. The main steps in the process were:

1. identifying all known active fault traces, and related features, in Wellington City;
2. mapping and defining the location of the fault traces, and related features, in a Geographic Information System (GIS);
3. classifying all parts of a fault in terms of the Fault Complexity of surface rupture;
4. defining Fault Avoidance Zones for each of these parts; and
5. determining the average recurrence interval of surface rupture faulting (i.e. Recurrence Interval Class) for each fault.

These data are then combined with standard tables for Building Importance Category (Table 2.5) and can thus be used to formulate appropriate risk-based planning measures to mitigate the adverse effects of fault rupture.

2.1 Data Sources

A review was undertaken of existing sources of data on the active faults in Wellington City, including: (1) the New Zealand Active Faults Database (both at 1:250,000 [Langridge et al. 2016] and high-resolution scale), (2) published papers and maps, (3) unpublished GNS Science consultancy and science reports and (4) the authors' first-hand knowledge of the geology and active faulting in the district.

At a regional scale, the active faults in Wellington City have been most recently mapped by Begg and Mazengarb (1996; 1:50,000-scale geological map) and Begg and Johnston (2000; 1:250,000-scale geological map). Ota et al. (1981) mapped the Wellington, Ohariu, Shepherds Gully and Terawhiti faults at a scale of 1:50,000, although no definitive scarps were identified or mapped for the Terawhiti Fault at the time.

At a more detailed scale, several active fault trace mapping projects have been conducted over the years. The Wellington Fault has previously been mapped in the area around Karori dam (Perrin and Wood 2003b), Tinakori Road (Perrin and Wood 2003a) and Thorndon (Perrin and Wood 2003a; Berryman 2019), and this work provides an update on earlier mapping by Ota et al. (1981). Offshore mapping of the Aotea and Evans Bay faults (Barnes et al. 2019) and onshore interpretation of the Aotea Fault by Kaiser et al. (2019) using their updated 3D basin model of Wellington CBD were utilised in an attempt to place constraints on the possible location of onshore portions of these two newly identified faults.

To maintain consistency with surrounding districts, Fault Avoidance Zone studies for Porirua (Litchfield and Van Dissen 2014), Lower Hutt City (Beetham et al. 2012), Upper Hutt City (Van Dissen et al. 2005) and Kāpiti Coast District (Van Dissen et al. 2003) were also accessed. Where faults in those districts extend into Wellington City, we have endeavoured to maintain a high degree of compatibility with adjoining work.

Three additional datasets were utilised during this project to review and modify the existing active fault trace mapping and to carry out new mapping, where applicable. These are: (1) the 2013 1 m Light Detection And Ranging (LiDAR) dataset commissioned by Greater Wellington Regional Council, (2) the 2017 urban aerial photograph survey commissioned by Wellington City Council (10 cm resolution) and (3) the 2017 rural aerial photograph survey commissioned

by Greater Wellington Regional Council (30 cm resolution). The LiDAR dataset was collected in January 2013 by Aerial Surveys and covers the entire Wellington district (Figure 1.1). The data were collected at an altitude of 1000 m and were originally supplied as a processed ground return point cloud. A 1 m Digital Elevation Model (DEM) was created from these data, and then a 1 m hillshade model, illuminated from both the northwest and northeast, was used for the fault mapping. Two sets of aerial photographs were used from the 2017 surveys: the 10 cm urban set, with only partial coverage of the district, and a 30 cm rural set, with full coverage. The Wellington City Council urban aerial photographs were collected by AAM New Zealand in February–March 2017, had been processed and ortho-rectified and have a 10 cm pixel resolution and spatial accuracy of ±20 cm at 90% confidence. The Greater Wellington Regional Council rural aerial photographs were collected by AAM New Zealand during the 2016/2017 season, had been processed and ortho-rectified and have a 30 cm pixel resolution and spatial accuracy of ±1 m.

2.2 Mapping Active Fault Features

Previous studies of active faulting in Wellington City have produced data on the location and type of fault-generated features present in the district. However, these data are often site-specific in nature, and, until this study, had not yet been compiled to provide comprehensive coverage of the district as a whole. The identified fault-generated features, such as fault scarps, offset river terraces, fans, spurs and streams, guided drainages, crush zones and aligned saddles, are line features that assist in locating the position of faults and provide evidence as to the timing and size of previous surface rupture earthquakes along these faults.

The accuracy with which the location of an active fault feature can be captured into a database is influenced by two types of uncertainty or error. The first is the error associated with how accurately the feature can be located on the ground. The second is the error associated with capturing that position into the database.

While a major active fault is typically a near-continuous geological structure, surface features generated by past surface ruptures of the fault are often intermittent. In some areas where fault features should exist, they cannot be seen. On hillslopes, for instance, geological processes such as landslides and slope wash can quickly destroy or modify topographic fault features. River processes such as erosion and sediment deposition can destroy fault features on the river valleys and plains. Urban development and earthworks are also quite efficient agents of landscape modification and destruction of fault location evidence. It is along the stretches of an active fault where fault features are not preserved that uncertainty as to the fault's precise location is greatest.

Where features are preserved, the accuracy with which the fault can be located on the ground depends on the type of feature. A fault scarp is one of the more definitive features that can be used to define the location of a fault. For example, the scarp of the Ohariu Fault is, in places, sharp and distinct (less than about 10 m wide), and here it is possible to define the location of the fault quite accurately (to within several metres). However, in other places, the fault trace may be a broad or ill-defined topographic feature (e.g. topographic saddle or fault-guided valley), expressed over a width of tens of metres or more. Without additional investigations at these sites, the ability to capture/define the position of the fault cannot be significantly more accurate than the distinctness/sharpness of the topographic expression of the fault feature. So, even when topographic fault features are preserved, the ability to use these features to define the precise location of the fault, and therefore future surface rupture hazard, varies according to the distinctness of topographic expression of the feature.

An additional uncertainty with regard to using topographic fault features to define the location of past, and future, surface rupture and hazard, is that the preservation potential of fault scarps, and other fault-generated topographic features, typically varies according to size. That is, a large scarp, or displacement, is more likely to be preserved in the landscape than a small scarp, or displacement. So, even when one can identify a distinct fault feature at a site, one cannot be entirely sure that smaller, but still life-threatening, displacements did not once extend through the site but are now no longer preserved. Thus, the identified fault feature may not indicate/record the true scale of fault rupture hazard at a site. As is discussed in more detail in Section 2.4, this type of uncertainty is typically addressed by prescribing a 20 m 'setback' distance either side of the fault.

In limited instances, active faults and fault-related features can be located absolutely, for example, in trenches that expose the fault plane. Global Navigational Satellite System (GNSS; formerly Global Positioning System [GPS]) or traditional survey techniques can be used to locate and capture the positions of these features to centimetre-scale accuracy. However, more typically for this project, once a fault feature was identified on the ground, or on aerial photographs, whether the feature be distinct or otherwise, its position was captured/ defined using LiDAR data in a GIS. An accuracy, in metres, was assigned to these features. For example, a feature considered to have an accuracy of ±10 m is denoted as 10 in the attribute tables (Table 2.1).

The mapped fault features were used to construct fault rupture zones (zones within which future rupture is likely to cause intense ground deformation). In some areas, these zones are based on the position of a simple linear fault-line, and the width of the zones reflects the accuracy of capture. In other places, the zone is based on complex features or inferred where no features are preserved. For example, mapping active faults through developed areas can be challenging because engineering works can obscure, remove or significantly modify these features used to identify active faults. In these areas, the width of the zone can be large and reflects both the complexity or uncertainty of the fault location on the ground, and the accuracy of capture. Fault Avoidance Zones were subsequently delineated around the fault rupture zones; see Section 2.4 for more detail.

The attributes assigned to each fault trace are listed in Table 2.1.

Table 2.1 Attributes for mapped active fault traces in Wellington City for the purposes of developing Fault Avoidance Zones.

Attribute	Name in Shapefile	Definition
Fault Name	NAME	The name given to an active fault.
Dominant Sense	DOM_SENSE	Dominant or primary sense of movement on the fault (dextral – see Appendix 1 for a full list and further details).
Down Quadrant	DOWN_QUAD	The direction of the down-thrown side of the fault described in terms of compass quadrants.
Fault Feature	FEATURE	Description of how the fault is expressed in the surface geomorphology (bedrock fault zone, bench, buried scarp, concealed fault, eroded scarp, fault-guided valley, gully, hillslope bench, lineament, modified scarp, saddle or scarp).
Tectonic Origin	TECTONIC_ORIGIN	Certainty that the feature is of tectonic (e.g. earthquake) origin (definite, likely, possible or unknown).

Attribute	Name in Shapefile	Definition
Accuracy	ACCURACY	Accuracy of the location of the fault on the ground surface (accurate, approximate or inferred).
Deformation Width of Local Fault Feature	LOCATION_DEF	Horizontal width of the visible fault feature or, for concealed faults or faults with no surface trace, the maximum width of where the deformation could be located. Value is in metres.
Recurrence Interval Class	RI_CLASS	The average time between surface-rupturing events on a fault, grouped into six classifications (RI Class I–IV – see Table 2.2 for a full list and further details).

Table 2.2 Definition of Recurrence Interval (RI) classes, from the MfE Active Fault Guidelines. In practise, all faults in Wellington City were only classified as RI Class I–IV. See Section 2.6 for more discussion regarding recurrence interval and Section 3 for detail regarding Recurrence Interval Class definition for each of the faults covered in this report.

RI Class	Average Recurrence Interval of Surface Rupture
I	≤2000 years
II	>2000 to ≤3500 years
III	>3500 to ≤5000 years
IV	>5000 to ≤10,000 years
V	>10,000 to ≤20,000 years
VI	>20,000 to ≤125,000 years

2.3 Fault Complexity of Surface Rupture

Surface rupture Fault Complexity is an important parameter used in the MfE Active Fault Guidelines to define rupture hazard at a site. When fault rupture deformation is distributed over a wide area, the amount of deformation at a specific locality within the distributed zone is less compared to where the deformation is concentrated on a single well-defined trace. The relative fault rupture hazard/risk is therefore less within a zone of distributed deformation than within a narrow well-defined zone. The fault feature data compiled for Wellington City were used to categorise the fault rupture complexity for all parts of each active fault in the district. Table 2.3 lists the Fault Complexity terms and definitions used throughout the rest of the report, including tables and figures. These Fault Complexity terms link directly into Resource Consent Category tables for the MfE Active Fault Guidelines (examples are provided in Appendix 3). These are also the same definitions used in similar active fault mapping projects in adjacent districts and elsewhere throughout the country (e.g. Kāpiti, Upper Hutt, Porirua, Horizons Region, Kaikōura and Taupō districts; Van Dissen and Heron 2003; Van Dissen et al. 2005; Litchfield and Van Dissen 2014; Langridge and Morgenstern 2018, 2019, 2020; Litchfield et al. 2019, 2020).

Table 2.3 Definitions of Fault Complexity terms used in this report (Van Dissen and Heron 2003; adapted from the MfE Active Fault Guidelines, Kerr et al. 2003).

Fault Complexity	Definition
Well-defined	Fault rupture deformation is well-defined and of limited geographic width (e.g. metres to tens of metres wide).
Well-defined extended	Fault rupture deformation has been either buried or eroded over short distances, but its position is tightly constrained by the presence of nearby distinct fault features.
Distributed	Fault rupture deformation is distributed over a relatively broad, but defined, geographic width (e.g. tens to hundreds of metres wide), typically as multiple fault traces and/or folds.
Uncertain constrained	Areas where the location of fault rupture is uncertain because evidence has been either buried or eroded, but where the location of fault rupture can be constrained to a reasonable geographic extent (≤300 m).
Uncertain poorly constrained	The location of fault rupture deformation is uncertain and cannot be constrained to lie within a zone less than 300 m wide, usually because evidence of deformation has been either buried or eroded away, or the features used to define the fault's location are widely spaced and/or very broad in nature.

2.4 Defining Fault Avoidance Zones

Generally, a fault is a zone of deformation rather than a single linear feature. The zone may range in width from metres to hundreds of metres. Structures sited directly across an active fault, or near a fault, are in a potentially hazardous area, and could be damaged in the event of fault rupture. As is suggested in the MfE Active Fault Guidelines, a Fault Avoidance Zone is created by defining a 20 m 'Setback Zone' (dark orange in Figure 2.1A) around the 'Deformation Zone' (light orange in Figure 2.1A), which defines the likely rupture zone of faults. This additional 20 m accommodates the intense deformation and secondary ruptures that can occur close to primary mapped fault rupture. The Deformation Zones are themselves generated from buffers surrounding the detailed active fault mapping linework (see Deformation Width of Local Fault Feature in Table 2.1A), with the width of this Deformation Zone generally determined by an expert assessment of fault location accuracy (or lack thereof). In Wellington City, the faults are considered to most likely be in the centre of the fault scarp, so the buffer zones are symmetrical about the fault lines.

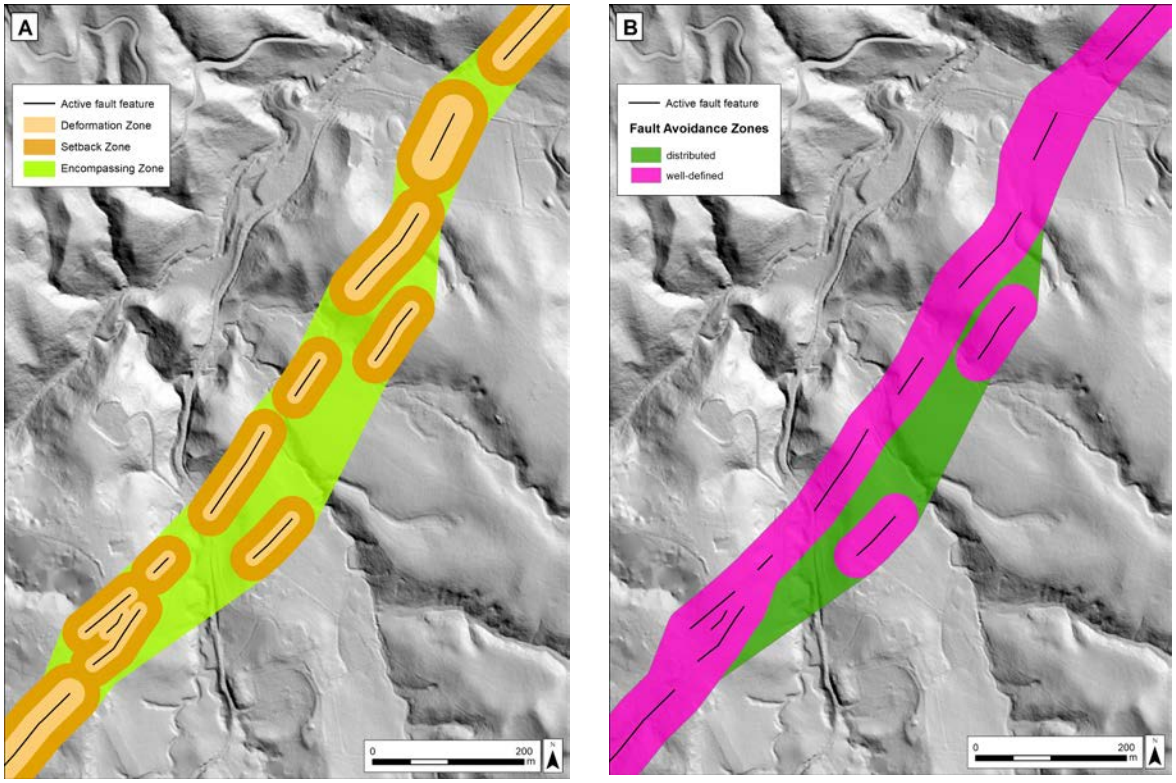

Figure 2.1 (A) The components of Fault Avoidance Zones separated into individual components (buffer zones). These are then used to create the overall Fault Avoidance Zones (B).

Once the resulting buffers are merged together and sharp edges and unnecessary kinks are manually smoothed out, the areas between the Setback Zones were connected with an 'Encompassing Zone' (light green in Figure 2.2A). This fills the gaps between active fault traces and accounts for any deformation that could occur between them. The combined zone is the Fault Avoidance Zone (Figure 2.2), with the Fault Complexity defined for that Fault Avoidance Zone typically assigned based on total width of the zone. In some instances, a narrow *well-defined* Fault Avoidance Zone can lie within a wider *distributed* or *uncertain* Fault Avoidance Zone (see centre and top right of Figure 2.2 for an example of this).

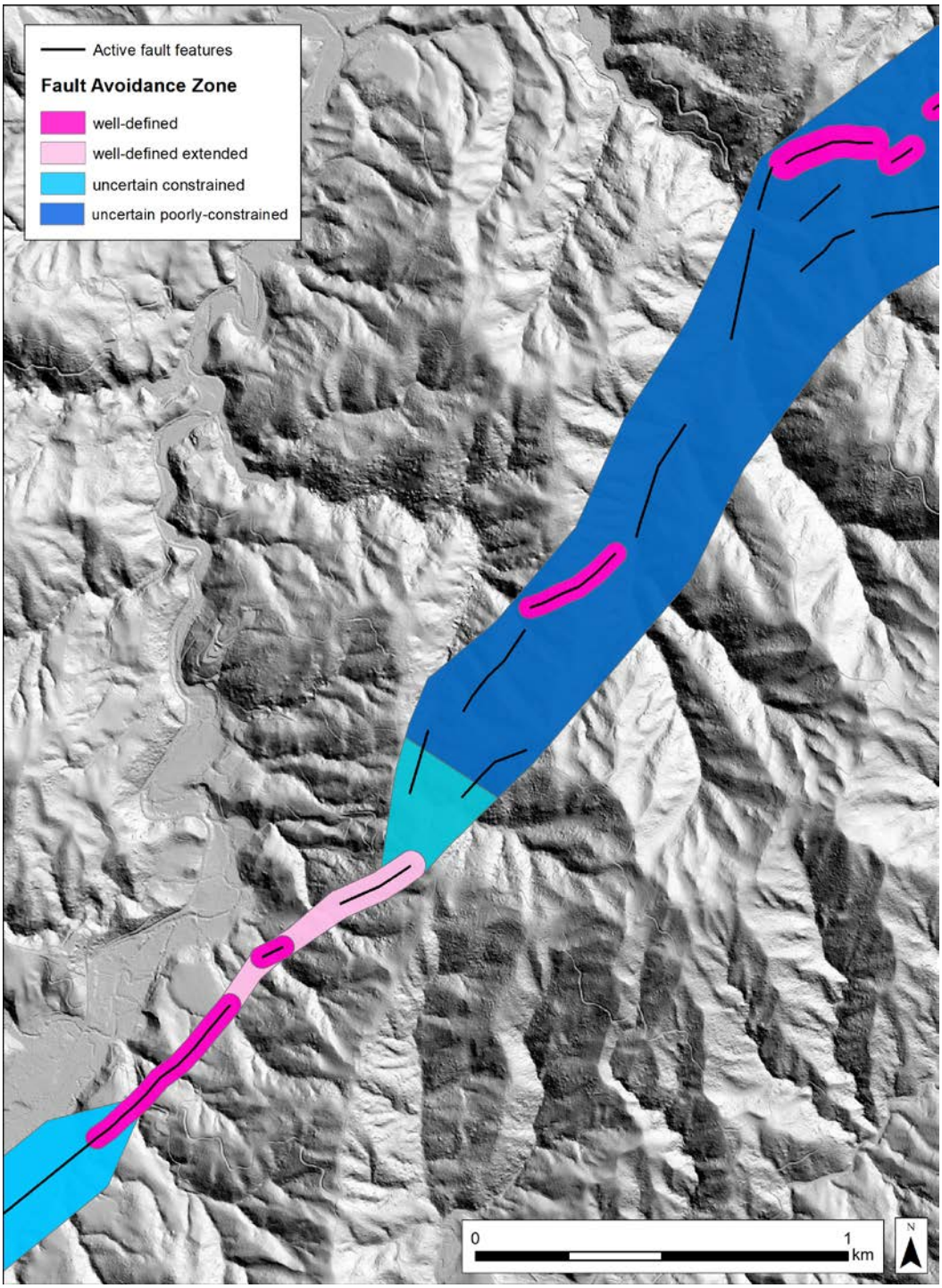

Figure 2.2 Examples of mapped Fault Avoidance Zones with differing Fault Complexities.

The above methodology for mapping and defining Fault Avoidance Zones (*well-defined*, *well-defined extended*, *distributed*, *uncertain constrained* or *uncertain poorly constrained*) has been followed for the Wellington, Ohariu and Shepherds Gully faults within Wellington City. A slight variation on this method was used to define Fault Avoidance Zones for the Terawhiti and Moonshine faults (see Sections 3.6 and 3.7, respectively, for more detail). We have also classified each of the seven faults according to Recurrence Interval Class, which is defined in Table 2.2 and discussed in detail for each fault in Section 3. Figures 3.1, 3.3, 3.4, 3.7 and 3.8 show, in a general sense, the distribution of the Fault Avoidance Zones defined in Wellington City during this study. The GIS data supplied with this report presents the complete coverage of the district.

2.5 Building Importance Category

In the event of fault rupture, buildings constructed across the fault will experience significant stress and can suffer extensive damage. Buildings adjacent to the fault and within the Fault Avoidance Zone may also be damaged. The MfE Active Fault Guidelines define five Building Importance Categories (Table 2.4) based on accepted risk levels for building collapse considering building type, use and occupancy. This categorisation is weighted toward life safety, but also allows for the importance of critical structures and the need to locate these wisely.

Table 2.4 Building Importance Categories from the MfE Active Fault Guidelines (Kerr et al. 2003).

Building Importance Category	Description	Examples
1	**Temporary structures** with low hazard to life and other property	• Structures with a floor area of <30 m^2 • Farm buildings, fences • Towers in rural situations
2a	**Timber-framed** residential construction	• Timber-framed single-storey dwellings
2b	**Normal structures** and structures not in other categories	• Timber-framed houses with area >300 m^2 • Houses outside the scope of NZS 3604 'Timber-Framed Buildings' • Multi-occupancy residential, commercial and industrial buildings accommodating <5000 people and <10,000 m^2 • Public assembly buildings, theatres and cinemas <1000 m^2 • Car parking buildings
3	**Important structures** that may contain people in crowds or contents of high value to the community or pose risks to people in crowds	• Emergency medical and other emergency facilities not designated as critical post-disaster facilities • Airport terminals, principal railway stations, schools • Structures accommodating >5000 people • Public assembly buildings >1000 m^2 • Covered malls >10,000 m^2 • Museums and art galleries >1000 m^2 • Municipal buildings • Grandstands >10,000 people • Service stations • Chemical storage facilities >500 m^2
4	**Critical structures** with special post-disaster functions	• Major infrastructure facilities • Air traffic control installations • Designated civilian emergency centres, medical emergency facilities, emergency vehicle garages, fire and police stations

2.6 Relationship between Fault Recurrence Interval Class and Building Importance Category

As noted earlier, the hazard posed by fault rupture is quantified using two parameters:

- Fault Complexity and its incorporation into the mapping of Fault Avoidance Zones; and
- average recurrence interval of surface rupture faulting.

The average recurrence interval of surface rupture is the average number of years between successive ground surface-rupturing earthquakes along a specific section or length of fault. Typically, the longer the average recurrence interval of surface rupture of a fault, the less likely the fault is to rupture in the near future. Likelihood of rupture is also a function of other variables, such as elapsed time since the last rupture of the fault, and the size, style and timing of large earthquakes on other nearby faults; however, these variables are not used to define rupture hazard in the MfE Active Fault Guidelines. Broadly speaking, a fault with a long recurrence interval typically poses less of a hazard than one with a short recurrence interval. In the MfE Active Fault Guidelines, active faults are grouped according to Recurrence Interval Class (Tables 2.2 and 2.5), such that the most hazardous faults, i.e. those with the shortest recurrence intervals, are grouped within Recurrence Interval Class I. The next most active group of faults are those within Recurrence Interval Class II, and so on. Recurrence Interval Classes for each WCC fault are provided in Table 3.1 and discussed in more detail in Section 3.

Table 2.5 Relationships between Recurrence Interval Class, average recurrence interval of surface rupture, and Building Importance Category for previously subdivided and greenfield sites. For more details, see Kerr et al. (2003) and King et al. (2003).

<table>
<tr><th rowspan="2">Recurrence Interval Class</th><th rowspan="2">Average Recurrence Interval of Surface Rupture</th><th colspan="2">Building Importance (BI) Category Limitations (Allowable Buildings)</th></tr>
<tr><th>Previously Subdivided or Developed Sites</th><th>‘Greenfield’ Sites</th></tr>
<tr><td>I</td><td>≤2000 years</td><td>BI Category 1
Temporary buildings only</td><td rowspan="2">BI Category 1
Temporary buildings only</td></tr>
<tr><td>II</td><td>>2000 years to ≤3500 years</td><td>BI Category 1 and 2a
Temporary and residential timber-framed buildings only</td></tr>
<tr><td>III</td><td>>3500 years to ≤5000 years</td><td>BI Category 1, 2a and 2b
Temporary, residential timber-framed and normal structures</td><td>BI Category 1 and 2a
Temporary and residential timber-framed buildings only</td></tr>
<tr><td>IV</td><td>>5000 years to ≤10,000 years</td><td rowspan="2">BI Category 1, 2a, 2b and 3
Temporary, residential timber-framed, normal and important structures (but not critical post-disaster facilities)</td><td>BI Category 1, 2a and 2b
Temporary, residential timber-framed and normal structures</td></tr>
<tr><td>V</td><td>>10,000 years to ≤20,000 years</td><td>BI Category 1, 2a, 2b and 3
Temporary, residential timber-framed, normal and important structures (but not critical post-disaster facilities)</td></tr>
<tr><td>VI</td><td>>20,000 years to ≤125,000 years</td><td colspan="2">BI Category 1, 2a, 2b, 3 and 4
Critical post-disaster facilities cannot be built across an active fault with a recurrence interval of ≤20,000 years</td></tr>
</table>

Note: Faults with average recurrence intervals >125,000 years are not considered active.

The MfE Active Fault Guidelines advocate a risk-based approach to dealing with development of land on, or close to, active faults. The risk is a function not only of the location and activity of a fault but also the type of structure/building that may be impacted by rupture of the fault. For a site on or immediately adjacent to an active fault, risk increases both as fault activity increases (i.e. fault recurrence interval and Recurrence Interval Class decrease) and Building Importance Category increases. In order to maintain a relatively constant/consistent level of risk throughout the district, it appears reasonable to impose more restrictions on the development of sites located on or immediately adjacent to highly active faults, compared to sites located on or immediately adjacent to low-activity faults. This hierarchical relationship between fault activity (Recurrence Interval Class) and building type (Building Importance Category) is presented in Table 2.5.

The MfE Active Fault Guidelines also make a pragmatic distinction between previously subdivided and/or developed sites, and undeveloped 'greenfield' sites, and allows for different conditions to apply to these two types of sites of differing development status (see Table 2.5). The rationale for this is that, in the subdivision/development of a greenfield area, a change of land usage is usually being sought, and it is much easier, for example, to require a building setback distance from an active fault or to plan subdivision of land around the location of an active fault. However, in built-up areas, buildings may have been established without knowledge of the existence or location of an active fault, and the community may have an expectation to continue to live there, despite the potential danger. Also, existing use rights under the Resource Management Act mean that, where an existing building over a fault is damaged, it can be rebuilt, even after the hazard/risk has been identified.

Using existing published geoscience literature, and unpublished GNS Science information, we characterise the Recurrence Interval Class (and attendant uncertainty) of each of the known active faults within WCC (Evans Bay, Aotea, Wellington, Moonshine, Ohariu, Shepherds Gully and Terawhiti faults). This was done in a fashion, as with the definition of Fault Avoidance Zones, that is wholly compatible with the MfE Active Fault Guidelines.

3.0 RESULTS

The Recurrence Interval Classes and confidence of classification for the seven active faults within Wellington City are given in Table 3.1. The reasons for these assignments and the description of the faults and Fault Avoidance Zones are presented on a fault-by-fault basis (in order of decreasing activity or increasing Recurrence Interval Class) in the following subsections.

Table 3.1 Recurrence Interval Classes of known active faults within Wellington City. For more detail, see Kerr et al. (2003) and Van Dissen et al. (2003).

Fault Name	Recurrence Interval Class	Recurrence Interval Range of Respective Recurrence Interval Class	Confidence of Recurrence Interval Classification*
Wellington Fault	I	≤2000 years	High
Ohariu Fault	II	>2000 years to ≤3500 years	Medium–Low
Aotea Fault	III	>3500 years to ≤5000 years	Medium
Shepherds Gully Fault	III	>3500 years to ≤5000 years	Low
Evans Bay Fault	IV	>5000 years to ≤10,000 years	Medium
Moonshine Fault	IV	>5000 years to ≤10,000 years	Low
Terawhiti Fault	IV	>5000 years to ≤10,000 years	Low

* Relative confidence that the fault can be assigned to a specific fault-avoidance Recurrence Interval Class.

High: Fault has a well-constrained recurrence interval (usually based on fault-specific data) that is well within a specific Recurrence Interval Class, or fault has such a high slip rate that it can be confidently placed within the ≤2000-year Recurrence Interval Class.

Medium: Uncertainty in average recurrence interval embraces a significant portion (> ~25%) of two Recurrence Interval Classes; the mean of the uncertainty range typically determines into which class the fault is placed.

Low: The range of uncertainty of the fault's recurrence interval embraces a significant portion of three or more Recurrence Interval Classes, or when there are no fault-specific data available for the fault to enable an estimation of its fault-specific recurrence interval (i.e. Recurrence Interval Class is assigned based only on subjective comparisons with other better-studied faults). The mean of the recurrence interval uncertainty range typically determines into which class the fault is placed.

3.1 Wellington Fault

The Wellington Fault is the most active fault in the district and one of the major earthquake-generating faults in the Wellington Region. It extends northeastwards for c. 12 km from an unnamed bay west of Sinclair Head at the south coast, along Long Gully and Zealandia, to, and through, Thorndon. From there, it extends offshore and out of the district (Figure 3.1). Trenching and other detailed paleoseismology studies on the Wellington Fault have determined that the fault has a right-lateral (dextral) slip rate of approximately 6 mm/yr (Rhoades et al. 2011; Ninis et al. 2013) and an average recurrence interval of ground surface-rupturing earthquakes of approximately 900 years (Langridge et al. 2011; Rhoades et al. 2011). It most recently ruptured the ground surface about 300 years ago (Langridge et al. 2011; Rhoades et al. 2011) and is considered capable of generating earthquakes in the order of magnitude 7.5 (Stirling et al. 2012). Individual surface-rupture earthquakes along the fault are expected to generate about 3.5–6.5 m of right-lateral displacement at the ground surface (Little et al. 2010) and a lesser and variable amount of vertical displacement.

The Wellington Fault passes through areas of both rural and urban development. In addition, it passes under, or very near to, numerous critical lifelines and infrastructure elements.

3.1.1 Recurrence Interval Class

The average recurrence interval of approximately 900 years for the Wellington Fault, and its relatively high slip rate, place the fault in Recurrence Interval Class I (≤2000 years) of the MfE Active Fault Guidelines, with a high degree of confidence (Table 3.1).

3.1.2 Fault Complexity

For the majority of its length through Wellington district, the Wellington Fault has a *well-defined* Fault Avoidance Zone (Figure 3.1A). It is generally well-constrained throughout the entire district, except for two areas where distributed deformation is likely to occur, the reasons for which are discussed in more detail below.

The position of the southern end of the Wellington Fault is well-constrained onshore, with clear and distinct scarps visible in the LiDAR data. There is a small gap where the fault is not clearly expressed at the surface, and a *well-defined extended* Fault Avoidance Zone has been assigned to this part of the fault (Figure 3.1). From here, the fault follows Long Gully in a northeastward direction, along which streams display clear and distinct lateral offsets. Surface expression has been modified to various extents, especially at the top of Long Gully, and here a *distributed* Fault Avoidance Zone has been defined. Northeast of the Karori Reservoir, urban development has obscured the trace of the fault, and we have adopted the fault rupture hazard zone defined by Perrin and Wood (2003a, b) along this section of the Wellington Fault from the Karori Reservoir to the harbour.

In the Thorndon area, the fault bends and changes strike by about 15°. Fault bends along strike-slip faults are places where fault deformation commonly widens and may comprise a number of discrete splays, as well as distributed deformation. To accommodate this possibility, we have tentatively mapped a *distributed* Fault Avoidance Zone in this area (Figure 3.1A). An archival photograph of Kaiwharawhara, taken in the 1870s, shows a possible fault scarp that could potentially represent such a splay on the Wellington Fault (Figure 3.2). Urban modification has occurred in this area since the photograph was taken; we therefore recommend further investigation in this area to confirm, or refute, the origin of that splay and therefore also the *distributed* Fault Avoidance Zone.

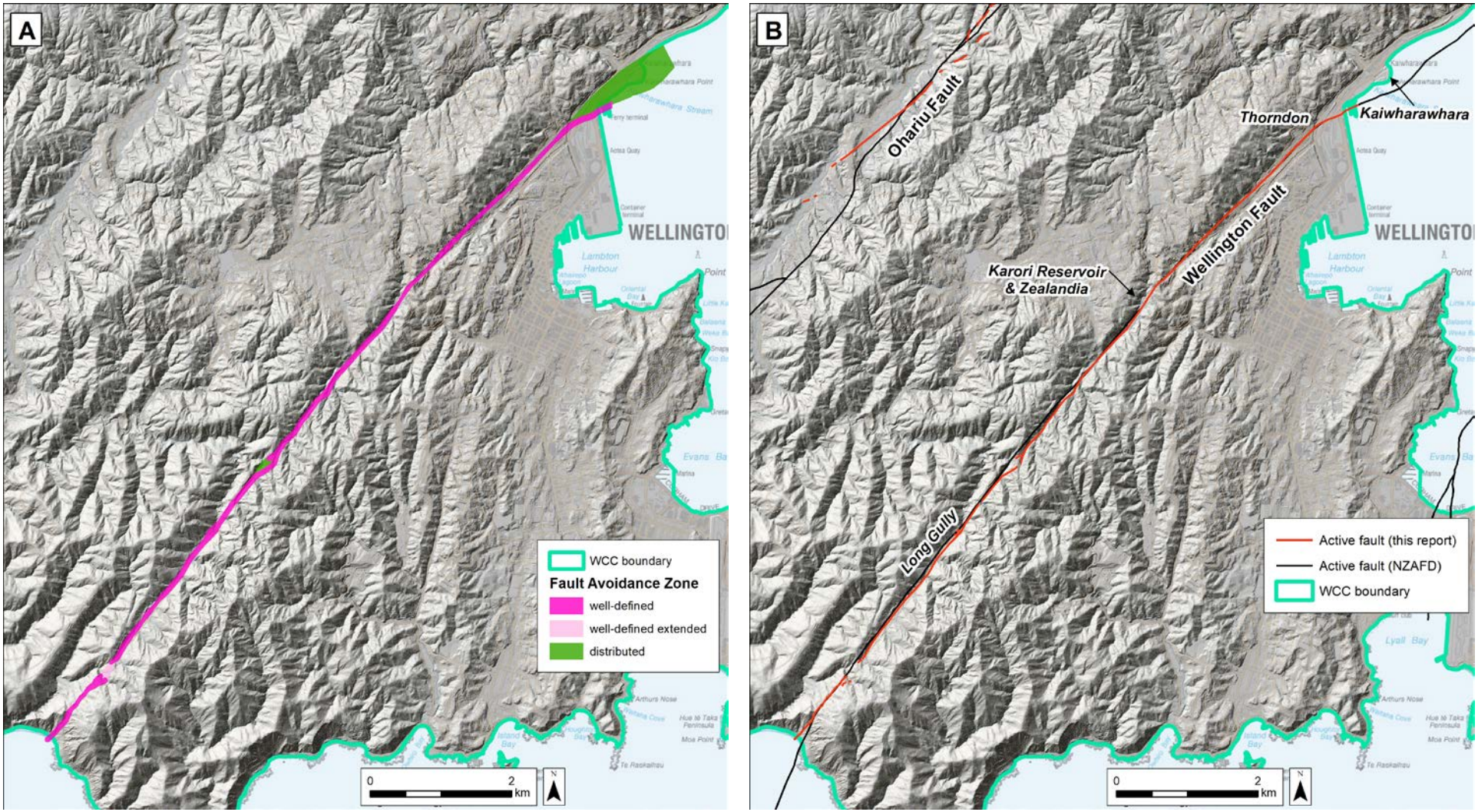

Figure 3.1 (A) Fault Avoidance Zones (pink and green – classified by Fault Complexity) developed for the Wellington Fault. (B) Previous active fault mapping from the high-resolution New Zealand Active Faults Database (NZAFD; black lines) versus new active fault mapping (this report; red lines). Offshore representations of faults in NZAFD are, at best, only approximate. WCC = Wellington City Council.

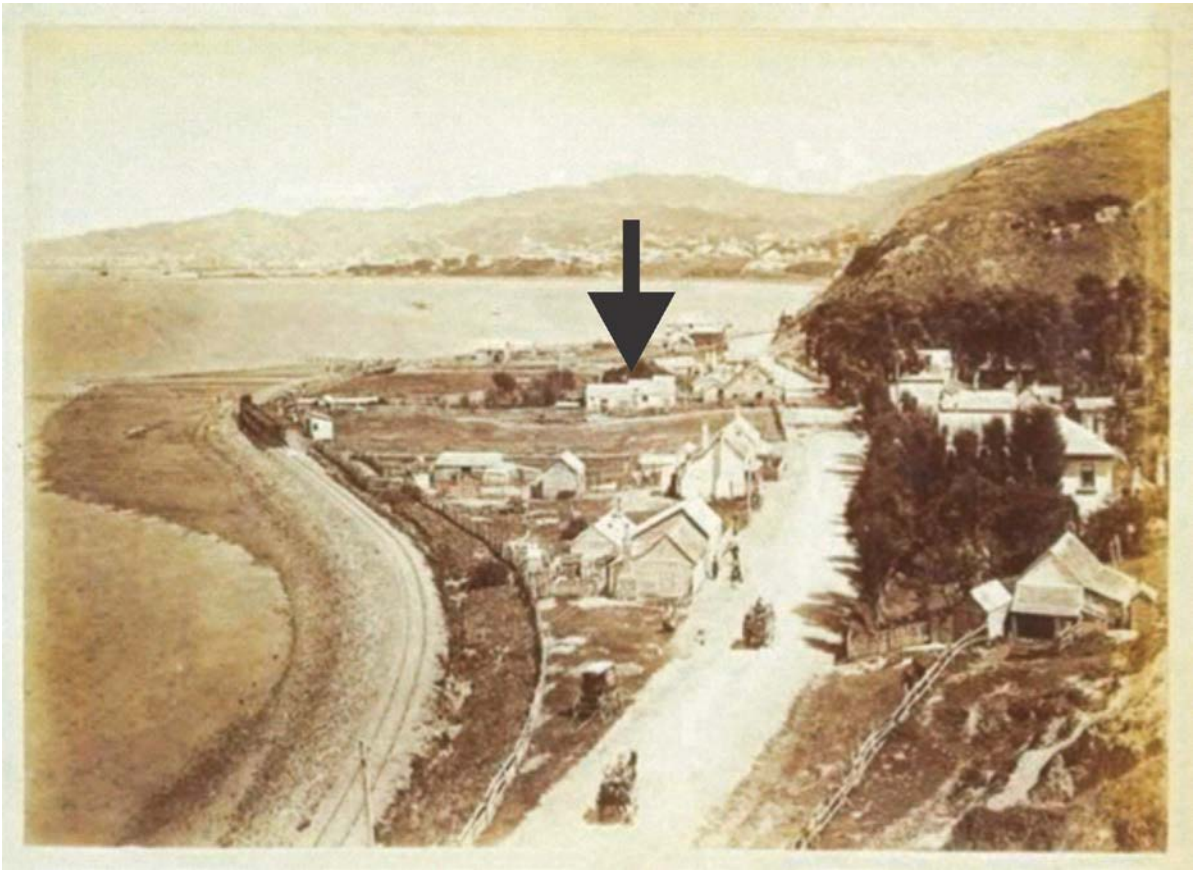

Figure 3.2 A possible scarp of a splay of the Wellington Fault at Kaiwharawhara, as photographed in the 1870s (view looking southwest). Possible scarp (black arrow) is northwest-side-up. Photograph taken from the album *Photographs of New Zealand Scenery – Wellington to the Wairarapa* by James Bragge (https://collections.tepapa.govt.nz/object/982829).

3.2 Ohariu Fault

The Ohariu Fault is another major earthquake-generating fault in the Wellington region. It extends for c. 23 km northeastward from Old Terawhiti, near Tongue Point and Karori Rock, along parts of the Makara and Ohariu valleys to the edge of the Wellington City boundary at Tawa, and beyond (Figure 3.3) (e.g. Heron et al. 1998; Begg and Johnston 2000; Pondard and Barnes 2010).

Trenching and other detailed studies of the Ohariu Fault (e.g. Heron et al. 1998; Litchfield et al. 2004, 2006, 2010) have determined that the fault has a right-lateral (dextral) slip rate of approximately 1–2 mm/yr and a recurrence interval of surface-rupturing earthquakes of 800–7000 years. The last major ground surface rupture was approximately 1000 years ago, although there appears to have been a small (a few tens of centimetres), localised rupture approximately 300 years ago, which may be either a small primary rupture or triggered slip resulting from a large earthquake on a nearby fault (Litchfield et al. 2010). It is considered capable of generating earthquakes in the order of magnitude 7.2–7.6 (Stirling et al. 2012). Individual surface rupture earthquakes along the fault are expected to generate 3–5 m of right-lateral displacement at the ground surface and a lesser and variable amount of vertical displacement.

The Ohariu Fault passes through areas of rural and semi-rural development in Wellington City, and passes under, or very near to, critical infrastructure.

3.2.1 Recurrence Interval Class

The recurrence interval of 800–7000 years for the Ohariu Fault spans several Recurrence Interval Class boundaries (Table 2.2). Statistical methods have been used to calculate a mean recurrence interval of 2200 years (Litchfield et al. 2006), and so the fault is placed in Recurrence Interval Class II (>2000 years to ≤3500 years), with a medium to low level of confidence (Table 3.1). Van Dissen et al. (2013) estimate that, within the next 100 years, the Ohariu Fault has a likelihood of ~5% of rupturing and producing a large magnitude earthquake.

3.2.2 Fault Complexity

Fault Avoidance Zones of *well-defined*, *well-defined extended*, *distributed* and *uncertain constrained* have been mapped along the Ohariu Fault within Wellington district. These are discussed in more detail below.

The surface expression of the Ohariu Fault is very clear on LiDAR data along the northern half of its extent through Wellington district but becomes less distinct to the south. At its southern onshore extent, a marine terrace at Old Terawhiti is vertically displaced by c. 20–30 m (west side up; Ota et al. 1981), which constrains the location of its southern onshore extent. The Ohariu Fault then follows Waiariki Stream northeastward, where it is exposed as a fault-bedrock crush zone, and crosses over the ridge crest at West Wind. From here, there are no clear fault scarps visible in the LiDAR data, and the fault is primarily denoted by fault-controlled saddles and fault-guided valleys. It separates into multiple splays southeast of Mt Wai-ariki (Figure 3.3A); the western-most trace follows a series of prominent fault-controlled saddles and fault-guided valleys and heads north-northeast towards the Shepherds Gully Fault. The other two lozenge-shaped splays of the Ohariu Fault have also been defined, primarily by fault-controlled saddles and fault-guided valleys on the LiDAR. Once it reaches Makara Valley, its location becomes even more poorly defined as it becomes concealed beneath younger river sediments and heads towards and through Makara township. This whole southern section of the Ohariu Fault from the south coast through Makara Valley has been defined as an *uncertain constrained* Fault Avoidance Zone of variable width depending on the nature of the fault feature(s) used to define the location of the zone.

Northeast of Makara, its surface expression starts to become clear and distinct in the LiDAR data, and it has therefore been mapped as a *well-defined* to *well-defined extended* Fault Avoidance Zone (Figure 3.3A). It then transitions into a zone of more widely spaced scarps, modified scarps and fault-guided valleys again, which are mapped as a *distributed* Fault Avoidance Zone. Further to the north – through the entire length of Ohariu Valley – the fault is, by and large, distinct in the LiDAR data, and it is mostly classified as a *well-defined* Fault Avoidance Zone. In Porirua City, the Ohariu Fault has previously been defined as an *uncertain constrained* Fault Avoidance Zone (Figure 3.3A; Litchfield and Van Dissen 2014), and this change to *well-defined* at the boundary to WCC reflects the intensity of ground modification in Porirua District when compared to WCC.

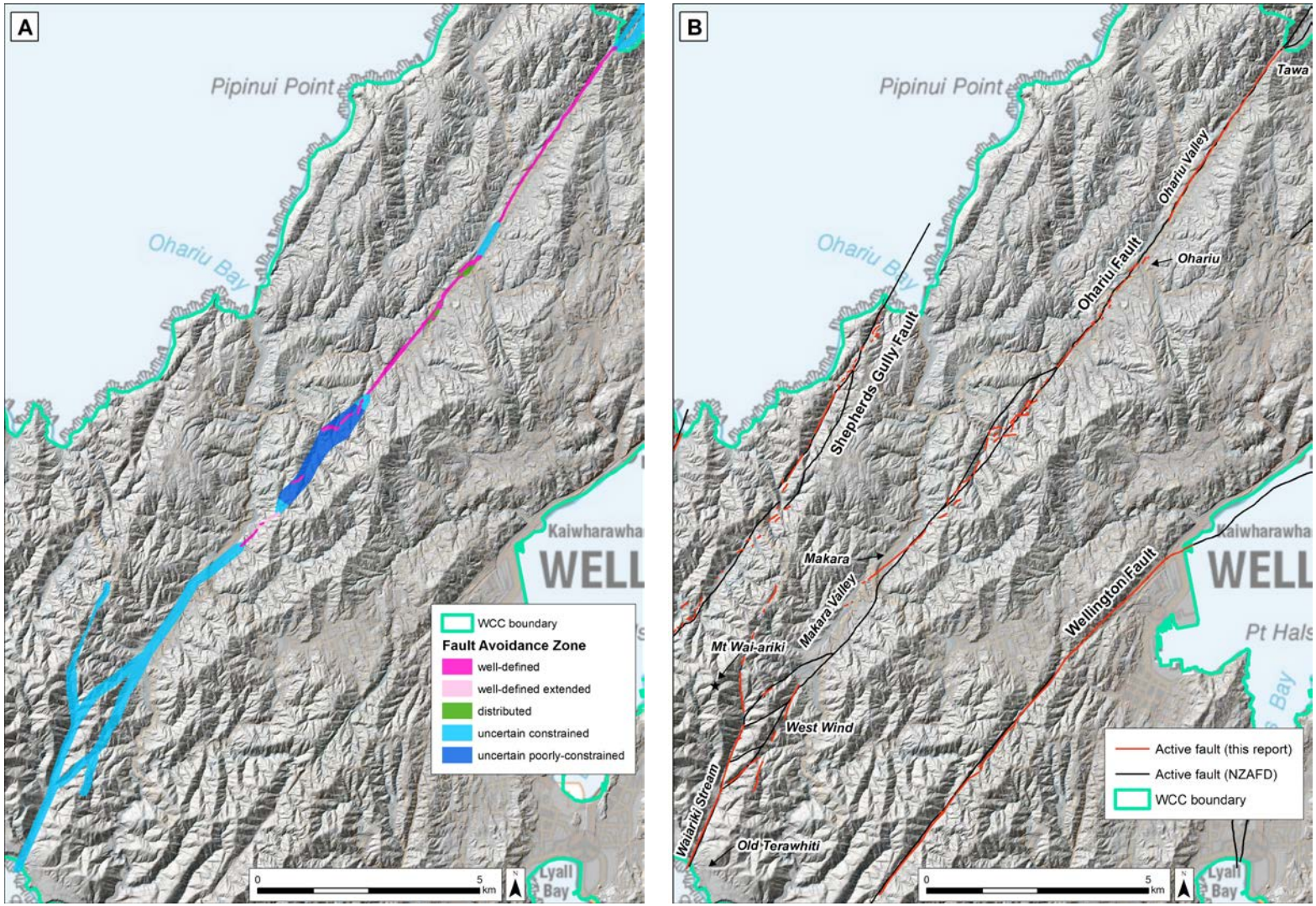

Figure 3.3 (A) Fault Avoidance Zones (pink, green and blue – classified by Fault Complexity) developed for the Ohariu Fault. The Fault Avoidance Zone previously mapped in Porirua District (Litchfield and Van Dissen 2014) is also shown for reference. (B) Previous active fault mapping from the high-resolution New Zealand Active Faults Database (NZAFD; black lines) versus new active fault mapping (this report; red lines). Offshore representations of faults in the NZAFD are, at best, only approximate. WCC = Wellington City Council.

3.3 Shepherds Gully Fault

The Shepherds Gully Fault extends for c. 11 km northeastwards from Oteranga Bay on the south coast along several valleys, including Shepherds Gully, to Ohariu Bay (Makara Beach) on the west coast (Figure 3.4) (e.g. Begg and Johnston 2000). Compared to the Wellington and Ohariu faults, the Shepherds Gully Fault has received little geological attention, and the parameterisation of its activity is relatively poorly constrained.

Van Dissen and Berryman (1996) describe the Shepherds Gully Fault as a right-lateral (dextral) strike-slip fault with a slip rate of approximately 1 mm/yr and a poorly defined recurrence interval of surface-rupturing earthquakes of c. 4000 years. Although the Shepherds Gully Fault is relatively short onshore in Wellington City, it is considered to link with the Pukerua Fault c. 20 km to the north (Porirua District), making it capable of generating earthquakes in the order of magnitude 7.2–7.4 (Stirling et al. 2012). Individual surface-rupture earthquakes along the fault are expected to generate metre-scale right-lateral displacement at the ground surface and a lesser and variable amount of vertical displacement.

The Shepherds Gully Fault passes only through rural areas but does pass under, or very near to, critical infrastructure.

The average recurrence interval of approximately 4000 years, and its moderate slip rate, place the Shepherds Gully Fault into Recurrence Interval Class III (>3500 years to ≤5000 years) of the MfE Active Fault Guidelines with a low degree of confidence (Table 3.1, see also Van Dissen et al. 2003).

3.3.1 Fault Complexity

Though less active than the neighbouring Ohariu Fault, the Shepherds Gully Fault has surface expression sufficiently strong enough to allow efficient and meaningful definition of Fault Avoidance Zones. Fault Avoidance Zones of *well-defined*, *well-defined extended*, *distributed*, *uncertain constrained* and *uncertain poorly constrained* have been defined along the Shepherds Gully Fault within Wellington district. These are discussed in more detail below.

Along the Shepherds Gully Fault, there are a number of distinct and obvious surface traces, especially in the north, south and middle; however, there are lots of gaps in its expression in between these (Figure 3.4). At the south coast, the active trace of the fault is expressed as a series of scarps, saddles and fault-guided valleys that allow for the distinction of *well-defined* and *well-defined extended* Fault Avoidance Zones to be made. However, there are many short traces off this main zone where distributed deformation is likely, and there is thus a wider *distributed* Fault Avoidance Zone mapped to the northwest of the main fault trace in this area. Within, and northeast of, Shepherds Gully, the location of the fault is poorly defined, with traces either eroded, concealed by the flood plain of Oteranga Stream or widely spaced apart. Fault Avoidance Zones along this stretch of fault have been defined as *uncertain constrained* and *uncertain poorly constrained*. West of Quartz Hill, there are a series of fault scarps and a narrow fault-guided valley that are obvious in the LiDAR data, and these have been used to map a *well-defined* Fault Avoidance Zone there. Northeast of Quartz Hill, the fault becomes obscured beneath young sediments in Opau Stream, which is interpreted as a fault-guided valley. From here, the fault is classified as *uncertain constrained*, with the exception of several *well-defined* Fault Avoidance Zones east of Opau Bay where there are clear scarps in the LiDAR data.

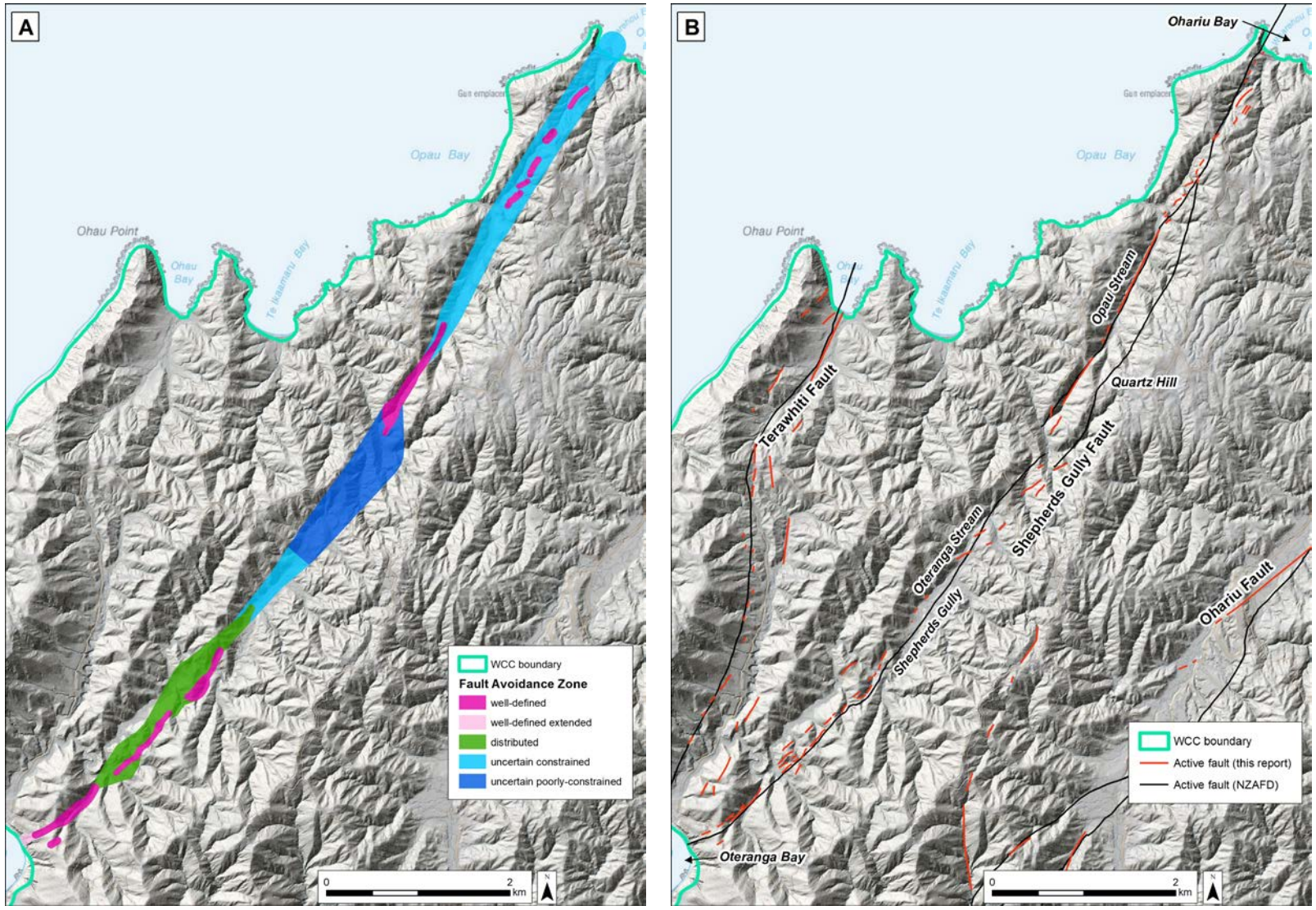

Figure 3.4 (A) Fault Avoidance Zones (pink, green and blue – classified by Fault Complexity) developed for the Shepherds Gully Fault. (B) Previous active fault mapping from the high-resolution New Zealand Active Faults Database (black lines) versus new active fault mapping (this report; red lines). WCC = Wellington City Council.

3.4 Aotea Fault

The Aotea Fault has recently been discovered and mapped offshore in Wellington Harbour by Barnes et al. (2019). It is believed to extend onshore somewhere between Whairepo Lagoon and Oriental Bay. Its extent further south is very poorly known, with interpretations as to its on-land location proposed by various authors differing by several hundred metres to over a kilometre (Figure 3.5) (Begg and Mazengarb 1996; Begg and Johnston 2000; Barnes et al. 2019; Kaiser et al. 2019).

Barnes et al. (2019) used a combination of high-resolution multibeam bathymetry data and marine seismic-reflection profiles tied to dated sediment cores to determine that the Aotea Fault, offshore, has a reverse slip rate of approximately 0.6 ± 0.3 mm/yr and shows evidence of at least two seabed-rupturing events in the last 10,000 years. Barnes et al. (2019) infer that it is capable of generating earthquakes in the order of magnitude 7.0 or greater.

Although the offshore Aotea Fault is demonstrably active (Barnes et al. 2019), its onshore location and activity is poorly constrained. The on-land areas that the fault may pass through are densely populated and highly modified by urban development. Our interrogation of LiDAR data did not identify any small-scale fault features (such as scarps) that would help define the location of the fault; however, it is likely that if any such features once existed, they have long since been destroyed. As noted above, previous interpretations of the Aotea Fault's on-land location differ, in places, by over a kilometre. Accordingly, because of the high degree of locational uncertainly, we have not attempted to define Fault Avoidance Zones along the Aotea Fault. Instead, we make a recommendation in Section 4.2 that additional investigations be undertaken in an attempt to better locate the fault and thus facilitate application of the MfE Active Fault Guidelines and formulation of meaningful land-use policy decisions.

Though the location and activity of the on-land portion of the Aotea Fault is uncertain, it is interpreted to pass through areas of significant urban development as well as passing under, or very near to, numerous critical lifelines and infrastructure elements.

3.4.1 Recurrence Interval Class

The occurrence of at least two seabed-rupturing earthquakes in the last 10,000 years, and its relatively low slip rate, place the Aotea Fault into Recurrence Interval Class III (>3500 years to ≤5000 years) of the MfE Active Fault Guidelines with a medium degree of confidence (Table 3.1).

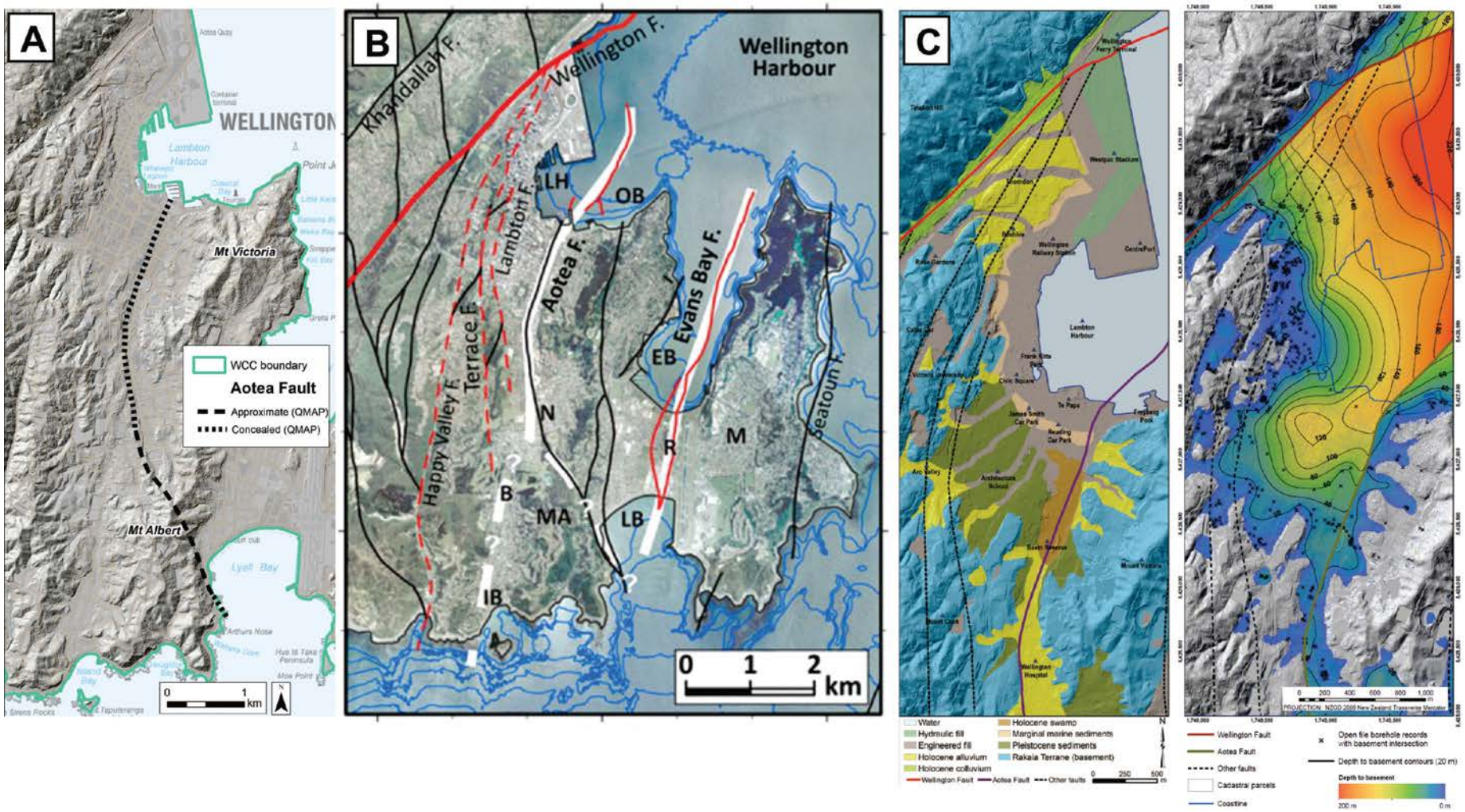

Figure 3.5 The location of the Aotea Fault as defined by (A) QMAP (Begg and Mazengarb 1996) (black dashed line = inactive), (B) Barnes et al. (2019) (solid red lines; demonstrably active) and (C) Kaiser et al. (2019) (purple/green line; interpreted). Panel (B) was taken directly from Figure 15 of Barnes et al. (2019); note that the two possible southern onshore extensions (dashed white lines) of the onshore Aotea Fault have a high level of uncertainty associated with their location and interpretation. Panel (C) was taken directly from Figure 4.1B and Appendix Map 3 of Kaiser et al. (2019); their new onshore interpretation of the Aotea Fault through Wellington CBD now places it c. 150 m further east than where it was originally mapped by Begg and Mazengarb (1996). Note that this new location still has a high locational uncertainty associated with it. WCC = Wellington City Council.

3.5 Evans Bay Fault

The Evans Bay Fault has been mapped by several researchers (e.g. Lewis and Carter 1976; Lewis et al. 1985; Stevens 1990; Begg and Mazengarb 1996; Begg and Johnston 2000), most recently by Barnes et al. (2019). It is interpreted to extend from Lyall Bay in the south across the Rongotai isthmus and through Evans Bay to near Point Halswell (Figure 3.6A). In Evans Bay, Barnes et al. (2019) demonstrate that the fault comprises two strands – a longer eastern strand and a shorter western one – both of which are active. The on-land extent and location of the fault is poorly constrained, however.

Barnes et al. (2019) used a combination of high-resolution multibeam bathymetry data and marine seismic-reflection profiles tied to dated sediment cores to determine that the Evans Bay Fault has a dip-slip rate of approximately 0.6 ± 0.3 mm/yr and shows evidence of at least one seabed-rupturing event in the last 10,000 years. Barnes et al. (2019) infer that it is capable of generating earthquakes in the order of magnitude 7.0 or greater.

Although the offshore Evans Bay Fault is demonstrably active (Barnes et al. 2019), its onshore location is still relatively poorly constrained. Because of the high degree of locational uncertainly, we have not attempted to define Fault Avoidance Zones along the Evans Bay Fault. Instead, we make a recommendation in Section 4.2 that additional investigations be undertaken in an attempt to better locate the fault and thus facilitate application of the MfE Active Fault Guidelines and formulation of meaningful land-use policy decisions.

Though the location of the on-land portion of the Evans Bay Fault is uncertain, it is interpreted to pass through areas of significant urban development as well as passing under, or very near to, numerous critical lifelines and infrastructure elements.

3.5.1 Recurrence Interval Class

The occurrence of at least one seabed-rupturing earthquake in the last 10,000 years, and the relatively low slip rate, place the Evans Bay Fault into Recurrence Interval Class IV (>5000 years to ≤10,000 years) of the MfE Active Fault Guidelines with a medium degree of confidence (Table 3.1).

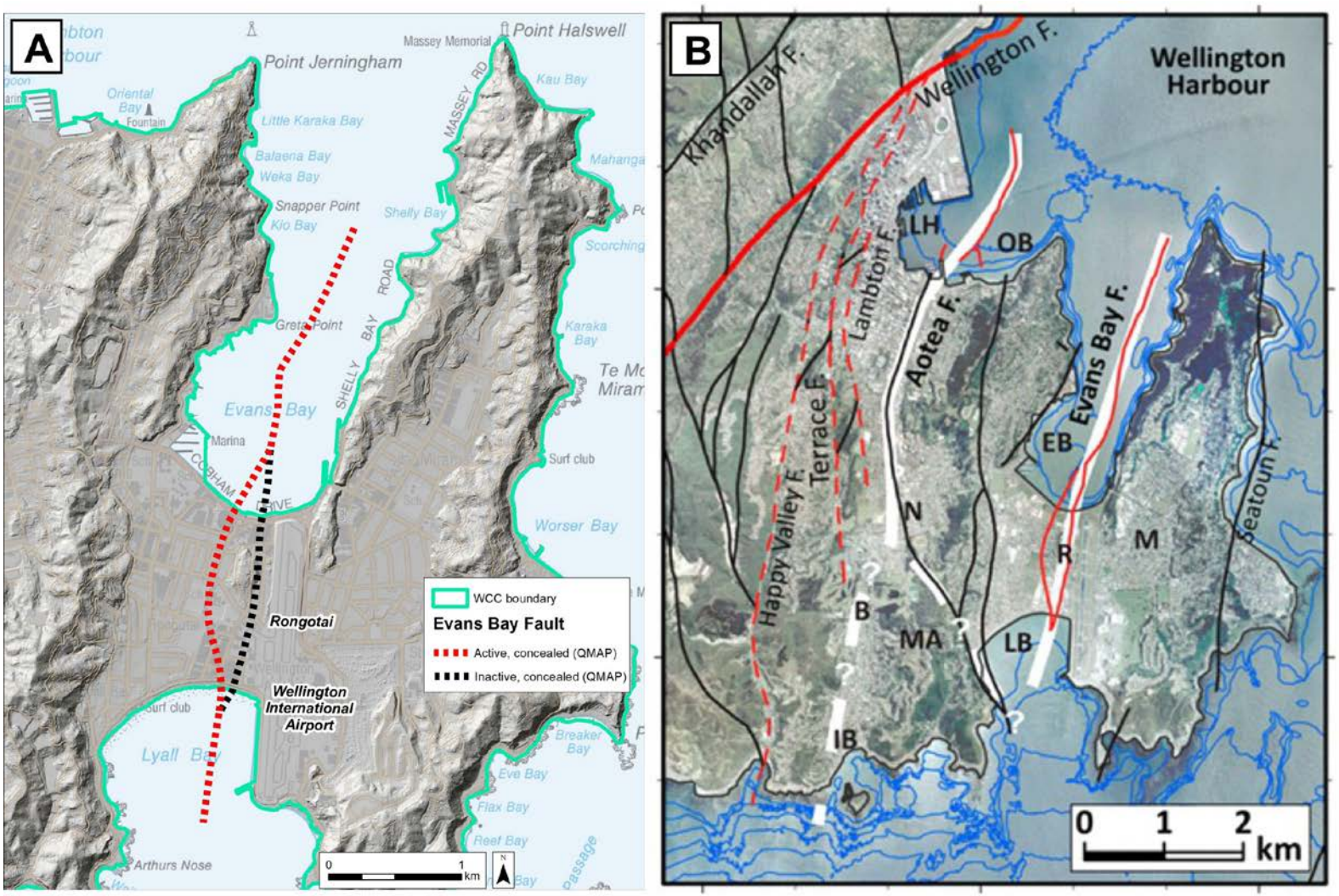

Figure 3.6 The location of the Evans Bay Fault as defined by (A) QMAP (Begg and Mazengarb 1996) (red dashed line = active or probably active, black dashed line = inactive) and (B) Barnes et al. (2019) (solid red lines; demonstrably active). Note that the eastern QMAP trace across the Rongotai isthmus in Panel (A) was not previously defined as active, and the offshore traces were previously defined as probably active. Also shown on Panel (B) is the inferred crustal extent of the Evans Bay Fault (solid white line) (taken directly from Figure 15 of Barnes et al. 2019). WCC = Wellington City Council.

3.6 Terawhiti Fault

The Terawhiti Fault is poorly located and very little is known about its activity (Ota et al. 1981). It extends for c. 6 km in a northeast orientation from Oteranga Bay on the south coast along Black Gully to Ohau Bay on the west coast (Figure 3.7).

Begg and Johnston (2000) define it is as a right-lateral (dextral) strike-slip fault, downthrown to the southeast. Based on general geomorphic expression, we suspect it is less active than the neighbouring Shepherds Gully Fault.

The Terawhiti Fault passes only through rural areas but does pass very near to infrastructure such as the wind farm near Makara (including associated transmission lines). Its southern onshore extent in Oteranga Bay is also located close to the power cable terminal that links the National Grid between the North and South islands.

3.6.1 Recurrence Interval Class

The Terawhiti Fault appears to be less active than the neighbouring Shepherds Gully Fault (Recurrence Interval Class III), it is therefore placed into Recurrence Interval Class IV (>5000 years to ≤10,000 years) of the MfE Active Fault Guidelines with a low degree of confidence (Table 3.1).

3.6.2 Fault Complexity

The Terawhiti Fault is expressed at the ground surface as a series of discontinuous and widely spaced, yet collectively aligned, fault-related features (Figure 3.7B). Along the southern half of the fault are a series of saddles and uphill-facing scarps visible in the LiDAR data on either side of Black Gully, which are especially prominent on the western side of the gully. Its surface expression becomes much more diffuse northeast of approximately the ‘stamping battery’, where it is expressed predominantly as fault-guided valleys, lineaments and saddles, with the exception of a few scarps visible on the slope above Ohau Bay.

Though less active than the Shepherds Gully Fault, the Terawhiti Fault has surface expression sufficiently strong enough to facilitate mapping of Fault Avoidance Zones. However, due to the nature of the mapped surface features, we applied a slightly different methodology to define a Fault Avoidance Zone for the Terawhiti Fault than that described in Section 2.4. Instead, a Fault Avoidance Zone of constant width was established to encompass all the widely spaced and discontinuous features. This eventuated in a Fault Avoidance Zone of ~600 width and was accordingly defined as *uncertain poorly constrained* (Figure 3.7A; Table 2.3).

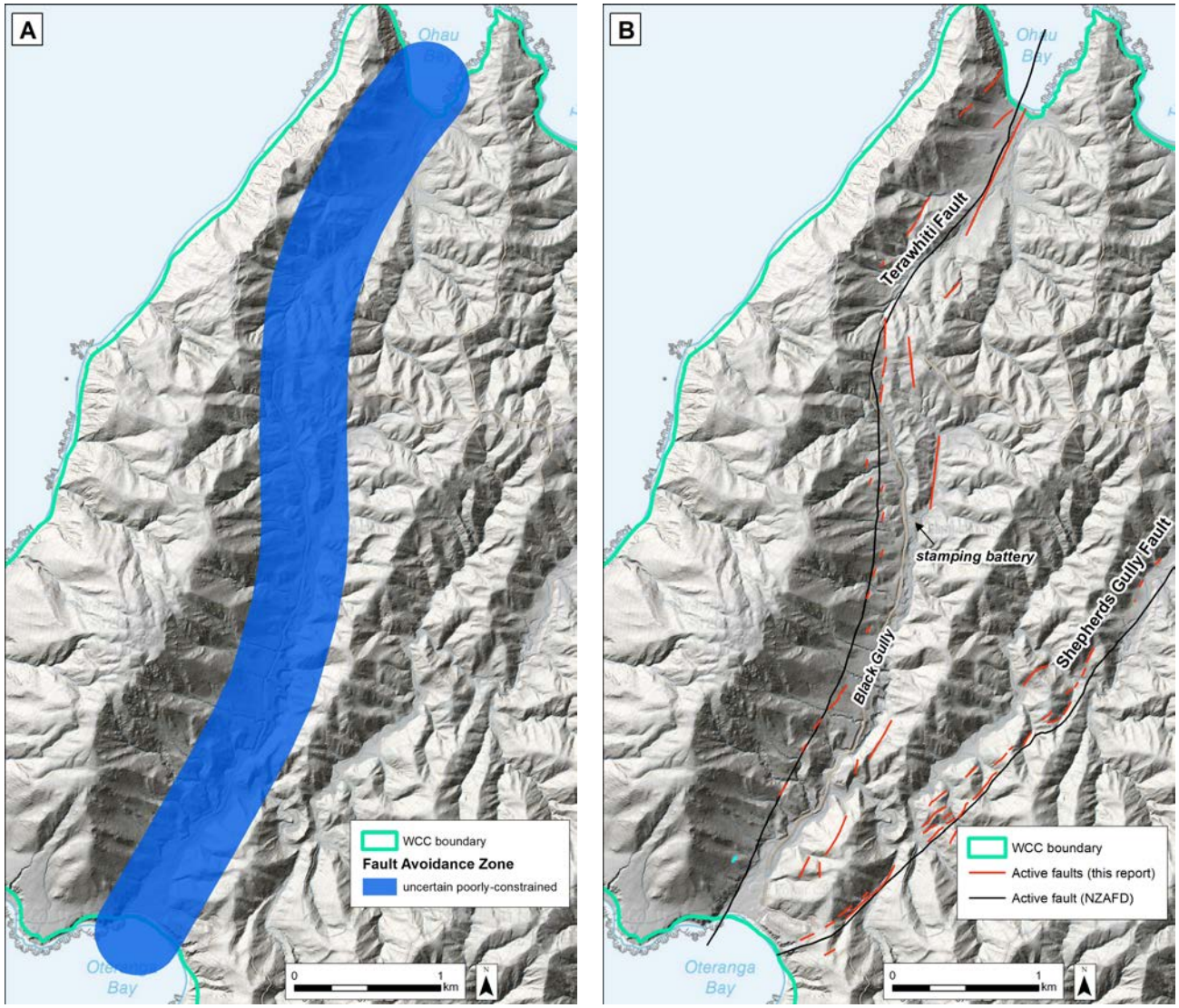

Figure 3.7 (A) Fault Avoidance Zone (blue – classified by Fault Complexity) developed for the Terawhiti Fault. (B) Previous active fault mapping from the high-resolution New Zealand Active Faults Database (black lines) versus new active fault mapping (this report; red lines). WCC = Wellington City Council.

3.7 Moonshine Fault

Very little is known about the Moonshine Fault in Wellington City. From its southern mapped active extent near Grenada North (Langridge et al. 2016), it extends northeastward through hill country above and along Takapu Road into Porirua District (Figure 3.8). The fault is only c. 5-km-long within Wellington City but has a total length, when combined with the along-strike Otaki Forks Fault, of ~70 km. The Moonshine Fault is interpreted to be a dextral strike-slip fault downthrown to the northwest (Begg and Johnston 2000), but there are no fault-specific data that constrain its slip rate or recurrence interval. However, in general, the gross geomorphic expression of this fault is less distinct and more subdued than other neighbouring faults in Wellington City or Porirua District. Its activity also appears to diminish to the south. It has been estimated to rupture in earthquakes of approximate magnitude 7.0–7.2 (Stirling et al. 2012).

The Moonshine Fault passes through areas of semi-urban and rural development and passes under, or very near to, critical infrastructure and lifelines.

3.7.1 Recurrence Interval Class

As noted above, there are no fault-specific data that constrain the recurrence interval of the Moonshine Fault. In a previous fault mapping investigation for Porirua District (Litchfield and Van Dissen 2014), the Moonshine Fault was assigned to Recurrence Interval Class IV (>5000 years to ≤10000 years) with a low degree of confidence. For consistency with fault mapping in adjacent districts, and in light of no new data, we have adopted that same Recurrence Interval Classification here; Recurrence Interval Class IV, with a low degree of confidence (Table 3.1).

3.7.2 Fault Complexity

The Moonshine Fault is mapped as *uncertain constrained* along its entire length in Wellington City (Figure 3.8A). The location is largely denoted by suspected, yet sparsely distributed, fault-controlled saddles and fault-guided valleys (Figure 3.8B). Due to the lack of surface features, we use the same methodology to define the Fault Avoidance Zone for the Moonshine Fault as that used for the Terawhiti Fault and which differs slightly from that described in Section 2.4. The Fault Avoidance Zone of the Moonshine Fault was positioned through WCC so as to encompass all of the mapped fault features, joining in the north to the Fault Avoidance Zone previously mapped for the Moonshine Fault in Porirua City (Litchfield and Van Dissen 2014). This resulted in a Fault Avoidance Zone that closely followed the previous geological mapping of Begg and Johnston (2000) and Langridge et al. (2016). Based on geomorphic expression, the Moonshine Fault within WCC appears to be less active than its along-strike extension in Upper Hutt City. Accordingly, we stop the Fault Avoidance Zone in the south near Grenada North where major earthworks have removed surface evidence of this fault. This position is similar to that depicted by Langridge et al. (2016), which is several kilometres further north than the depiction offered by Begg and Johnston (2000). As noted above, the Fault Avoidance Zone of the Moonshine Fault through WCC has a constant width and has been defined as *uncertain constrained* (Figure 3.8A).

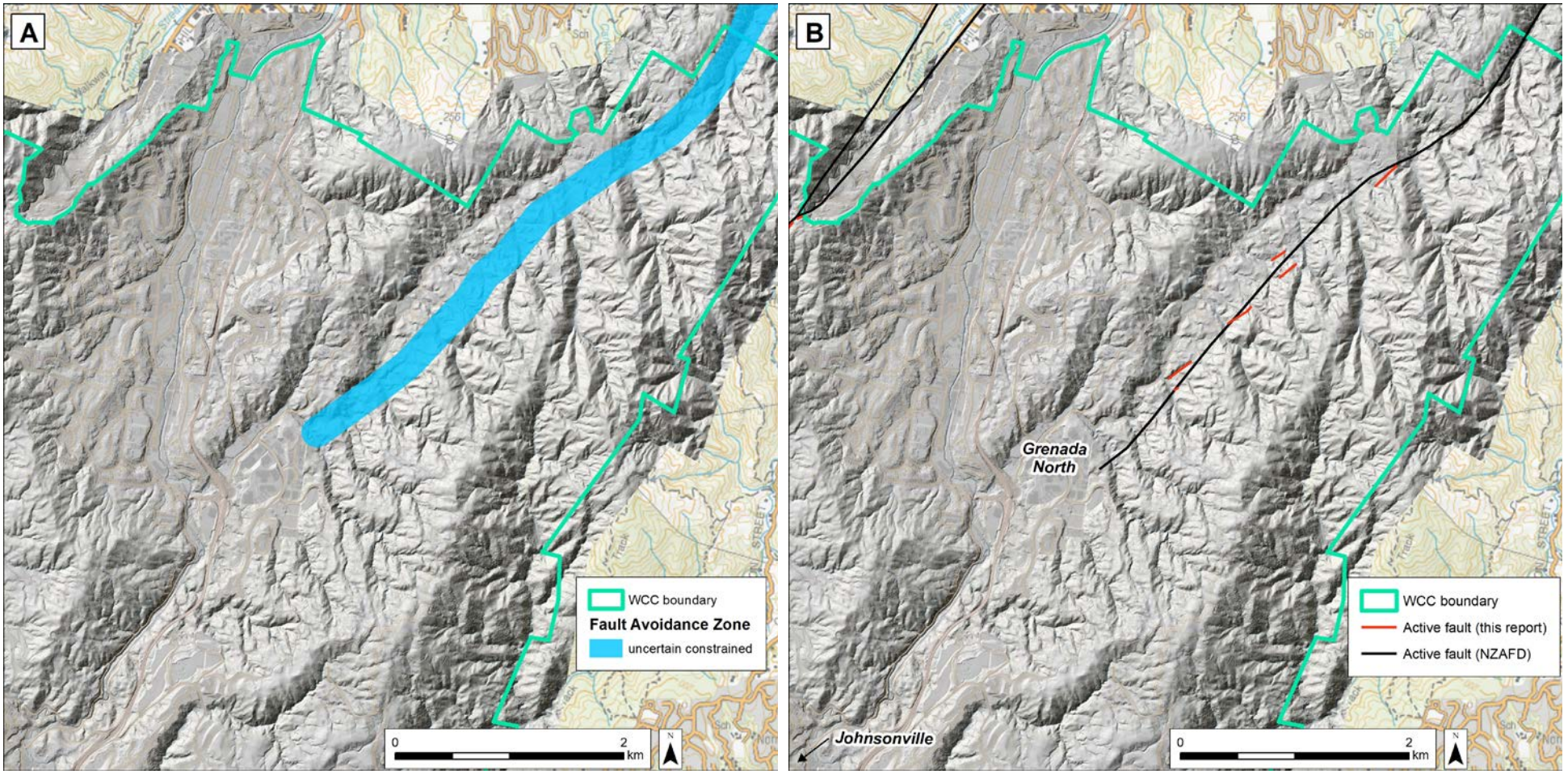

Figure 3.8 (A) Fault Avoidance Zones (blue – classified by Fault Complexity) developed for the Moonshine Fault. The Fault Avoidance Zone previously mapped in Porirua District (Litchfield and Van Dissen 2014) is also shown for reference. (B) Previous active fault mapping from the high-resolution New Zealand Active Faults Database (black lines) versus new active fault mapping (this report; red lines). WCC = Wellington City Council.

4.0 CONCLUSIONS AND RECOMMENDATIONS

4.1 Conclusions

Fault Recurrence Interval Class and Fault Avoidance Zones based on Fault Complexity have been defined for the Wellington, Ohariu, Shepherds Gully, Terawhiti and Moonshine faults within Wellington City. These fault rupture hazard parameters, when combined with Building Importance Category, enable a risk-based approach to be taken when making planning decisions about development of land on, or close to, active faults that is consistent with the MfE Active Fault Guidelines. For the Aotea and Evans Bay faults, Recurrence Interval Class has been defined, but, due to a large locational uncertainty, Fault Avoidance Zones have not been defined.

4.2 Recommendations

Based on the findings in this report, GNS Science recommends that Wellington City Council:

Formulate Planning Policy and Assessment Criteria

Fault Recurrence Interval Class, Fault Complexity and Building Importance Category are the three key elements in the MfE Active Fault Guidelines that, when brought together, enable a risk-based approach to be taken when making planning decisions about development of land on, or close to, active faults. Understanding the inter-relationships between these key parameters is critical to the development of consistent, risk-based objectives, policies and methods to guide development of land that may be impacted by surface rupture faulting. The critical relationships between Recurrence Interval Class and Building Importance Category are summarised in Table 2.5. These interrelationships are expanded in tables presented in Appendix 3, which provide indicative examples of Resource Consent Category suggestions for various combinations of Recurrence Interval Class, Fault Complexity and Building Importance Category for active faults in Wellington City. We would encourage Wellington City Council to develop and apply tables such as these for the Fault Avoidance Zones developed in this study.

Determining appropriate fault rupture hazard mitigation strategies for different scenarios/ combinations of Recurrence Interval Class, Fault Complexity and Building Importance Category is a complex task, especially when trying to anticipate the level of risk that a community may or may not be willing to accept. Certainly, as the risk increases, the mitigation strategies should become more restrictive, and the range of matters that Council needs to consider increases. Ultimately, the Council needs to be able to impose consent conditions, such as those regarding the use, size, location and foundations of structures, to avoid or reduce the adverse effects of fault rupture.

It is important to remember that surface fault rupture is a seismic hazard of relatively limited geographic extent, compared to strong ground shaking, and can, in many cases, be avoided. If avoidance of fault rupture hazard at a site is not practicable, then planning and design measures need to be prescribed/incorporated to mitigate and accommodate the co-seismic surface rupture displacements anticipated at the site. The planning and design measures need to also be consistent with the appropriate combination of Fault Complexity, Recurrence Interval Class and Building Importance Category relevant to that site.

Also worth reiterating is that when a Fault Avoidance Zone is classified as, for example, *uncertain poorly constrained*, specific fault studies at or near the site may provide more certainty as to the fault's location and thus allow the Fault Avoidance Zone to be reduced in width and reclassified to, for example, *well-defined* or *uncertain constrained*. Commensurate with a reclassification of Fault Avoidance Zone is a re-assessment as to the most appropriate fault rupture hazard mitigation strategies applicable to the site.

With respect to planning for fault rupture, the Council will ideally want to apply one or a number of strategies that mitigate the hazard. These strategies should be tailored to suit the individual setting and requirements of the Council.

In light of the current study, the Council may wish to review objectives, policies and methods (which may include rules) that address fault rupture during the District Plan review. The exact nature of these objectives, policies and methods will need to be determined in consultation with a number of relevant parties, including within the Council itself, the community and other relevant organisations. As part of the process, matters that the Council may wish to consider include the:

- risk to life, property and the environment posed by fault rupture hazard;
- likely frequency and size of displacement;
- type, scale and distribution of potential effects from surface rupture;
- combined effects of ground shaking and displacement caused by earthquakes;
- distance of the proposed structure from the fault itself; and
- degree to which the building, structure or design work can avoid or mitigate the effects of the fault rupture.

If applying for a resource consent in a Fault Avoidance Zone, the District Plan should make provisions to ensure that the Council has the option of requiring applicants to provide evidence of the location for fault rupture hazard. Alternatively, if it is impractical to locate the fault to the accuracy that is necessary, then the developer should prove that the proposed building is resilient enough to withstand fault rupture, from a life safety standpoint.

Apply Consistent Policies throughout the Region

Natural hazards, including fault rupture hazard, do not stop at local authority boundaries. It is important to consider how the District Plan will co-ordinate with other adjoining local authorities that share the same hazards to ensure that hazard avoidance and/or mitigation issues can be suitably integrated across councils. Examples of these are the Ohariu and Moonshine faults that cross into the adjoining Porirua City (and continue on into Kāpiti Coast District and Upper Hutt City, respectively) and the continuation of the Wellington Fault through Lower Hutt City before it heads northeast into Upper Hutt City and beyond.

Obtain Better Constraints on Recurrence Interval Class

Using the terminology and definitions put forward in the MfE Active Fault Guidelines, the confidence of Recurrence Interval Classification for many of the active faults in Wellington City is generally low, with the exception of the Wellington Fault (Table 3.1). For the second-most active fault in the district, the Ohariu Fault, this is because the range of uncertainty of the recurrence interval estimates span a significant portion of several Recurrence Interval Classes. The mean rate is used to define the Recurrence Interval Class, but an alternative, more conservative, approach would be to assign the Recurrence Interval Class based on the

minimum value rather than the mean. This would result in the Ohariu Fault being placed in the more hazardous/restrictive Recurrence Interval Class I. The Recurrence Interval Class of the Shepherds Gully Fault is very poorly-constrained, while those of the Aotea and Evans Bay faults only have a medium level of certainty. Recurrence Interval Classes for the Terawhiti and Moonshine faults are assigned purely based on subjective comparisons with the neighbouring faults.

Additional paleoearthquake studies on these faults could yield data that would better constrain their respective recurrence intervals. This may warrant a re-assessment of the faults' Recurrence Interval Classes compared to those listed in Table 3.1. Regardless if new work leads to the re-classification of a fault's Recurrence Interval Class, better-constrained recurrence interval data will allow a Recurrence Interval Class to be assigned with more confidence.

Also, less as a recommendation, but more as a comment, it needs to be acknowledged that, with future geological work in Wellington City, new active faults may be discovered, and evidence may be uncovered to show that faults now regarded as not active may, in fact, be active. In this regard, it is fitting to remember that the Aotea Fault was only discovered a few years ago.

Reduce the Width of Some Fault Avoidance Zones

Some of the Fault Avoidance Zones defined in this study are quite wide, largely owing to uncertainty in the location of the fault. Detailed fault studies (e.g. mapping, trenching and other forms of subsurface investigation) could provide better constraints on fault locations in some of these areas, and, consequently, the width of the Fault Avoidance Zones could be reduced. This would mean fewer properties would fall within Fault Avoidance Zones, and, consequently, fewer properties would need consideration by Council with regard to fault rupture hazard.

Additionally, with better constraints on fault location, and a possible reduction in width of a Fault Avoidance Zone, the zone may warrant reclassification, for example, from *uncertain poorly constrained* to *uncertain constrained*. Depending on Building Importance Category, a reclassification of Fault Complexity (i.e. Fault Avoidance Zone) may also warrant a re-think regarding decisions pertaining to development of that land.

Such detailed fault studies are particularly needed for the Aotea and Evans Bay faults to better define/constrain their onshore location to the extent that meaningful Fault Avoidance Zones can be established for them. This would enable application of the MfE Active Fault Guidelines and facilitate the formulation of appropriate land-use planning policy.

Similarly, we have tentatively mapped a *distributed* Fault Avoidance Zone in the Kaiwharawhara area along the Wellington Fault. We recommend further investigation in this area to confirm or refute the veracity of this mapping.

It also needs to be acknowledged that there are some areas in the district (e.g. the *uncertain poorly constrained* Fault Avoidance Zones) where expensive geological investigations may be the only methods available to better constrain the fault's location. The results of these surveys may still leave uncertainty as to the precise location of the fault, particularly with respect to the location of future surface rupture. In these areas, it may be more expedient to mitigate rupture hazard by appropriate assessment criteria (e.g. the degree to which the proposed building, structure or design work can accommodate/mitigate the effects of fault rupture) rather than by locating the fault.

Investigate Engineering Mitigation Measures

Characterising the hazards associated with surface fault rupture and developing design strategies to mitigate those hazards have been the focus of several publications by JD Bray (e.g. Bray 2001, 2009; Bray and Kelson 2006). In these, he consistently highlights four principal means for mitigating the hazard posed by ground-surface fault rupture:

- land-use planning
- engineering geology
- geotechnical engineering, and
- structural engineering.

Depending on fault rupture characteristics and site conditions, he advocates several potentially effective design measures that include establishing non-arbitrary setback distances; constructing earth fills to partially absorb and distribute underlying rupture; isolating foundations from underlying ground movement (e.g. through the use of slip layers); and designing strong, ductile foundations that resist imposed earth pressures.

The MfE Active Fault Guidelines is the primary document in New Zealand providing guidance with regard to the mitigation of ground-surface fault rupture hazard. In these guidelines, the recommended mitigation strategy is avoidance; however, engineering mitigation strategies are also permitted in appropriate circumstances, though little, if any, guidance is provided regarding what those engineering strategies and appropriate circumstances might be. This deficiency was largely the consequence of a lack of data. That is, at the time that the guidelines were issued, there were very few New Zealand examples to draw from where New Zealand engineered structures had been impacted by ground-surface fault rupture and the impacts of that rupture evaluated with regard to: (1) the characterisation of the ground strains and displacements generated by that surface rupture, (2) the structural damage that the surface rupture produced and (3) the possible engineering strategies that could be employed to mitigate that damage.

Since the MfE Active Fault Guidelines were published, there have been two large New Zealand earthquakes that have generated ground-surface fault rupture that has directly impacted engineered buildings; the 2010 Darfield earthquake and the 2016 Kaikōura earthquake (Van Dissen et al. 2011, 2019). The amount and style of surface-rupture deformation varied considerably, ranging from decimetre-scale distributed folding with estimated shear strains in the order of $\leq 10^{-2}$ to metre-scale discrete rupture with estimated shear strains up to 10^{0}. Collectively, about two-dozen buildings were directly damaged by ground-surface fault rupture resulting from these two earthquakes. These were typically single-storey timber-framed houses, barns and woolsheds with regular-shaped floor plans and lightweight roofing materials. Based on these examples (which are elaborated on in Appendix 2), several pertinent observations can be made regarding the performance of New Zealand residential structures when subjected to surface fault-rupture deformation of varying levels of strain and amounts of displacement.

1. Single-storey, regular-shaped, timber-framed residential structures with light roofs and of modest dimensions (floor area of ≤~200 m^2) subjected to low/moderate surface fault rupture deformation (i.e. shear strains $\leq 10^{-2}$ and discrete displacements of decimetre-scale or less) do not appear to pose a collapse hazard.

2. At those levels of deformation, the prospects of damage-control and repairability (and therefore post-event functionality) appear to be improved for such residential structures if the cladding contributes to the robustness of the superstructure (e.g. plywood, timber weatherboard) and is not brittle.
3. This favourable behaviour is enhanced if building systems moderate the direct transmission of ground deformation into the superstructure (either by decoupling or by other means) and allow for re-levelling of the structure post-event.
4. For residential structures with the above-mentioned attributes, non-collapse performance can be achieved at even higher levels of strain (~100) and larger discrete displacements (metre-scale) in a predominantly horizontal displacement setting (i.e. strike-slip) if the superstructure decouples from (is isolated from) the underlying ground deformation. The New Zealand dataset does not contain examples of the performance of residential structures subjected to such large surface fault rupture strains and displacements in a predominantly vertical displacement setting. In a horizontal displacement setting, the decoupled superstructure still rests on (and is supported by) the ground. This may not be the case in a predominantly vertical displacement setting, where there is the possibility that fault rupture will leave a significant portion of the decoupled superstructure un-supported, and this may lead, if not to collapse, then at least to significant tilting and angular distortions. In addition, in a reverse/thrust vertical displacement setting there is the potential for a 'bulldozer zone' to develop at the base of the scarp where fault displacement forces the scarp to thrust horizontally across the ground surface, and this too can severely impact structures.

The surest and most successful way to mitigate the damage and loss that may result for ground-surface fault rupture is to avoid the hazard (i.e. to not build across the fault). However, we acknowledge that there has been significant urban development over the Wellington, Aotea and Evans Bay faults through Wellington City centre and surrounding suburbs. In this instance, it may be more practicable to mitigate the fault rupture hazard through engineered solutions rather than by fault avoidance, if it is feasible to reduce the risk to an acceptable level. For buildings, the aim of these solutions would be to firstly prevent collapse (i.e. to preserve life safety) and secondly to limit damage (and facilitate repair) due to ground surface fault rupture. In Appendix 2, we present case study examples from the 2010 Darfield and 2016 Kaikōura earthquakes, and the 1987 Edgecumbe earthquake also, showing the impacts that surface fault rupture had on residential (or residential-type) structures. These examples provide insight into construction styles that could be employed, in suitable circumstances, to facilitate non-collapse performance resulting from surface fault rupture and, in certain instances, post-event functionality. We also provide comment on how these examples may enable a more nuanced application of the MfE Active Fault Guidelines in, again, appropriate circumstances.

Similarly, attention should be given to critical lifelines that cross active faults. For example, consideration should be given to designing or retro-fitting lifelines to be rupture-resilient or to facilitate ease and speed of reparability and to limit damage.

Socialise the Fault Avoidance Zones during the District Plan Review Phase

In the interest of transparency and information sharing, it is recommended that the Council socialises the Fault Avoidance Zones and their implications within a District Plan setting, first with internal Council departments (resource consents, building consents, infrastructure controllers, parks and reserves, emergency managers) and then with the Council's Executive and Councillors, before proceeding with any incorporation of the Fault Avoidance Zones into

the revised District Plan. Next, it is recommended that Fault Avoidance Zones and their implications are socialised with landowners, focusing on land with significant and short- to mid-term development potential. Finally, Fault Avoidance Zones will also need to be socialised with other groups, including Mana Whenua, Regional Council, ratepayers associations, residents groups, local boards, other landowners, infrastructure providers, development groups and regional planning branches.

5.0 ACKNOWLEDGEMENTS

Nicola Litchfield and Robert Langridge (GNS Science) provided peer review of this report.

6.0 REFERENCES

Alloway BV, Lowe DJ, Barrell DJA, Newnham RM, Almond PC, Augustinus PC, Bertler NAN, Carter L, Litchfield NJ, McGlone MS, et al. 2007. Towards a climate event stratigraphy for New Zealand over the past 30 000 years (NZ-INTIMATE project). *Journal of Quaternary Science*. 22(1):9–35. doi:10.1002/jqs.1079.

Barnes PM, Nodder SD, Woelz S, Orpin AR. 2019. The structure and seismic potential of the Aotea and Evans Bay faults, Wellington, New Zealand. *New Zealand Journal of Geology and Geophysics*. 62(1):46–71. doi:10.1080/00288306.2018.1520265.

Beetham RD, Cousins WJ, Craig M, Dellow GD, Van Dissen RJ. 2012. Hutt Valley trunk wastewater earthquake vulnerability study. Lower Hutt (NZ): GNS Science. 51 p. Consultancy Report 2012/234. Prepared for MWH NZ Ltd.

Begg JG, Johnston MR, compilers. 2000. Geology of the Wellington area [map]. Lower Hutt (NZ): Institute of Geological & Nuclear Sciences. 1 sheet + 64 p., scale 1:250,000. (Institute of Geological & Nuclear Sciences 1:250,000 geological map; 10).

Begg JG, Mazengarb C. 1996. Geology of the Wellington area: sheets R27, R28, and part Q27 [map]. Lower Hutt (NZ): Institute of Geological & Nuclear Sciences. 1 folded map + 128 p., scale 1:50,000. (Institute of Geological & Nuclear Sciences geological map; 22).

Berryman KR. 2019. Wellington Fault: earthquake shaking and tsunami hazards for KiwiRail Project iRex. Lower Hutt (NZ): GNS Science. 8 p. Consultancy Report 2019/138LR. Prepared for KiwiRail.

Bray JD. 2001. Developing mitigation measures for the hazards associated with earthquake surface fault rupture. In: *Proceedings of the Workshop on Seismic Fault-Induced Failures, Tokyo, Japan, 11–12 January 2001*. Tokyo (JP): Japan Society for the Promotion of Science. p. 55–79.

Bray JD. 2009. Designing buildings to accommodate earthquake surface fault rupture. In: Goodno B, editor. *Improving the seismic performance of existing buildings and other structures*. 2009 Dec 9–11; San Francisco, California. Reston (VA): American Society of Civil Engineers. p. 1269–1280.

Bray JD, Kelson KI. 2006. Observations of surface fault rupture from the 1906 earthquake in the context of current practice. *Earthquake Spectra*. 22(2):69–89. doi:10.1193/1.2181487.

Heron DW, Van Dissen RJ, Sawa M. 1998. Late Quaternary movement on the Ohariu Fault, Tongue Point to MacKays Crossing, North Island, New Zealand. *New Zealand Journal of Geology and Geophysics*. 41(4):419–439. doi:10.1080/00288306.1998.9514820.

Kaiser AE, Hill MP, Wotherspoon L, Bourguignon S, Bruce ZR, Morgenstern R, Giallini S. 2019. Updated 3D basin model and NZS 1170.5 subsoil class and site period maps for the Wellington CBD: Project 2017-GNS-03-NHRP. Lower Hutt (NZ): GNS Science. 48 p. + appendix. Consultancy Report 2019/01. Prepared for Natural Hazards Research Platform.

Kerr J, Nathan S, Van Dissen RJ, Webb P, Brunsdon D, King AB. 2003. Planning for development of land on or close to active faults: a guideline to assist resource management planners in New Zealand. Lower Hutt (NZ): Institute of Geological & Nuclear Sciences. 71 p. Client Report 2002/124. Prepared for Ministry for the Environment.

King AB, Brunsdon DR, Shephard RB, Kerr JE, Van Dissen RJ. 2003. Building adjacent to active faults: a risk-based approach. In: *Proceedings of the 2003 Pacific Conference on Earthquake Engineering*. 2003 Feb 13–15; Christchurch, New Zealand. Wellington (NZ): New Zealand Society for Earthquake Engineering. Paper 158.

Langridge RM, Morgenstern R. 2018. Active fault mapping and fault avoidance zones for Horowhenua District and Palmerston North City. Lower Hutt (NZ): GNS Science. 72 p. Consultancy Report 2018/75. Prepared for Horizons Regional Council.

Langridge RM, Morgenstern R. 2019. Active fault mapping and fault avoidance zones for the Manawatū District. Lower Hutt (NZ): GNS Science. 69 p. Consultancy Report 2019/123. Prepared for Horizons Regional Council.

Langridge RM, Morgenstern R. 2020. Active fault mapping and fault avoidance zones for the Rangitikei District. Lower Hutt (NZ): GNS Science. 66 p. Consultancy Report 2019/168. Prepared for Horizons Regional Council.

Langridge RM, Ries WF, Litchfield NJ, Villamor P, Van Dissen RJ, Barrell DJA, Rattenbury MS, Heron DW, Haubrock S, Townsend DB, et al. 2016. The New Zealand Active Faults Database. *New Zealand Journal of Geology and Geophysics*. 59(1):86–96. doi:10.1080/00288306.2015.1112818.

Langridge RM, Van Dissen RJ, Rhoades DA, Villamor P, Little T, Litchfield NJ, Clark KJ, Clark D. 2011. Five thousand years of surface ruptures on the Wellington Fault, New Zealand: implications for recurrence and fault segmentation. *Bulletin of the Seismological Society of America*. 101(5):2088–2107. doi:10.1785/0120100340.

Lewis KB, Carter L. 1976. Depths, sediments and faulting on each side of the Rongotai Isthmus, Wellington. Wellington (NZ): New Zealand Oceanographic Institute. 31 p. (NZOI oceanographic summary; 11).

Lewis KB, Mildenhall DC, Clowes CD. 1985. The late Quaternary seismic, sedimentary and palynological stratigraphy beneath Evans Bay, Wellington Harbour. *New Zealand Journal of Geology and Geophysics*. 28(1):129–152. doi:10.1080/00288306.1985.10422281.

Litchfield NJ, Morgenstern R, Van Dissen RJ, Langridge RM, Pettinga JR, Jack H, Barrell DJA, Villamor P. 2019. Updated assessment of active faults in the Kaikōura District. Lower Hutt (NZ): GNS Science. 71 p. Consultancy Report 2018/141. Prepared for Canterbury Regional Council (Environment Canterbury).

Litchfield NJ, Morgenstern R, Villamor P, Van Dissen RJ, Townsend DB, Kelly SD. 2020. Active fault hazards in the Taupō District. Lower Hutt (NZ): GNS Science. 114 p. Consultancy Report 2020/31. Prepared for Taupō District Council.

Litchfield NJ, Van Dissen RJ. 2014. Porirua district fault trace study. Lower Hutt (NZ): GNS Science. 53 p. Consultancy Report 2014/213. Prepared for Greater Wellington Regional Council; Porirua Council.

Litchfield NJ, Van Dissen RJ , Hemphill-Haley M, Townsend DB, Heron DW. 2010. Post c. 300 year rupture of the Ohariu Fault in Ohariu Valley, New Zealand. *New Zealand Journal of Geology and Geophysics*. 53(1):43–56. doi:10.1080/00288301003631780.

Litchfield NJ, Van Dissen RJ, Heron DW, Rhoades DA. 2006. Constraints on the timing of the three most recent surface rupture events and recurrence interval for the Ohariu Fault: trenching results from MacKays Crossing, Wellington, New Zealand. *New Zealand Journal of Geology and Geophysics*. 49(1):57–61. doi:10.1080/00288306.2006.9515147.

Litchfield NJ, Van Dissen RJ, Langridge RM, Heron DW, Prentice C. 2004. Timing of the most recent surface rupture event on the Ohariu Fault near Paraparaumu, New Zealand: short communication. *New Zealand Journal of Geology and Geophysics*. 47(1):123–127. doi:10.1080/00288306.2004.9515041.

Little TA, Van Dissen RJ, Rieser U, Smith EGC, Langridge RM. 2010. Coseismic strike slip at a point during the last four earthquakes on the Wellington Fault near Wellington, New Zealand. *Journal of Geophysical Research: Solid Earth*. 115(B5):B05403. doi:10.1029/2009jb006589.

Ninis D, Little TA, Van Dissen RJ, Litchfield NJ, Smith EGC, Wang N, Rieser U, Henderson CM. 2013. Slip rate on the Wellington fault, New Zealand, during the Late Quaternary: evidence for variable slip during the Holocene. *Bulletin of the Seismological Society of America*. 103(1):559–579. doi:10.1785/0120120162.

Ota Y, Williams DN, Berryman KR. 1981. Late Quaternary tectonic map of New Zealand, parts Sheets Q27, R27 & R28, Wellington [map]. Wellington (NZ): Department of Scientific and Industrial Research. 1 map + 1 booklet, scale 1:50,000.

Perrin ND, Wood PR. 2003a. Defining the Wellington Fault within the urban area of Wellington City. Lower Hutt (NZ): Institute of Geological & Nuclear Sciences. 33 p. Client Report 2002/151. Prepared for Wellington City Council.

Perrin ND, Wood PR. 2003b. Location of the Wellington Fault at the lower Karori dam. Lower Hutt (NZ): Institute of Geological & Nuclear Sciences. 11 p. Client Report 2002/143. Prepared for Wellington Regional Council.

Pondard N, Barnes PM. 2010. Structure and paleoearthquake records of active submarine faults, Cook Strait, New Zealand: implications for fault interactions, stress loading, and seismic hazard. *Journal of Geophysical Research: Solid Earth*. 115(B12):B12320. doi:10.1029/2010jb007781.

Rhoades DA, Van Dissen RJ, Langridge RM, Little TA, Ninis D, Smith EGC, Robinson R. 2011. Re-evaluation of conditional probability of rupture of the Wellington-Hutt Valley segment of the Wellington Fault. *Bulletin of the New Zealand Society for Earthquake Engineering*. 44(2):77–86. doi:10.5459/bnzsee.44.2.77-86.

Stevens GR. 1990. Rugged landscape: the geology of central New Zealand, including Wellington, Wairarapa, Manawatu, and the Marlborough Sounds. Wellington (NZ): Department of Scientific and Industrial Research. 286 p. (DSIR information series; 169).

Stirling M, McVerry G, Gerstenberger M, Litchfield N, Van Dissen RJ, Berryman K, Barnes P, Wallace L, Villamor P, Langridge R, et al. 2012. National Seismic Hazard Model for New Zealand: 2010 update. *Bulletin of the Seismological Society of America*. 102(4):1514–1542. doi:10.1785/0120110170.

Van Dissen RJ, Barrell DJA, Litchfield NJ, Villamor P, Quigley M, King AB, Furlong K, Begg JG, Townsend DB, Mackenzie H, et al. 2011. Surface rupture displacement on the Greendale Fault during the M_w 7.1 Darfield (Canterbury) Earthquake, New Zealand, and its impact on man-made structures. In: *Proceedings of the Ninth Pacific Conference on Earthquake Engineering: building an earthquake resilient society*. 2011 Apr 14–16; Auckland, New Zealand. Auckland (NZ): 9PCEE. Paper 186.

Van Dissen RJ, Berryman KR. 1996. Surface rupture earthquakes over the last ~1000 years in the Wellington region, New Zealand, and implications for ground shaking hazard. *Journal of Geophysical Research: Solid Earth*. 101(B3):5999–6019. doi:10.1029/95JB02391.

Van Dissen RJ, Berryman KR, Webb TH, Stirling MW, Villamor P, Wood PR, Nathan S, Nicol A, Begg JG, Barrell DJA, et al. 2003. An interim classification of New Zealand's active faults for the mitigation of surface rupture hazard. In: *Proceedings of the 2003 Pacific Conference on Earthquake Engineering*. 2003 Feb 13–15; Christchurch, New Zealand. Wellington (NZ): New Zealand Society for Earthquake Engineering. Paper 155.

Van Dissen RJ, Heron DW. 2003. Earthquake Fault Trace Survey, Kapiti Coast District. Lower Hutt (NZ): Institute of Geological & Nuclear Sciences. 45 p. Client Report 2003/77. Prepared for Kāpiti Coast District Council.

Van Dissen RJ, Heron DW, Becker JS, King AB, Kerr JE. 2006. Mitigating active fault surface rupture hazard in New Zealand: development of national guidelines, and assessment of their implementation. In: *100th anniversary earthquake conference, April 18–22, 2006, San Francisco, California: proceedings*. Oakland (CA): Earthquake Engineering Research Institute. Paper 633.

Van Dissen RJ, Heron DW, Hinton S, Guerin A. 2004. Mapping active faults and mitigating surface rupture hazard in the Kapiti Coast District, New Zealand. In: Gregory G, editor. *Getting the message across and moving ahead: conference 2004 technical papers*. Rotorua, New Zealand. Wellington (NZ): New Zealand Society for Earthquake Engineering. Paper 21.

Van Dissen RJ, Litchfield NJ, Begg JG. 2005. Upper Hutt City fault trace project. Lower Hutt (NZ): Institute of Geological & Nuclear Sciences. 28 p. Client Report 2005/151. Prepared for Greater Wellington Regional Council, Upper Hutt City Council.

Van Dissen RJ, Rhoades DA, Little T, Litchfield NJ, Carne R, Villamor P. 2013. Conditional probability of rupture of the Wairarapa and Ōhariu faults, New Zealand. *New Zealand Journal of Geology and Geophysics*. 56(2):53–67. doi:10.1080/00288306.2012.756042.

Van Dissen RJ, Stahl T, King A, Pettinga JR, Fenton C, Little TA, Litchfield NJ, Stirling MW, Langridge RM, Nicol A, et al. 2019. Impacts of surface fault rupture on residential structures during the 2016 Mw 7.8 Kaikōura earthquake, New Zealand. *Bulletin of the New Zealand Society for Earthquake Engineering*. 52(1):1–22. doi:10.5459/bnzsee.52.1.1-22.

Williams DN. 1975. Ohariu Fault Zone at Porirua, Wellington, New Zealand. *New Zealand Journal of Geology and Geophysics*. 18(5):659–665. doi:10.1080/00288306.1975.10421566.

This page left intentionally blank.

APPENDICES

This page left intentionally blank.

APPENDIX 1 ACTIVE FAULT DEFINITIONS

A1.1 What is an Active Fault?

Active faults are those faults considered capable of generating strong earthquake shaking and/or ground-surface fault rupture. An active fault in New Zealand is generally defined as one that has deformed the ground surface within the past 125,000 years (Langridge et al. 2016). In part, this is defined, for practical reasons, as those faults that deform marine terraces and alluvial surfaces that formed during the 'Peak Last Interglacial period' or Marine Isotope Stage (MIS) 5e or younger (MIS 1–4; e.g. Alloway et al. 2007). For Wellington City, we therefore define active faults as those with evidence of activity in the last 125,000 years.

The purpose of this Appendix is to introduce how active faults express themselves, i.e. their behaviour, styles of deformation, activity and geomorphic expression. Active faults are typically expressed in the landscape as linear traces displacing surficial geologic features, which may include hillslopes, alluvial terraces and fans. The age of these displaced features can be used to define how active a fault is.

Active faults are often defined by a fault scarp or trace. A fault scarp is formed when a fault displaces or deforms the land surface or seafloor and produces an abrupt linear step, which smooths out with time to form a scarp (Figure A1.1). In some cases, where a fault moves horizontally, only a linear trace or furrow may be observed.

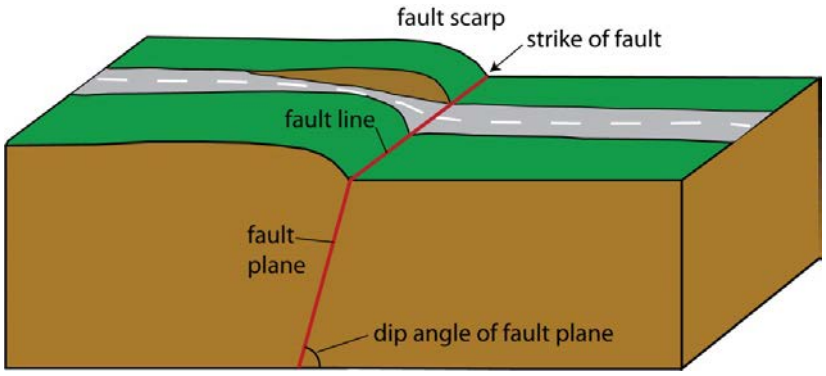

Figure A1.1 Block model of a generic active fault. Fault displacement produces a scarp along the projection of the fault plane at the Earth's surface (fault line or trace).

A1.2 Styles of Fault Movement

Faults can be categorised as: strike-slip faults, where the dominant style (sense) of motion is horizontal (movement in the strike direction of the fault); and dip-slip faults, where the dominant sense of motion is vertical (defined by movement in the dip direction of the fault).

Strike-slip faults are defined as either right-lateral (dextral), where the motion on the opposite side of the fault is to the right (Figure A1.2), or left-lateral (sinistral), where the opposite side of the fault moves to the left. The Wellington, Ohariu, Shepherds Gully and Moonshine faults are predominantly dextral strike-slip faults, except for the Terawhiti Fault, which also has a component of normal slip (see below for more details).

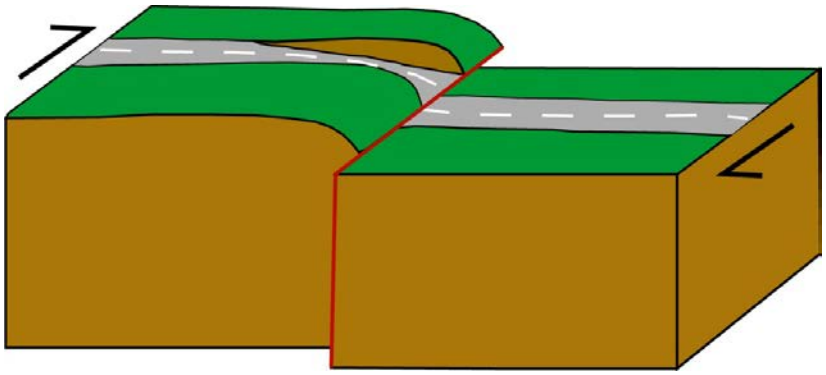

Figure A1.2 Block model of a strike-slip fault (red line). The fault is a right-lateral (dextral) fault, as shown by the black arrows and the sense of movement across the two blocks and a right separation across the road.

Dip-slip faults can be divided into reverse faults, formed mainly under contraction (where the hanging-wall block of the fault is pushed up; Figure A1.3), and normal faults, formed under extension (where the hanging-wall block of the fault drops down; Figure A1.4). The Aotea Fault is an example of a fault in WCC with a component of reverse dip-slip movement (Barnes et al. 2019).

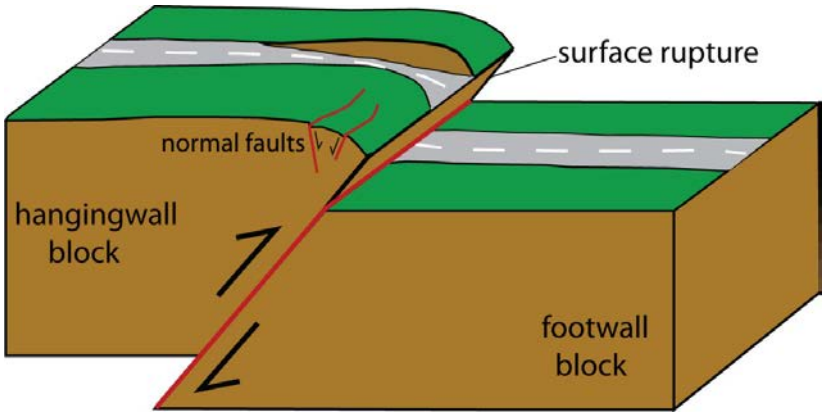

Figure A1.3 Block model of a reverse dip-slip fault that has recently ruptured. Movement of the blocks is vertical and in the dip direction of the fault plane. In this case, the hanging-wall block has been pushed up over the footwall block. Folding and normal faulting are common features of deformation in the hanging-wall block of reverse faults.

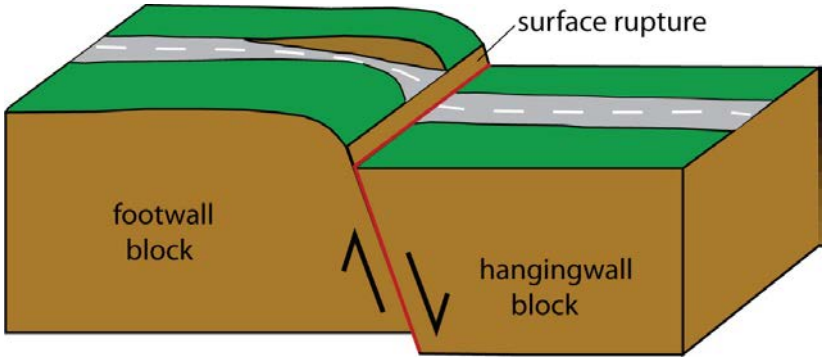

Figure A1.4 Block model of a normal dip-slip fault. The relative movement of the blocks is vertical and in the dip direction of the fault plane. The hanging-wall block has dropped down, enhancing the height of the fault scarp.

APPENDIX 2 IMPACTS OF SURFACE FAULT RUPTURE ON RESIDENTIAL STRUCTURES IN RECENT NEW ZEALAND EARTHQUAKES AND IMPLICATION FOR THE MITIGATION OF SURFACE FAULT RUPTURE HAZARD

A2.1 Introduction

The New Zealand Ministry for the Environment's active fault guidelines titled 'Planning for development of land on or close to active faults: A guideline to assist resource management planners in New Zealand' (Kerr et al. 2003) is the primary document providing guidance with regard to the mitigation of ground-surface fault rupture hazard. In these guidelines (hereafter referred to as the MfE Active Fault Guidelines), the recommended mitigation strategy is avoidance; however, engineering mitigation strategies are also permitted in appropriate circumstances, though little, if any, guidance is provided regarding what those engineering strategies and appropriate circumstances might be. This deficiency was largely the consequence of a lack of data. That is, at the time that the guidelines were issued, there were very few New Zealand examples to draw from where New Zealand engineered structures had been impacted by ground-surface fault rupture and the impacts of that rupture evaluated with regards to: (a) the characterisation of the ground strains and displacements generated by that surface rupture, (b) the structural damage the surface rupture produced and (c) possible engineering strategies that could be employed to mitigate that damage.

Since the MfE Active Fault Guidelines were published, there have been two large earthquakes in New Zealand that have generated ground-surface fault rupture that has directly impacted engineered buildings; the 2010 Darfield earthquake and the 2016 Kaikōura earthquake (Figure A2.1). Collectively, about two dozen buildings or residential-type structures were directly damaged by ground-surface fault rupture resulting from these two earthquakes. In this Appendix, we present approximately a dozen case-study examples from these two earthquakes, and the 1987 Edgecumbe earthquake also, illustrating the impacts surface fault rupture had on residential (or residential-type) structures. These examples provide insight into construction styles that could be employed, in suitable circumstances, to facilitate non-collapse performance resulting from surface fault rupture and, in certain instances, post-event functionality. We also provide comment on how these examples may enable a more nuanced application of the MfE Active Fault Guidelines in, again, appropriate circumstances.

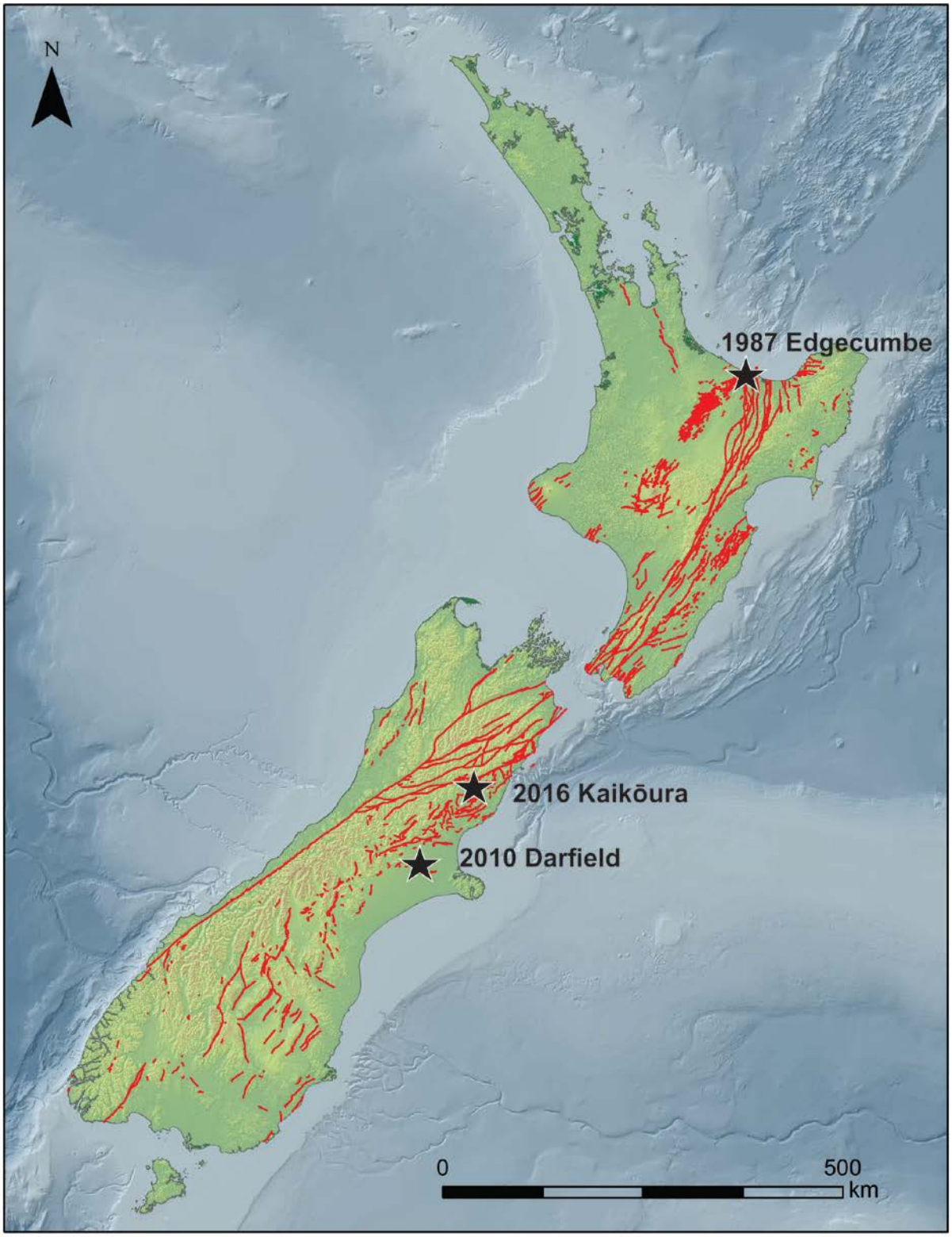

Figure A2.1 On-land known active faults of New Zealand (red lines) and epicentres of New Zealand's three most recent ground-surface-rupturing earthquakes (black stars): 1987 M_W 6.5 Edgecumbe earthquake, 2010 M_W 7.1 Darfield earthquake and 2016 M_W 7.8 Kaikōura earthquake. Active faults from Langridge et al. (2016).

A2.2 1987 Edgecumbe Earthquake

The Edgecumbe earthquake struck the Rangitaiki Plains, eastern Bay of Plenty, on 2 March 1987 (Figure A2.2). The earthquake had a magnitude of M_L 6.3, and generated metre-scale ground-surface fault rupture along the Edgecumbe Fault (maximum displacement, 2.5 m vertical and 1.8 m extension) (Figures A2.3 and A2.4) and decimetre- to centimetre-scale surface rupture displacement on several other nearby faults (Anderson and Webb 1989, Beanland et al. 1989, Nairn and Beanland 1989). The predominant sense of displacement on all these faults was normal.

Damage to residential structures caused by the Edgecumbe earthquake was primarily the result of strong ground shaking and, subordinately, liquefaction (e.g. Pender and Robertson 1987). However, ground-surface fault rupture along the Edgecumbe Fault did extend through and severely damage the concrete yards of two milking sheds in the McCracken Road area (Figures A2.5 and A2.6). The impact that Edgecumbe Fault ground-surface rupture had on these yards provides an informative illustration of the severe structural damage that could be expected to result from metre-scale normal fault rupture extending though a lightly reinforced concrete slab foundation of a residential structure.

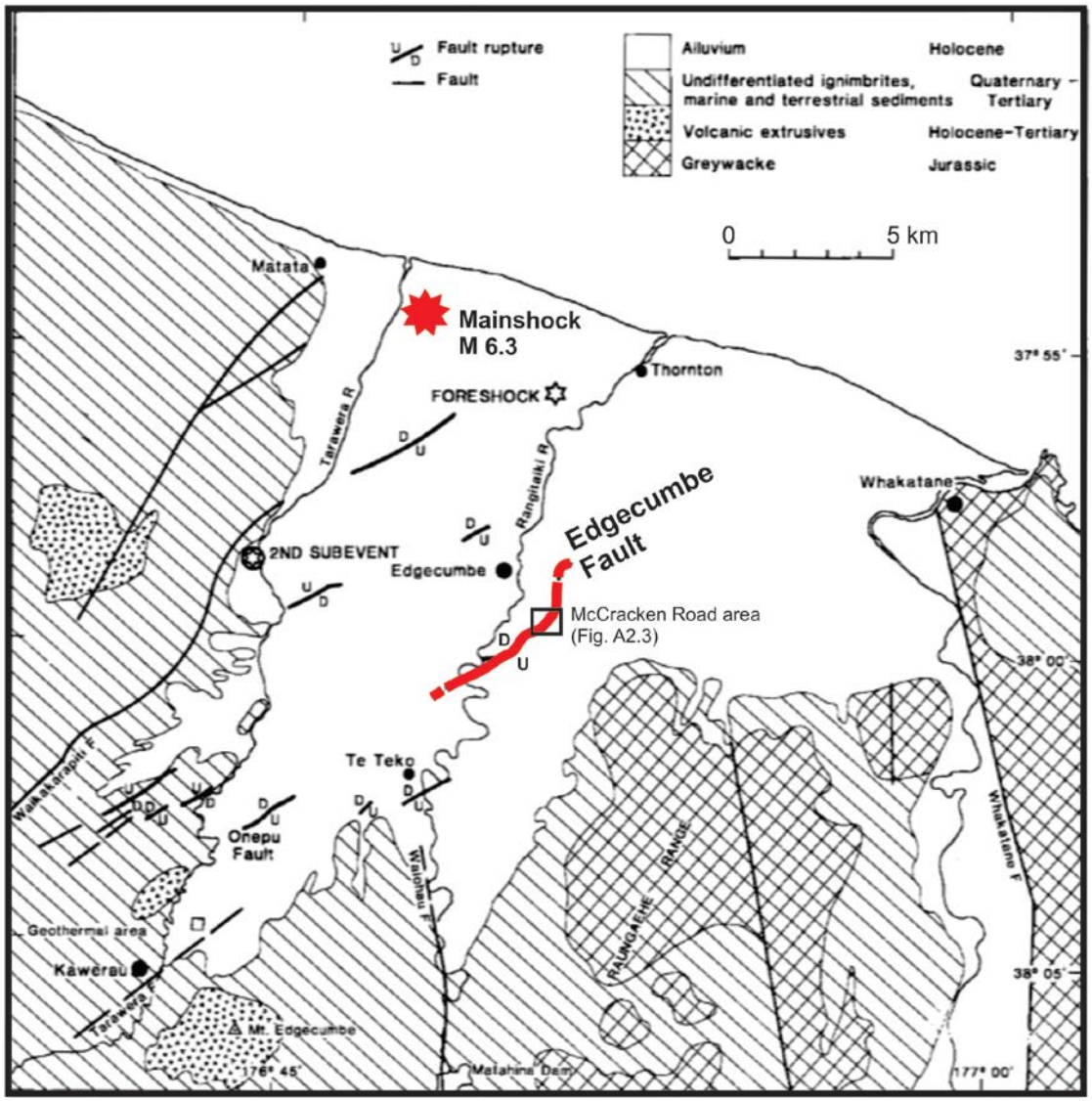

Figure A2.2 Edgecumbe earthquake: 2 March 1987, M_W 6.5 (M_L 6.3). Map shows location of mainshock epicentre (red star) and Edgecumbe Fault rupture (red line). Also shown is the location of the McCracken Road area depicted in Figure A2.3. After Figure 1 of Anderson and Webb (1989).

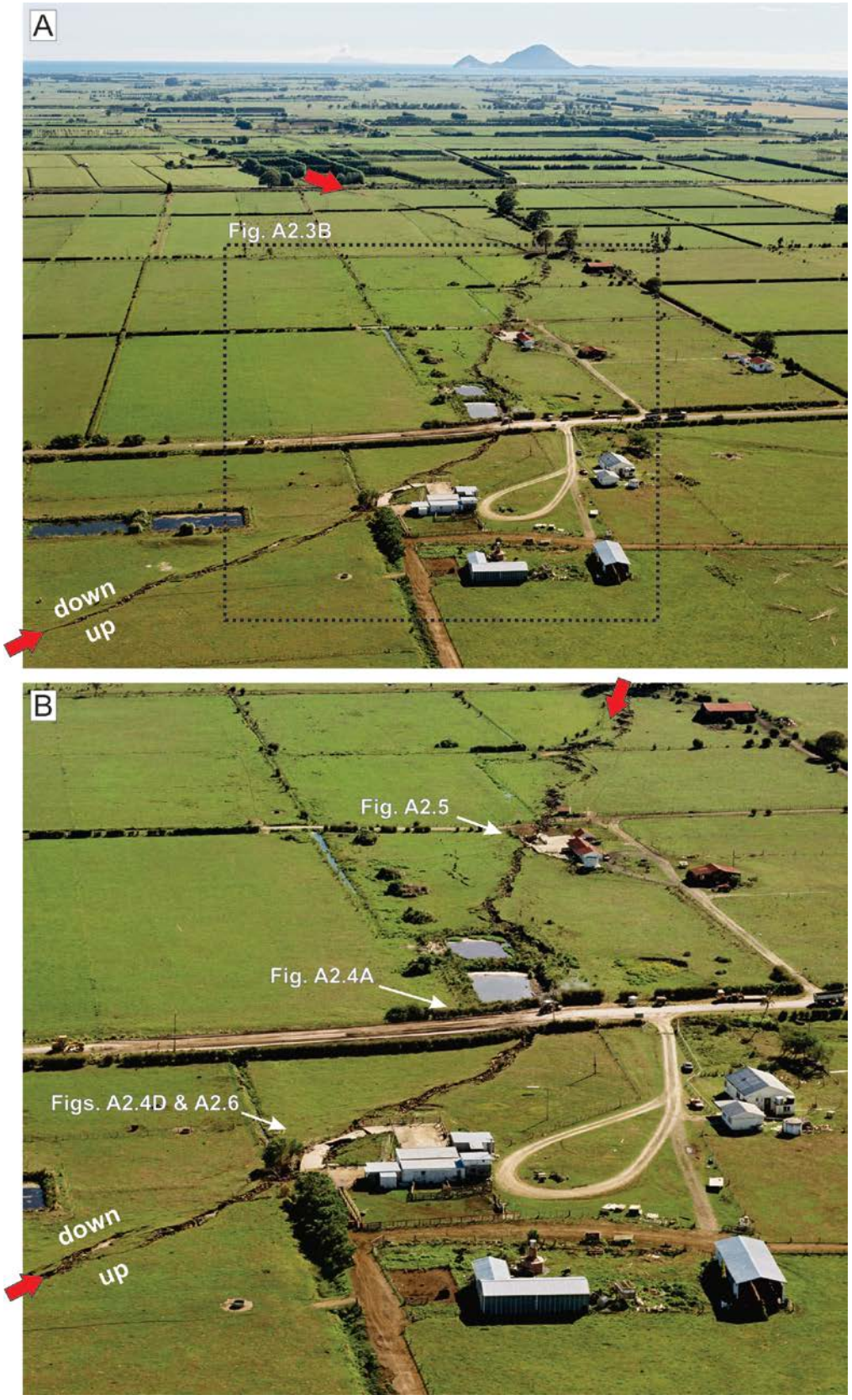

Figure A2.3 Edgecumbe Fault ground-surface rupture (red arrows) in the McCracken Road area, 1987 Edgecumbe earthquake. (A) Oblique aerial view looking northeast. (B) Enlarged portion of (A), showing locations of Figures A2.4A, D; A2.5; and A2.6. Photos by Lloyd Homer.

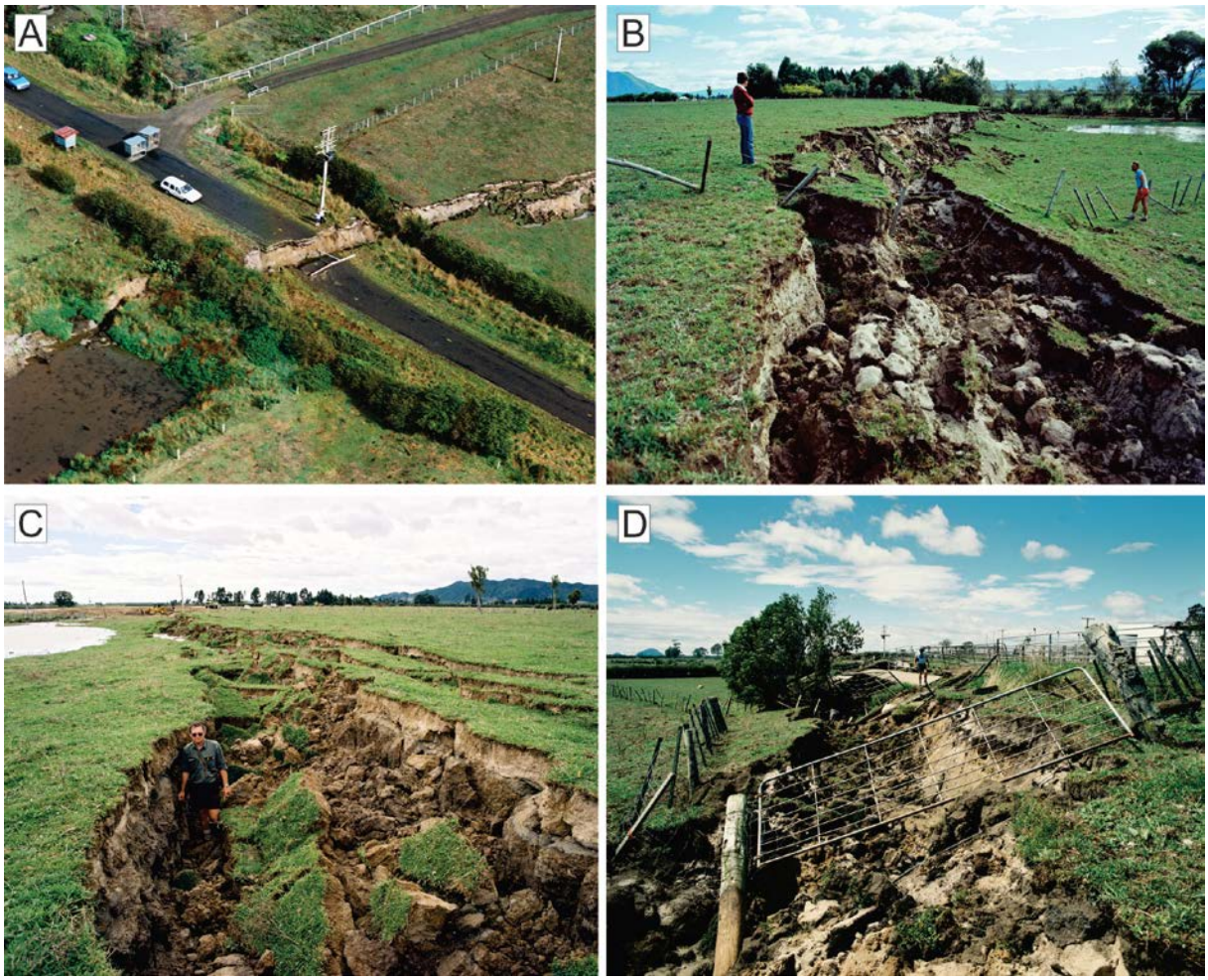

Figure A2.4 Examples of metre-scale normal ground-surface fault rupture along the Edgecumbe Fault, 1987 Edgecumbe earthquake. Photos by Lloyd Homer.

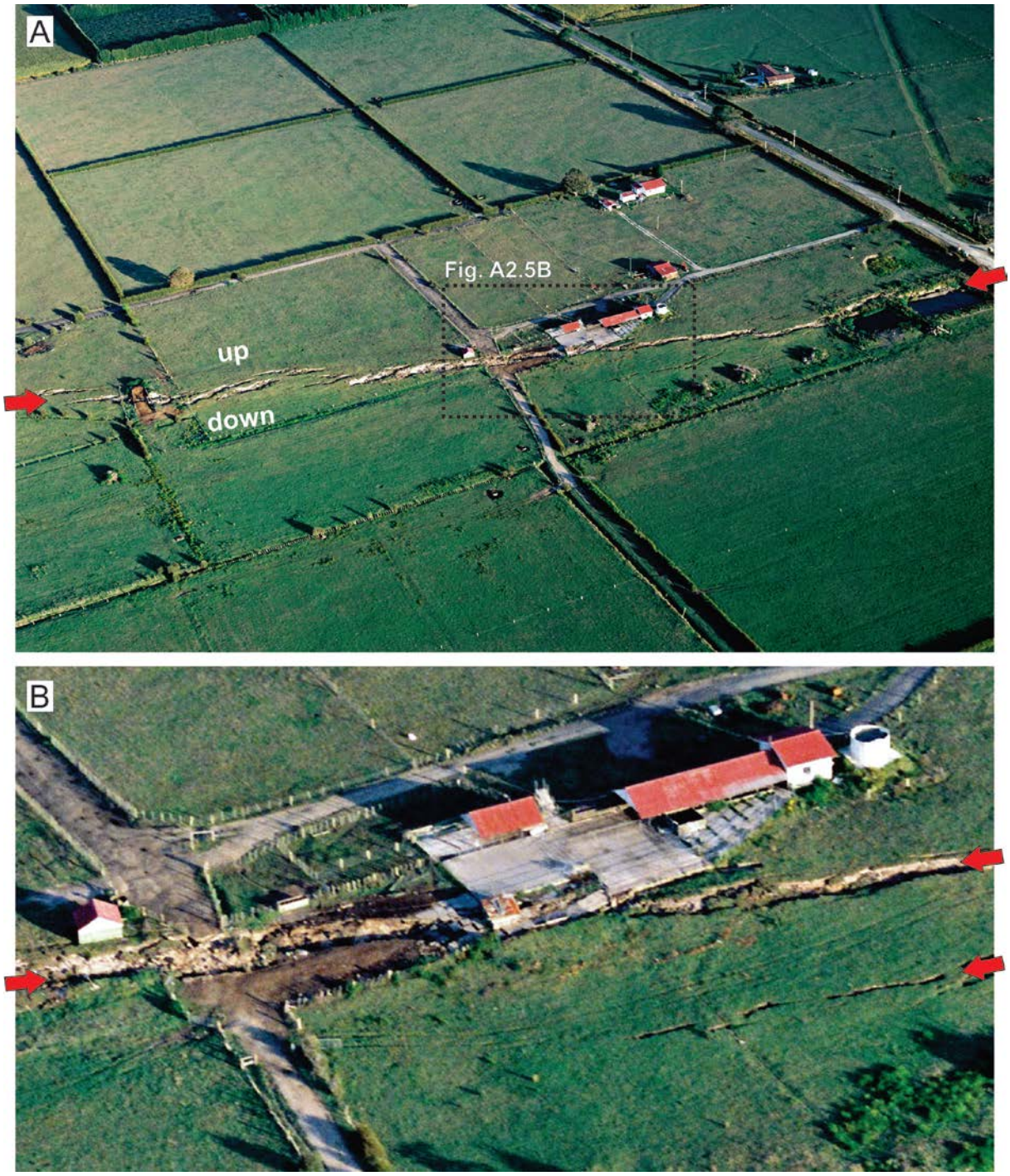

Figure A2.5 Edgecumbe Fault ground-surface rupture (red arrows) and damage to concrete yard of milking shed north of McCracken Road, 1987 Edgecumbe earthquake. (A) Oblique aerial view looking east-southeast. (B) Enlarged portion of (A). See Figure A2.3B for location. Photos by Lloyd Homer.

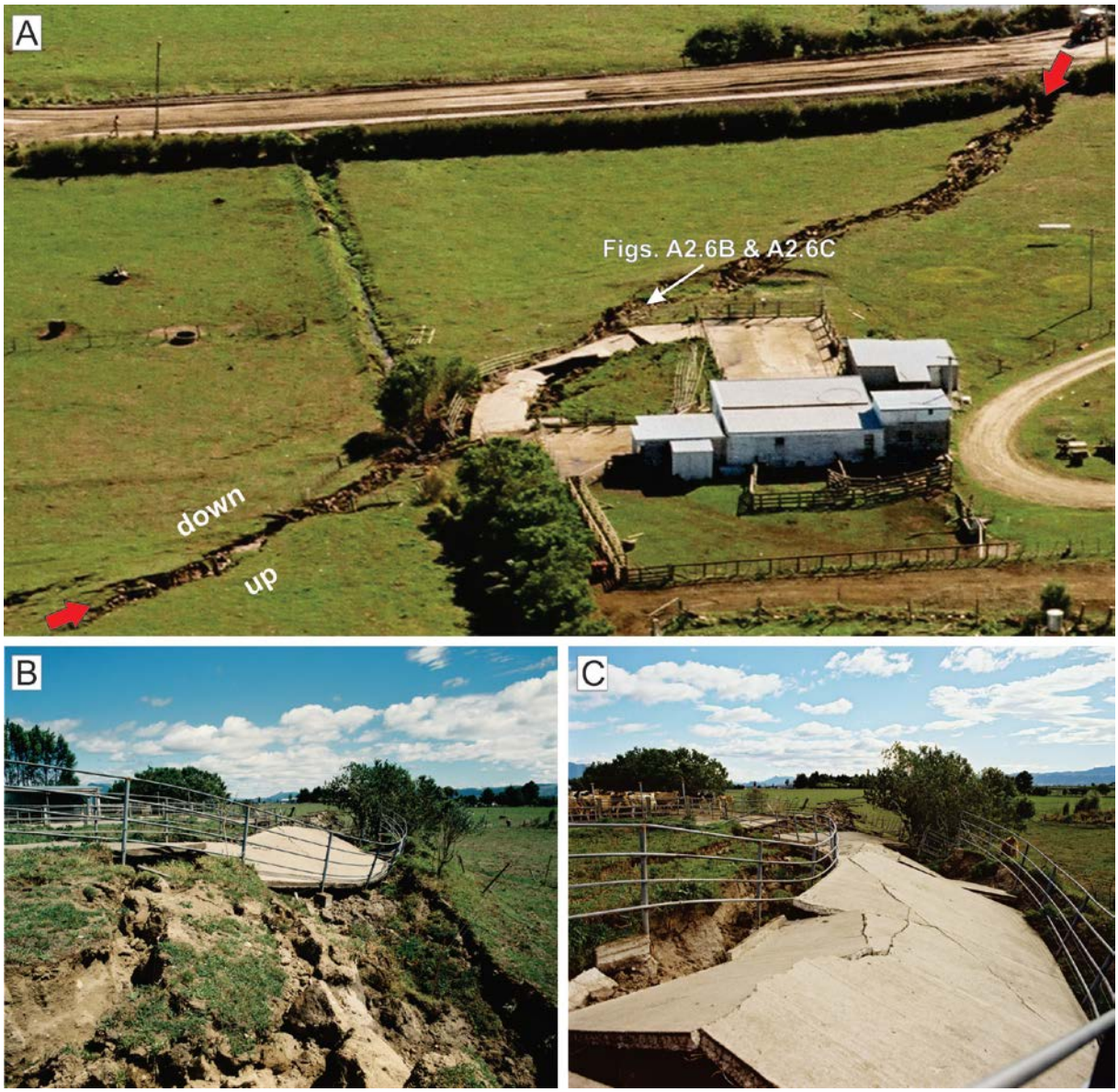

Figure A2.6 Edgecumbe Fault ground-surface rupture (red arrows) and damage to concrete race of milking shed south of McCracken Road, 1987 Edgecumbe earthquake. (A) Oblique aerial view looking northeast. See Figure A2.3B for location. (B, C) Details of reinforced concrete milking shed race damaged by metre-scale normal fault rupture. Views looking west-southwest. Photos by Lloyd Homer.

A2.3 2010 Darfield Earthquake

Much of the material presented in this section comes from Van Dissen et al. (2011).

A2.3.1 Introduction

The M_W 7.1 Darfield earthquake of 4 September 2010 had a shallow focus (~11 km deep) and an epicentre located within ~40 km west of Christchurch (Figure A2.7). It was a complex event, involving rupture of multiple fault planes with most of the earthquake's moment release resulting from slip on the previously unknown Greendale Fault (Beavan et al. 2010, Gledhill et al. 2010, Holden et al. 2011). Greendale Fault rupture propagated to the ground surface and extended east–west for ~30 km (Quigley et al. 2010, 2012). Surface rupture was mainly dextral strike-slip (Figures A2.7–A2.9).

About a dozen buildings, mainly single-storey houses and farm sheds, were affected by Greendale Fault ground-surface rupture but none collapsed, largely because most of the buildings were relatively flexible and resilient timber-framed structures and also because deformation was distributed over a relatively wide zone. In this section of the Appendix, we present a summary of the characteristics of Greendale Fault surface rupture deformation and the impacts this deformation had on residential (or residential-type) structures.

A2.3.2 Greendale Fault Surface Rupture Displacement and Expression

A variety of methods were used to map and characterise the Greendale Fault surface rupture, including tape and compass, GPS surveys, aerial photography, airborne LiDAR and shallow excavations (Quigley et al. 2010, 2012; Duffy et al. 2013; Hornblow et al. 2014). The zone of Greendale Fault ground-surface rupture deformation extends for about 30 km from ~4 km west of the hamlet of Greendale (from which the fault gets its name) to an eastern tip ~2 km north of the town of Rolleston (Figure A2.7). The gross morphology of the surface rupture is that of an *en-echelon* series of east–west-striking, left-stepping surface traces (Figures A2.7 and A2.8). The largest step-over is ~1 km wide, and there is a multitude of smaller ones. Push-up 'bulges' formed at most of these restraining left-steps, with amplitudes up to ~1 m but typically less than 0.5 m (Figure A2.8B, C).

Displacement along the full length of surface rupture averages ~2.5 m (predominantly dextral) with maximum of ~5 m along the central section of fault trace. Perpendicular to the strike of the Greendale Fault, surface rupture displacement is distributed across a ~30–300-m-wide deformation zone, largely as horizontal flexure. The width of the surface rupture deformation zone is greatest at step-overs and damaging ground strains developed within these. On average, 50% of the horizontal displacement occurs over 40% of the total width of the deformation zone, with offset on discrete shears, where present, typically accounting for less than about 30% of the total displacement. Across the paddocks deformed by fault rupture, there is a threshold of surface rupture displacement of ~1–1.5 m; greater than this discrete ground cracks and shears occur and form part of the surface rupture deformation zone and less than this they are rarely present. The distributed nature of Greendale Fault surface rupture displacement undoubtedly reflects a considerable thickness of poorly consolidated alluvial gravel deposits underlying the Canterbury Plains at this location.

A2.3.3 Engineered Structures Impacted by Surface Fault Rupture

About a dozen buildings, typically single-storey timber-framed houses and farm sheds with lightweight roofs, lay either wholly, or partially, within the Greendale Fault's surface rupture deformation zone (Figures A2.7, A2.8, A2.10–A2.13). None of these buildings collapsed, but all were more damaged than comparable structures immediately outside the zone of surface rupture deformation. From a life-safety standpoint, all these buildings performed satisfactorily, but, with regard to post-event functionality, there are notable differences. Houses with only lightly reinforced concrete slab foundations suffered moderate to severe structural and non-structural damage. Three other buildings performed more favourably: one had a robust concrete slab foundation, another had a shallow-seated pile foundation that isolated ground deformation from the superstructure, and the third had a structural system that enabled the house to tilt and rotate as a rigid body. Below, we present four informative case-study examples.

A2.3.3.1 Telegraph Road House – Greendale Fault

The Telegraph Road house (Figure A2.10) was a timber-framed, brick-clad residential structure with a concrete slab foundation (at most, only lightly reinforced) and lightweight roof. It was located within the Greendale Fault's ground-surface fault rupture deformation zone (~150 m wide at this site) that accommodated a total of 4–5 m of dextral displacement. The house was badly damaged by distributed deformation, and ~0.5 m of discrete strike-slip rupture that entered the house through the front door (Figure A2.10B) passed through the house's foundation (including living room) and exited through the back door (Figure A2.10D).

Not long after the earthquake, this house was demolished and a new one constructed nearby.

A2.3.3.2 Kivers Road Woolshed – Greendale Fault

The Kivers Road woolshed was a timber-framed structure located within a 25–50-m-wide ground-surface fault rupture deformation zone of the Greendale Fault. At this site, surface fault rupture deformation comprised both discrete shears and distributed deformation and accommodated ~2.7 m of net slip (predominantly strike-slip) (Figure A2.11). The woolshed was made up of two parts, a larger metal-clad structure with a timber floor founded on shallow-seated ~700-mm-high concrete piles (Figure A2.11D) and a smaller lean-to structure attached to the side (Figure A2.11A, C). The lean-to was a pole building (part metal-clad and part wood-clad) with an unreinforced concrete floor. The response of the two different construction styles to surface fault rupture was noticeably different. The support poles of the lean-to were set into the ground; dextral fault rupture under the lean-to led to lateral displacement of the support poles on either side of the rupture and significant distortion of the walls and roof (Figure A2.11C). In contrast, surface rupture deformation under the larger piled structure was, in large measure, isolated from the superstructure by rotation of the shallow-seated piles. The timber flooring and framing and metal cladding proved a resilient structural system that limited internal distortion.

This woolshed has subsequently been demolished.

A2.3.3.3 Greendale Substation – Greendale Fault

The Greendale substation (Figure A2.12) is a light-industrial building with a reportedly well-reinforced concrete slab foundation. During the Darfield earthquake, the building was tilted and rotated, but relatively undamaged by ~1.7 m dextral and < 1 m vertical displacement (south-side up) distributed across a ~100-m-wide surface rupture deformation zone of the Greendale Fault. The long axis of the building is oriented ~55° counter-clockwise to the general strike of the fault rupture. Distributed displacement imposed tensile ground strains across the site with an orientation roughly sub-parallel to the building's long axis. The foundation of the building was robust enough to resist these strains (i.e. no cracking of the foundation was evident) and, instead, the soil pulled away from either end of the building's foundation (yellow 't' in Figure A2.12C, D).

The Greendale substation is still in service today, ten years after the Darfield earthquake and the Greendale Fault's ground-surface rupture.

A2.3.3.4 Gillanders Road House – Greendale Fault

The Gillanders Road house (Figure A2.13) is a light-gauge steel-framed, plywood- and weatherboard-clad residential structure with a steel pile foundation, steel I-beam bearers, steel joists and plywood flooring. As a result of Greendale Fault ground-surface rupture,

the house was tilted and rotated, but only slightly damaged, by ~1 m of distributed vertical and dextral fault rupture spread over several tens of metres width. Despite this house being essentially 'locked' into the ground (piles are concreted to ~1 m depth into the ground), it suffered only slight damage because surface rupture deformation was distributed and relatively evenly spread across the site, and because the structural system was strong and stiff enough to tilt and rotate as a rigid body. Given this structure's resilient, and somewhat uncommon, construction style, it proved a relatively straightforward process to reinstate.

This building was subjected to both ground-surface fault rupture and strong ground shaking and performed in a fashion that not only greatly exceeded life-safety objectives, but also greatly facilitated post-event reinstatement. However, if the building had been subjected to greater amounts of deformation, especially discrete displacement, the pile foundation may have been able to transfer enough deformation into the superstructure to damage it. Design modifications to potentially mitigate this, yet still retain the building's noteworthy resilience, could be to: (1) use piles specifically designed to yield during surface fault rupture; and/or (2) use two sets of bearers, with one set attached to the piles and oriented parallel to the strike of the fault and another orthogonal set on top, onto which the floor joists are attached. With due geological and engineering consideration, both of these options (and conceivably others) could potentially be employed to successfully isolate ground rupture from the superstructure and still retain the advantageous ease of re-levelling qualities of this type of construction.

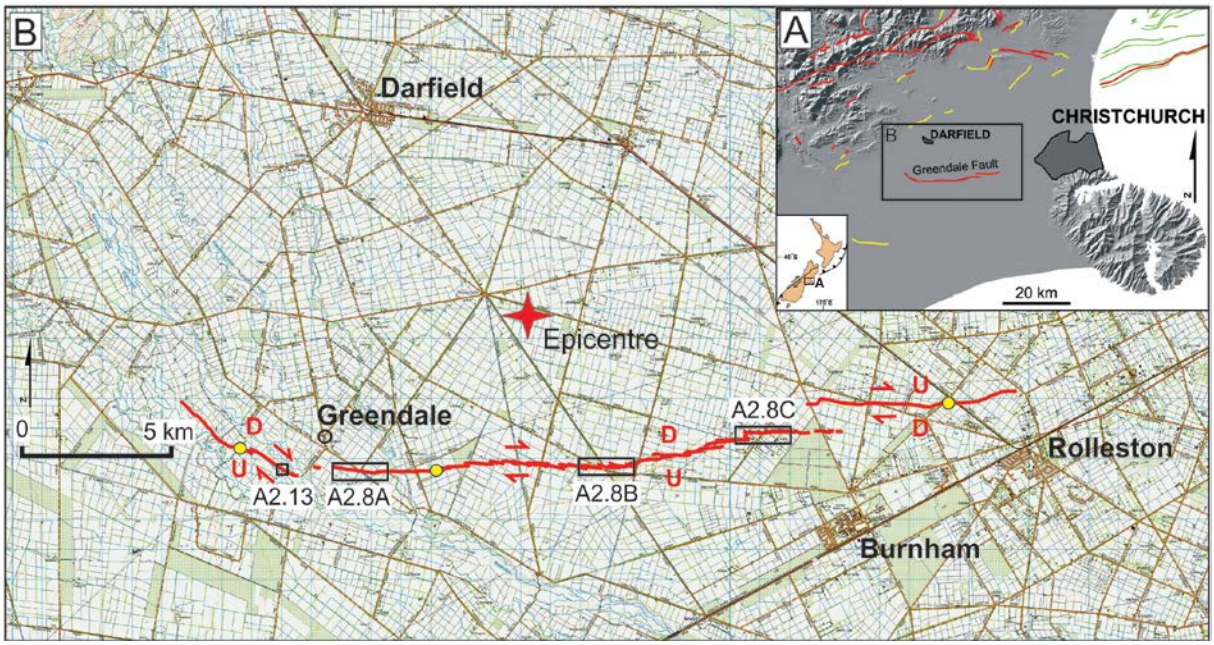

Figure A2.7 (A) Digital Elevation Model (DEM) of the Christchurch area of the Canterbury region showing locations of the Greendale Fault and other known tectonically active structures. Red lines are active faults, and yellow and green lines are, respectively, on-land and offshore active folds (combined data from Forsyth et al. [2008] and GNS Active Faults Database, http://data.gns.cri.nz/af/). (B) Mapped surface trace of the Greendale Fault (Quigley et al. 2010). Red arrows indicate relative sense of lateral displacement, while vertical displacement is denoted by red U = up and D = down. Also shown are locations of Figures A2.8A–C and A2.13, Darfield earthquake epicentre (red star; Gledhill et al. 2010) and buildings damaged by surface fault rupture (yellow dots) that are neither encompassed by Figure A2.8 nor depicted elsewhere in this Appendix.

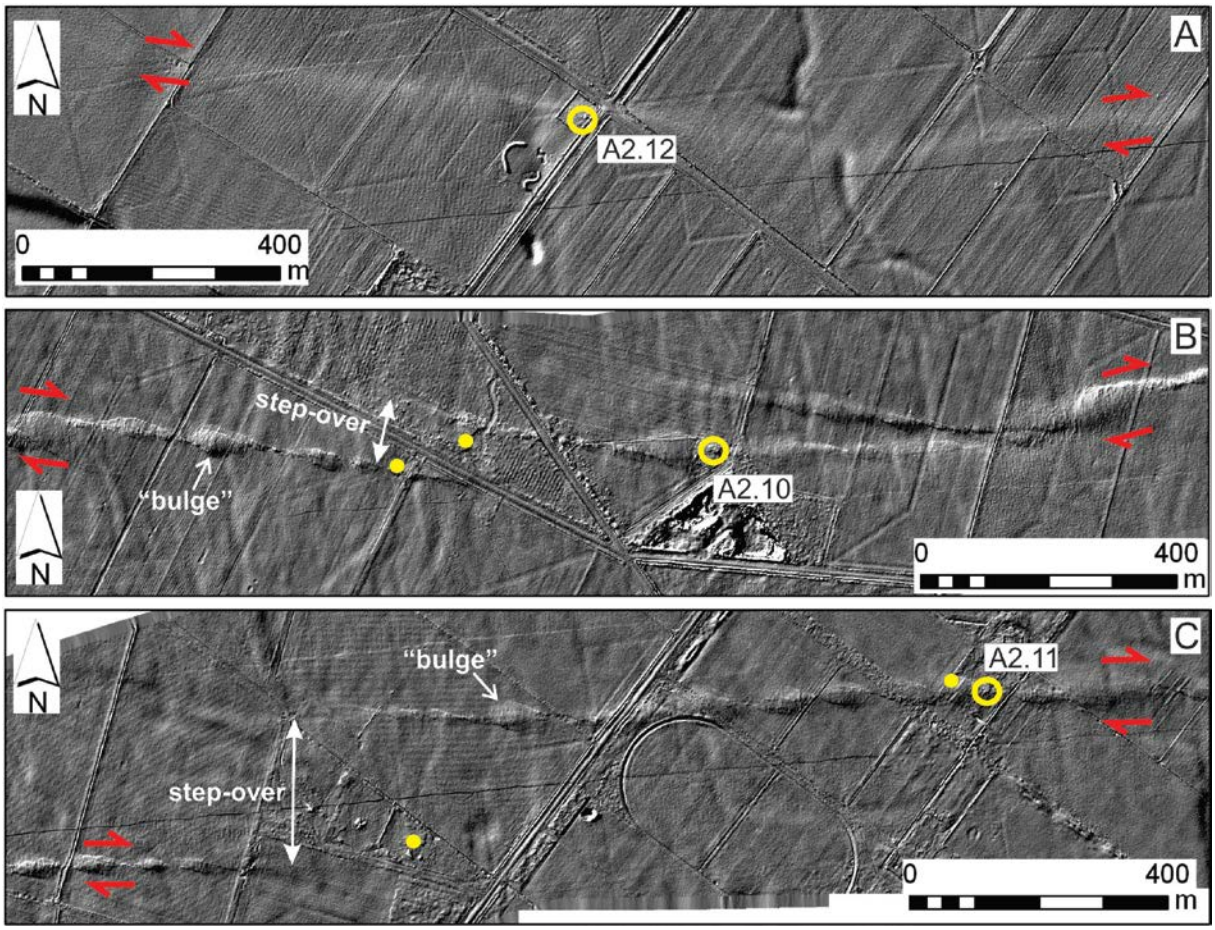

Figure A2.8 LiDAR hillshade DEMs (illuminated from the northwest) of three ~1.8-km-long sections of the Greendale Fault (see Figure A2.7 for locations), showing characteristic left-stepping *en-echelon* rupture pattern (especially evident in B and C) and dextral offset of roads, fences, irrigation channels, hedges and crop rows. Red arrows straddle the surface fault rupture and show the sense of lateral displacement. Representative examples of fault step-overs and push-up 'bulges' are identified in B and C. Open yellow circles show the locations of buildings damaged by surface fault rupture that are depicted in Figures A2.10–A2.12. Small yellow dots show the locations of other buildings damaged by surface rupture deformation that are not discussed in this appendix. The general amount of net surface rupture displacement in A, B and C is, respectively, 1.5–2.5 m (horizontal to vertical ratio ~3:1, south-side up), 4–5 m (predominantly dextral) and 2.5–4 m (predominantly dextral).

Figure A2.9 Examples of metre-scale dextral strike-slip ground-surface fault rupture along the Greendale Fault, 2010 Darfield earthquake.

Figure A2.10 Telegraph Road house and Greendale Fault surface rupture; see Figures A2.7 and A2.8 for location. Red arrows denote location of discrete surface fault rupture. (A) Aerial view looking south. Photo by Richard Cosgrove. (B) View looking west-northwest. Photo by Hayden Mackenzie. (C) View looking south-southwest. Photo by Hayden Mackenzie. (D) View looking east-southeast. Photo by Dougal Townsend.

Figure A2.11 Kivers Road woolshed and Greendale Fault surface rupture; see Figures A2.7 and A2.8 for location. Red arrows denote location of discrete surface fault rupture. (A) Aerial view looking northeast – note dextral offset of irrigation channel in right-hand side of photograph. Photo by Richard Cosgrove. (B) View looking west. Photo by Dougal Townsend. (C) View looking east. Photo by Dougal Townsend. (D) View looking southwest showing detail of shallow-seated concrete piles. Photo by Russ Van Dissen.

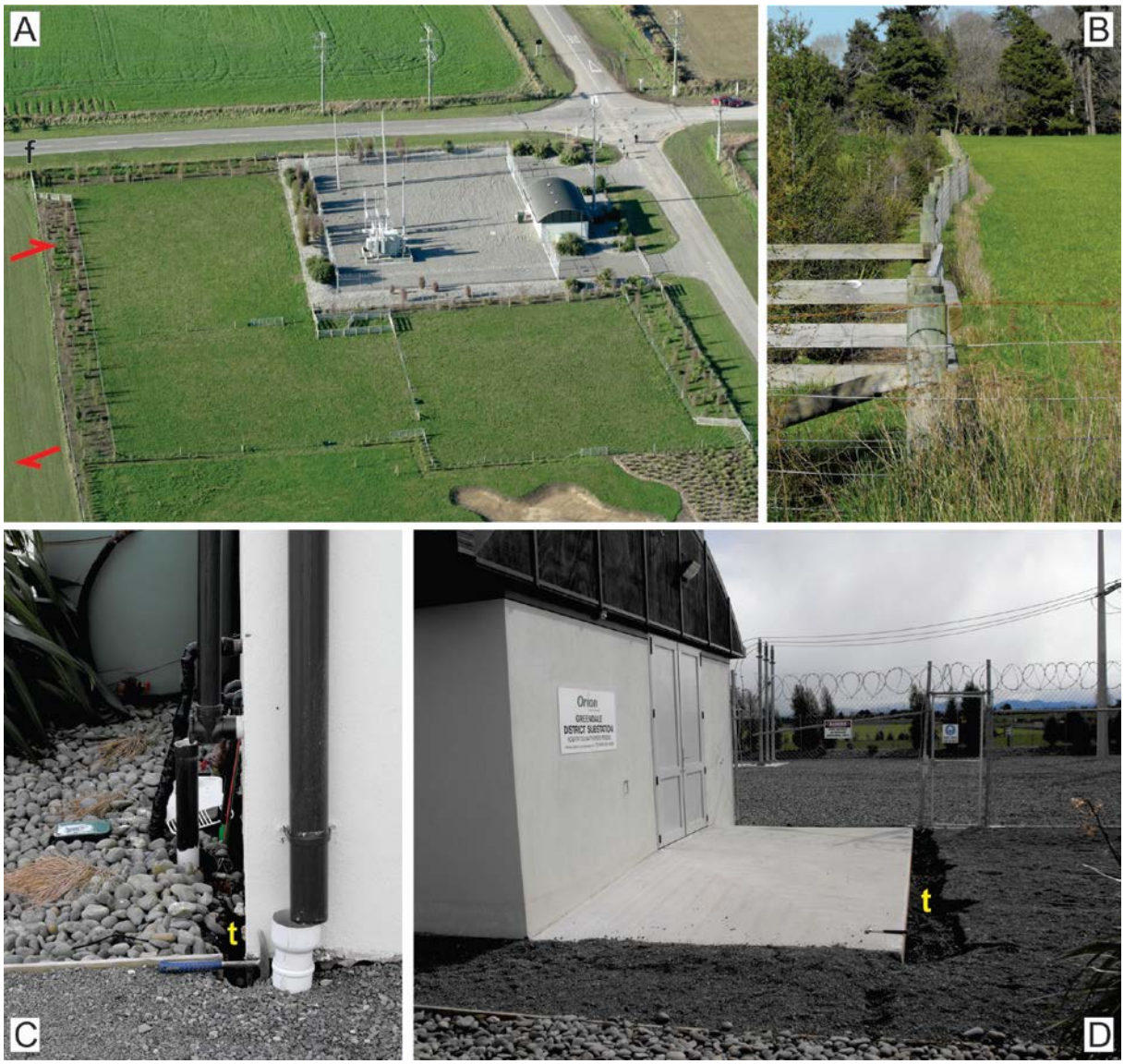

Figure A2.12 Greendale substation and Greendale Fault surface rupture; see Figures A2.7 and A2.8 for location. (A) Aerial view looking northeast. Red arrows denote location, strike and sense of lateral displacement of the surface rupture deformation zone. Photo by Richard Jongens. (B) View looking southwest along fence line adjacent to the substation that crosses the surface rupture deformation zone and records the amount, width and distributed style of fault displacement here (camera location for B is shown by black 'f' in A). Photo by Russ Van Dissen. (C, D) Views looking northwest. 't' is where soil has pulled away from the building's foundation. See text for details. Photos by Russ Van Dissen.

Figure A2.13 Gillanders Road house and Greendale Fault surface rupture; see Figure A2.7 for location. (A) View looking east. (B) View looking northwest. (C) Close-up of detached down-pipe on east-southeast side of the house. View looking west-northwest. (D) Close-up of pile, bearer and deformed bolted connection. View looking west-northwest. Photos by Russ Van Dissen.

A2.4 2016 Kaikōura Earthquake

Much of the material presented in this section comes from Van Dissen et al. (2019).

A2.4.1 Introduction

The Kaikōura earthquake struck at two minutes past midnight on 14 November 2016. Its epicentre was located near the South Island township of Waiau (Figure A2.14) and, with a magnitude of M_W 7.8, it was the largest on-land earthquake to hit New Zealand in more than a century (Downes and Dowrick 2014). The Kaikōura earthquake generated damaging levels of ground shaking throughout much of north Canterbury, eastern Marlborough and beyond (Bradley et al. 2017; Kaiser et al. 2017). It triggered thousands of landslides (Dellow et al. 2017; Massey et al. 2018) and locally significant liquefaction (Cubrinovski et al. 2017; Stringer et al. 2017; Bastin et al. 2018). The earthquake caused vertical deformation, primarily uplift, along more than 100 km of coastline between Cape Campbell and the Hundalee Fault south of Kaikōura (Clark et al. 2017) (Figure A2.14) and spawned a tsunami with up to ~7 m run-up height – the impacts of which were lessened by the fact that the earthquake occurred at low tide and much of the potentially affected coastline had been uplifted (Power et al. 2017).

In a global context, the Kaikōura earthquake was also one of the most complex earthquakes yet documented, with about two dozen major and minor faults rupturing the ground surface (Figure A2.14) (Hamling et al. 2017; Stirling et al. 2017; Litchfield et al. 2018). Collectively, over 220 km of surface fault rupture was generated by the Kaikōura earthquake (Figure A2.14). This rupture directly impacted several residential (or residential-type) structures. In this section of the Appendix, we document several examples of the impacts this surface fault rupture had on these buildings.

A2.4.2 Residential Structures Impacted by Surface Fault Rupture

About a dozen buildings, mostly single-storey timber-framed houses, barns and woolsheds, were directly impacted by surface fault rupture in the Kaikōura earthquake. Here we present seven instructive case-study examples.

A2.4.2.1 Bluff Cottage – Kekerengu Fault

Of the residential structures impacted by surface fault rupture during the Kaikōura earthquake, Bluff Cottage (Figures A2.15 and A2.16) deserves special mention because of its noteworthy life-safety (non-collapse) performance when subjected to extreme surface fault rupture deformation. Bluff Cottage – which has since been demolished – was a timber-framed single-storey residential structure (house) with a corrugated metal roof and a combination of timber weatherboard and concrete brick cladding. It had a roughly rectangular floor plan (area of ~90 m^2), a timber floor comprising a combination of particle board sheets and tongue and groove hardwood strips/planks and a pre-cast concrete chimney and fireplace (with some steel-rod reinforcing) encased by concrete brick. It had a concrete perimeter foundation with shallow-seated concrete piles. The timber floor joists were skew-nailed to the timber wall plates, which were in turn bolted to the perimeter foundation, and the timber floor bearers were attached to the piles via wire ties.

The age of construction of Bluff Cottage is composite, and not known in detail. The original hut that formed the core of the cottage was constructed prior to the late 1940s (the oldest set of aerial photographs for this part of the country date from 1947 and show that the hut was already in existence). Later, in the late 1970s / early 1980s, a kitchen and sitting room were

added, along with the concrete perimeter foundation. Bluff Cottage was sited on a relatively thin layer (<1–2 m thick) of Holocene loosely packed gravel-dominated Kekerengu River alluvium overlying weak, fault-damaged, bedrock.

Approximately 10 m of discrete (i.e. concentrated, as opposed to distributed) horizontal and 1–2 m vertical surface fault rupture displacement extended through the footprint of Bluff Cottage on the Kekerengu Fault (Figure A2.16) (Kearse et al. 2018). Offset fence lines within ~450 m either side of the cottage also document lateral displacements of ~10–11 m and narrow fault deformation zone widths (Figures A2.15 and A2.17). The foundation of Bluff Cottage was cut in half and displaced by fault rupture. The superstructure of the house was low mass, flexible, regular in shape, timber-floored and relatively weakly attached to the foundation. These properties allowed the superstructure to detach from the mainly laterally displacing foundation and isolate it from the extreme ground deformation taking place beneath. The house suffered severe structural damage, but it did not collapse. From a life-safety perspective, and considering the large displacement and small fault zone width at this site (i.e. metre-scale strike-slip displacements and shear strains in the order of 10^0), this house performed admirably.

A2.4.2.2 Harkaway Villa – Papatea Fault

Harkaway Villa is a timber-framed single-storey house with timber weatherboard cladding and a corrugated metal roof on framed rafters, with internal load-bearing walls (Figures A2.14, A2.18–A2.20). It has a roughly square floor plan (area of ~130 m^2), timber strip (plank) flooring and a timber pile foundation (~60 cm above ground), with joists attached to piles via wire ties and skew nails.

The age of construction of Harkaway Villa is composite. It was built around 1910. About a hundred years later, in 2009, it was moved onto the site (in three pieces) and, at this time, significant renovations were undertaken. The villa is sited on several metres of late Holocene fan alluvium (comprising interbedded silt, sand and loosely packed gravel) which, in turn, likely overlies gravel-dominated Clarence River alluvium.

Harkaway Villa is located within the surface rupture deformation zone of the Papatea Fault which, at this site, is ~90 m wide, comprising both discrete fault rupture and distributed deformation and accommodating ~5 m of vertical deformation (reverse, southwest-side up) and a comparable (or lesser) amount of left-lateral horizontal slip (Figures A2.18–A2.20) (Langridge et al. 2018). The villa is situated ~200 m west from the true-right bank of the Clarence River on the hanging-wall side (southwest side) of the Papatea Fault in the hinge zone between the higher vertical displacement gradient fold/fault scarp to the northeast and the lower vertical displacement gradient ‘back limb’ to the southwest (Figure A2.20). The ground encompassed by the footprint of the structure experienced decimetre-scale folding, horizontal sinistral flexure (i.e. fault drag) and up to ~80 cm of distributed N–S-oriented extension (Figures A2.19 and A2.20). The villa was also tilted ~5° in a down-to-the-NE sense. Fortunately, the superstructure of the house is low mass, flexible, regular in shape, timber-floored and relatively weakly attached to the pile foundation, all of which allowed the superstructure to detach from the foundation and thus isolate much of the ground extension from the superstructure. Despite this house suffering damage significant enough to be ‘red-tagged’, it performed commendably, from a life-safety perspective. It experienced very strong ground shaking, local decimetre-scale surface fault rupture deformation and is located within the hinge zone of a reverse fault scarp that has been classified in other earthquakes as a zone of ‘severe building damage’ (Kelson et al. 2001), yet the villa did not collapse. Not only

did it not collapse, it appears that it could potentially be re-piled and re-levelled, suggesting the possibility of post-event reinstatement (as opposed to demolition and reconstruction).

As stated above, and illustrated in Figure A2.20, Harkaway Villa is located in the transition zone between the higher strain fold/fault scarp to the northeast and the lower strain 'back limb' to the southwest. Utilising a combination of field observations, a differential LiDAR digital elevation model (DEM; 2013 LiDAR subtracted from post-earthquake 2016 LiDAR) at the site (Figure A2.20B, C) and assuming simple shear, ground strains at the villa site can be approximated.

At the steepest portion of the fold/fault scarp region to the northeast of the villa, dip-slip shear strains of ~0.2–0.4 can be derived based on ~1.5 m of elevation gain over 7 m of fault-perpendicular horizontal distance (Figure A2.20C), an estimated/observed fault dip of 45˚–90˚ (Langridge et al. 2018) and assuming simple shear. Strike-slip shear strains of ≤0.2 can be estimated based on an observed horizontal-to-vertical ratio of displacement of ≤1 (Langridge et al. 2018), ~1.5 m of elevation gain over 7 m of fault-perpendicular horizontal distance and assuming simple shear. Based on the above dip-slip and strike-slip shear strain considerations, net shear strains oriented parallel to the plane of the fault of ~0.2–0.4 (rounded to 10^{-1}) are approximated in the region of the fold/fault scarp.

In the 'back limb' area, dip-slip shear strains of ~0.02–0.04 can be estimated based on ~1 m of elevation gain over 50 m of fault-perpendicular horizontal distance (Figure A2.20C), an estimated/observed fault dip of 45˚–90˚ (Langridge et al. 2018) and assuming simple shear. Strike-slip shear strains of ≤0.02 can be estimated based on an observed horizontal-to-vertical ratio of displacement of ≤1 (Langridge et al. 2018), ~1 m of elevation gain over 50 m of fault-perpendicular horizontal distance and assuming simple shear. In the 'back limb' area, and based on the above dip-slip and strike-slip shear strain considerations, net shear strains oriented parallel to the fault plane of approximately 0.02–0.04 (rounded to 10^{-2}) are estimated.

Because Harkaway Villa is located between the fold/fault scarp and 'back limb' regions, we estimate that the ground-surface beneath Harkaway Villa experienced fault-parallel net shear strains in the order of 10^{-2}–10^{-1}, comprising a combination of reverse dip-slip and left-lateral shear strain.

In addition, at the villa site, N–S-oriented horizontal tensile strains of ~0.06 (rounded to 10^{-2}) are estimated based on the observation that the N–S extent of the villa's foundation piles was about 0.8 m greater than the ~13 m N–S length of the superstructure (Figure A2.19D).

A2.4.2.3 Grey House – Papatea Fault

Grey House is a timber-framed single-storey residential structure with a corrugated metal roof and timber weatherboard cladding (Figures A2.18 and A2.21). It has a concrete slab foundation that the owner reports as having been poured 'double thick'. It has a roughly square floor plan with an approximate area of 140 m^2.

Grey House was moved onto its present site in 1933. In 2004, the owner had the house placed on a concrete slab and renovated the house 'from top to bottom'. The only original components of the house are the roof and some weatherboards, windows and interior doors. The site conditions at Grey House are similar to those at Harkaway Villa (i.e. several metres of late Holocene fan alluvium that most likely overlie gravel-dominated Clarence River alluvium).

Grey House is located about 100 m west of Harkaway Villa within the surface rupture deformation zone of the Papatea Fault. At this locality, the Papatea Fault accommodates approximately 6 m of vertical deformation (reverse, southwest-side up), a comparable (or lesser) amount of left-lateral horizontal slip (Langridge et al. 2018) and defines a ~100+-m-wide surface fault rupture deformation zone comprising both discrete fault rupture and distributed deformation (Figure A2.21). The house is located on the hanging-wall side (southwest side) of the Papatea Fault, with metre-scale surface fault rupture passing within ~45 m northeast of the house, metre- to decimetre-scale surface fault rupture passing within ~10 m southwest of the house and centimetre-scale surface fault rupture intersecting the footprint of the house (Figure A2.21A, B). Nevertheless, the house came through the earthquake in good shape. It did not suffer significant structural damage and, following the earthquake, it was judged suitable for habitation and is currently occupied (as at 2020). In addition, the house is located within a portion of the surface rupture deformation zone that experienced minimal tilt; this, too, no doubt facilitated post-event occupation.

Utilising a combination of field observations, a differential LiDAR DEM at the site (Figure A2.21D, E) and assuming simple shear, ground strains at the Grey House site can be approximated. At the location of the house, dip-slip shear strains of ~0.02–0.03 can be estimated based on ~0.5 m of elevation gain over 25 m of fault-perpendicular horizontal distance (Figure A2.21E), an estimated/observed fault dip of 45˚–90˚ (Langridge et al. 2018) and assuming simple shear. Strike-slip shear strains of ≤0.02 can be estimated based on an observed horizontal to vertical ratio of displacement of ≤1 (Langridge et al. 2018), ~0.5 m of elevation gain over 25 m of fault-perpendicular horizontal distance and assuming simple shear. Based on the above dip-slip and strike-slip shear strain considerations, net shear strains oriented parallel to the fault plane of ~0.03–0.04 (rounded to 10^{-2}) are approximated at the Grey House site.

A2.4.2.4 Middle Hill Cottage – Papatea Fault

Middle Hill cottage was a timber-framed single-storey residential structure with a corrugated metal roof, timber weatherboard cladding and timber pile foundation (Figures A2.14, A2.22 and A2.23). It had a roughly rectangular floor plan with an approximate area of 75 m^2.

Middle Hill Cottage was probably constructed in the mid-1900s (the oldest aerial photographs we have access to for this part of the country date from 1961 and show that the cottage was already in existence). It was sited on several metres of Holocene gravel-dominated fan alluvium that likely overlies gravel-dominated Clarence River alluvium.

Middle Hill Cottage was located within the surface rupture deformation zone of the Papatea Fault which, at this site, is ~100 m wide, comprising both discrete fault rupture and distributed deformation and accommodating ~7.5 m of vertical deformation (reverse, west-side up) and a comparable (or lesser) amount of left-lateral horizontal slip (Figures A2.22 and A2.23) (Langridge et al. 2018). The cottage was located on the hanging-wall side of the Papatea Fault, close to the crest of the broad fold/fault scarp that is cut by extensional fissures (Figure A2.22C). The ground encompassed by the footprint of the structure experienced decimetre-scale folding, horizontal sinistral flexure (i.e. fault drag), tilting and distributed E–W-oriented extension. As a result of the Kaikōura earthquake, this house suffered damage significant enough to be ‘red-tagged’, and it has since been demolished. However, from a life-safety perspective, this house performed creditably – it experienced very strong ground shaking, tilting and decimetre-scale surface fault rupture deformation, but it did not collapse.

Utilising a combination of field observations, a differential LiDAR DEM at the site (Figure A2.23B, C), assuming simple shear and adopting a fault dip of 45°–90° and a horizontal to vertical ratio of displacement of ≤1 (Langridge et al. 2018), we estimate that the ground-surface beneath Middle Hill Cottage experienced fault parallel net shear strains in the order of 10^{-2}–10^{-1}, comprising a combination of left-lateral and reverse dip-slip shear strain.

A2.4.2.5 Paradise Cottage – Papatea Fault

Paradise Cottage is a timber-framed single-storey house with corrugated metal roof and cladding (Figures A2.24 and A2.25). It has a roughly square floor plan (area of ~85 m^2). Most of the structure is founded on timber piles, but the laundry room at the back (west side) of the cottage has a concrete slab foundation. About 13 m to the south of the cottage, there is a timber-framed and timber-clad shed.

Paradise Cottage was constructed prior to the early 1960s (aerial photographs from 1961 show that the cottage was already in existence). Paradise Cottage is sited on several metres of Holocene gravel-dominated colluvium and alluvium, and beach sand and gravel, overlying moderately strong bedrock.

At the coast, where Paradise Cottage is located, the Papatea Fault comprises several main strands; the cottage is located across and immediately adjacent to the westernmost of these (Langridge et al. 2018). Here, the western strand of the Papatea Fault accommodates approximately 3.5 m of vertical deformation (east-side up) (Figure A2.24D), a subordinate amount of left-lateral horizontal slip (Langridge et al. 2018) and defines an 8–10-m-wide surface fault rupture deformation zone primarily comprising discrete fault rupture. The cottage is located on the up-thrown side of the fault, at the eastern edge of the surface rupture deformation zone and has had its back-side ripped out by surface fault rupture. The nearby timber shed is located entirely within the fault scarp and has been severely tiled and deformed. Neither the house nor the shed collapsed.

Employing a combination of field observations and a differential LiDAR DEM at the site (Figure A2.24C, D), assuming simple shear and adopting a sub-vertical fault dip and a horizontal to vertical ratio of displacement of <1 (Langridge et al. 2018), we estimate that the ground-surface beneath the shed and the southwest corner of the cottage experienced fault-parallel net shear strains in the order of 10^{-1}.

A2.4.2.6 Glenbourne Woolshed – The Humps Fault

The Glenbourne woolshed is a single-storey, timber-framed structure with corrugated metal roof and cladding (Figures A2.26 and A2.27) and a rectangular floor plan (area of ~300 m^2). The structure stands on concrete piles and has timber flooring overlying timber joists.

The Glenbourne woolshed was constructed in 1980. It is sited on a 2–4 m thickness of late Pleistocene–Holocene loosely packed fluvial gravel above moderately strong bedrock.

Glenbourne Farm is located near the north-east margin of the Culverden Basin, where the low relief topography of the Emu Plains transitions into the steeper slopes of the Mt Stewart Range (Figure A2.14). Here, surface rupture of The Humps Fault comprises three to four main traces mapped over a 3.5 km width perpendicular to fault strike (Figure A2.27) (Nicol et al. 2018). Net dextral displacement across these traces is a factor of 2 larger compared to the average dextral displacement on the western ~20 km of the fault (Nicol et al. 2018). Along the fault, vertical displacements are variably north- or south-side up. At the Glenbourne woolshed,

surface rupture displacement was measured using RTK-GPS with the primary trace, located only ~5 m from the woolshed (Figures A2.26A, C and A2.27A), having ~1–2 m of dextral and ~1.2 m of north-side-up vertical displacement. The woolshed is situated on the down-thrown side of the primary discrete trace in a 10–20-m-wide zone of decimetre-scale ground subsidence that encompasses minor fracturing and small faults with vertical displacements of up to 10 cm (Figure A2.26A). This zone of ground subsidence extends from the stockyard adjacent to, and southwest of, the woolshed to the northeast for over 50 m. Fault-rupture-induced damage to the Glenbourne woolshed appears to be limited to rotation of some of the shallow-seated concrete piles (Figure A2.26B). The superstructure itself is relatively undamaged and intact. We suspect that rotation of the piles isolated the superstructure from the decimetre-scale fault rupture ground deformation underneath. It is pertinent to note that a similarly constructed and piled woolshed sited across the 2010 surface rupture of the Greendale Fault displayed similar performance, with rotation of shallow-seated piles isolating, to a large extent, the superstructure from the underlying fault rupture ground deformation (Figure A2.11) (Van Dissen et al. 2011).

At this location, and elsewhere along The Humps and Leader faults, we have access to pre- and post-earthquake photogrammetric point clouds. Iterative closest point (ICP) differencing of pre- and post-earthquake point clouds (e.g. Nissen et al. 2012) yields gridded values of displacements in the vertical, northing and easting directions at 50 m grid spacings. These gridded values were interpolated into three separate 10 m grid-size rasters (one for each component/direction), and we construct fault-perpendicular transects on these rasters, crossing the structures, to estimate the fault-parallel net shear strains at the location of the structures that incorporate both horizontal and vertical displacements (Figure A2.27). Given the decametre-scale resolution of the ICP method, our shear strain estimations need to be augmented by field observations to accommodate the location, and amount, of discrete displacements that would otherwise be smoothed by the ICP method. Nevertheless, the ICP method provides the opportunity to document the amount and style of broad-scale net displacement across the surface rupture deformation zone, and distributed deformation within the deformation zone, that may otherwise not be readily apparent, or well-characterised, by field measurements of discrete displacement alone. While the ICP method is used here to estimate 3D displacements that should be internally consistent across fault profiles, there is some uncertainty introduced in both gridding processes, and this yields uncertainty regarding the exact amount and distribution of deformation along the profiles at the specific location of the structures. This, in turn, yields uncertainty in our strain estimations. However, we expect that this effect is small, given the order of magnitude strain estimates reported in this Appendix, and acknowledging that field observations of discrete displacement are taken into account. Using these data, and assuming simple shear and a sub-vertical fault dip (80–90°) at the woolshed site, we estimate net shear strains of ~10^{-2}.

A2.4.2.7 Hillview Cottage – The Humps Fault

Hillview Cottage is a timber-framed, single-storey residential structure with a corrugated metal roof and Fibrolite cladding. It has a concrete slab foundation and a rectangular floor plan with an area of ~50 m^2 (Figures A2.28 and A2.29).

Hillview Cottage was constructed prior to the early 1950s (aerial photographs from 1950 show that the cottage was already in existence). It is sited on late Pleistocene loosely to tightly packed fan-gravel and stiff loess >15 m thick.

Hillview Cottage is located on a zone of concentrated deformation in the central section of The Humps Fault. Just west of the cottage, there is a prominent, ~25-m-wide pull-apart depression that transitions to the east into a narrow zone of Riedel shears and tension fractures (Figures A2.28 and A2.29A). In the field, an adjacent fault-offset fence yielded RTK-derived offset measurements of 0.9 m dextral and 0.5 m vertical (Nicol et al. 2018). The cottage experienced a chimney collapse (Figure A2.28B) and multiple fractures to the concrete foundation (Figure A2.28C, D). Timber supports for the roof/veranda at the front of the cottage experienced minor amounts of shear and were deformed out-of-plumb (Figure A2.28C, D). Several cladding planks at the base of the exterior of the cottage were broken (Figure A2.28D). Although surface rupture caused structural damage to the cottage, it appears to be far from collapse. Using a combination of the ICP-based analysis (see Glenbourne section) and field observations, we estimate centimetre-scale vertical and decimetre-scale dextral displacement at the site of the cottage. Assuming simple shear and a sub-vertical fault plane, we estimate a net shear strain across the footprint of the structure of ~10^{-2}.

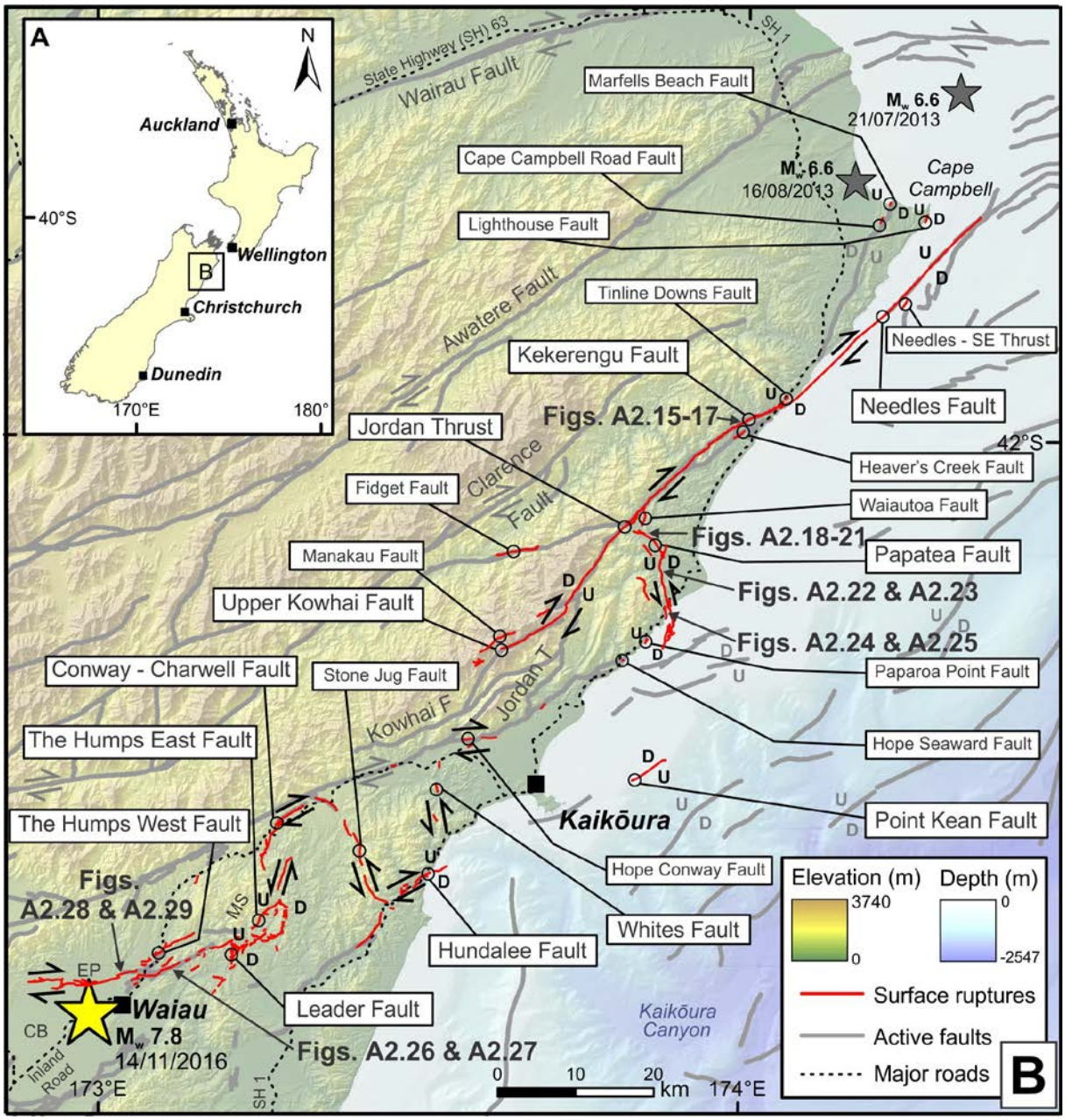

Figure A2.14 Kaikōura earthquake surface fault ruptures (red lines) from Litchfield et al. (2018). Also shown are the locations of Figures A2.15–A2.29, the epicentre of the 2016 Kaikōura earthquake (large yellow star) from Nicol et al. (2018) and the epicentres for the two 2013 Cook Strait earthquakes (small grey stars) from Holden et al. (2013). Abbreviations: CB = Culverden Basin, EP = Emu Plains, F = fault, MS = Mt Stewart Range, T = thrust. A 1:250,000-scale digital version of 2016 surface ruptures is available for download at https://data.gns.cri.nz/af/ (choose 'Download data – Kaikōura'; Langridge et al. 2016).

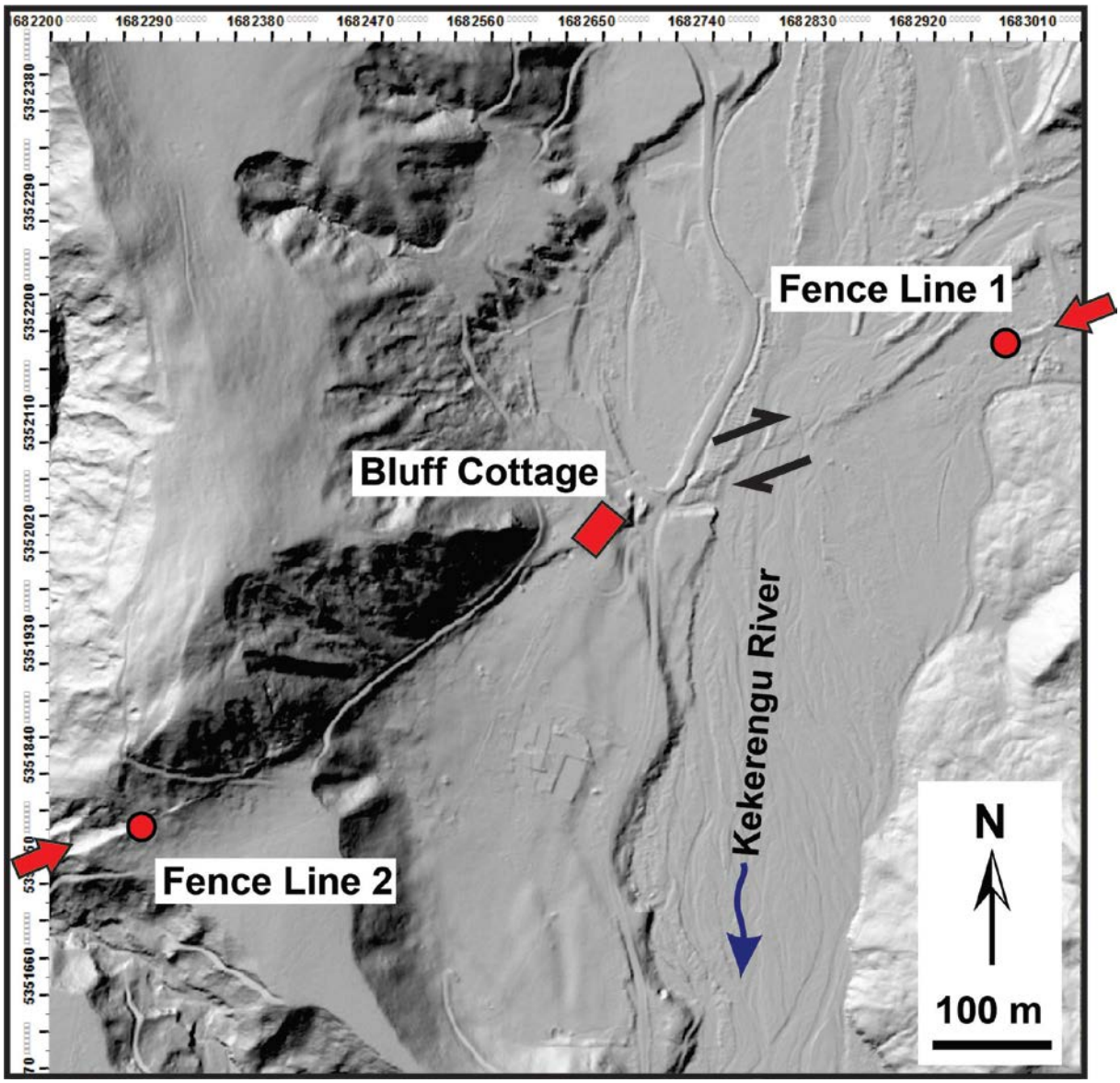

Figure A2.15 2016 post-earthquake LiDAR hill shade DEM, illuminated from the northwest showing location of surface rupture trace of the Kekerengu Fault (red arrows), Bluff Cottage (Figure A2.16), the two offset fence lines depicted in Figure A2.17 and the sense of strike-slip on the Kekerengu Fault (black arrows). Though the size of Bluff Cottage portrayed in this figure is significantly exaggerated, its orientation is accurate. Coordinates are New Zealand Transverse Mercator 2000.

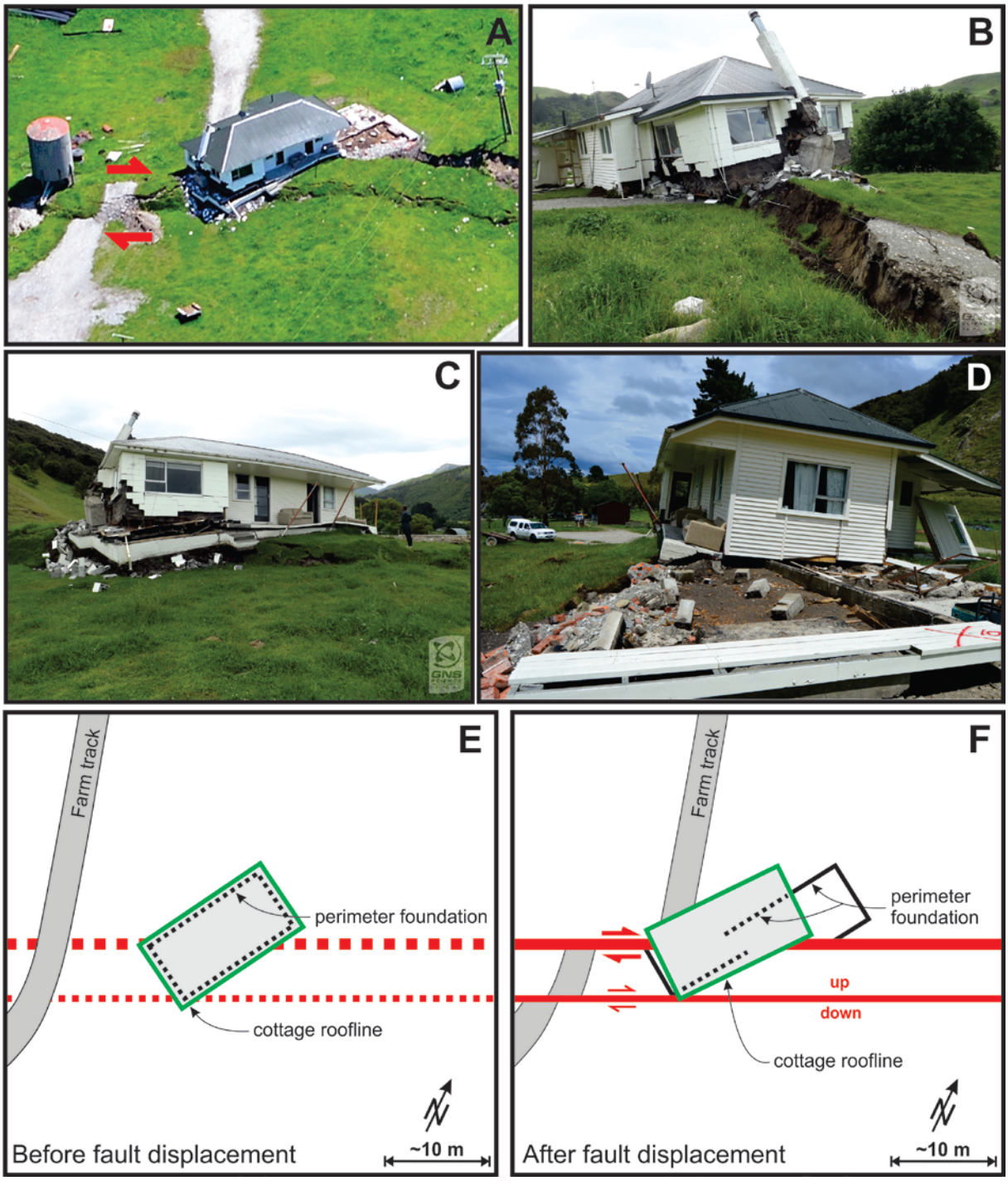

Figure A2.16 Bluff Cottage and Kekerengu Fault surface rupture; see Figures A2.14 and A2.15 for location (Lat: -41.9796, Long: 173.9976). (A) Oblique aerial view looking northwest. Red arrows show the sense of slip of the Kekerengu Fault that generated ~10 m of right-lateral surface rupture displacement at this locality. Photo by Dougal Townsend, taken in November 2016. (B) View of Bluff Cottage looking northeast along the strike of the surface rupture of the Kekerengu Fault. Right-laterally offset farm track to left of cottage in Figure A2.16A is the same farm track visible in lower right and middle left of Figure A2.16B. Photo by Nicola Litchfield, taken in November 2016. (C) View looking northwest. Photo by Nicola Litchfield, taken in November 2016. (D) View looking southwest. Note that the concrete perimeter foundation and piles that were once under the cottage have now been torn from the superstructure of the cottage and laterally displaced toward the viewer, relative to the cottage. Photo by Robert Zinke, taken in November 2016. (E) Schematic map of Bluff Cottage and farm track prior to surface rupture of the Kekerengu Fault. (F) Schematic map of Bluff Cottage and farm track after fault displacement.

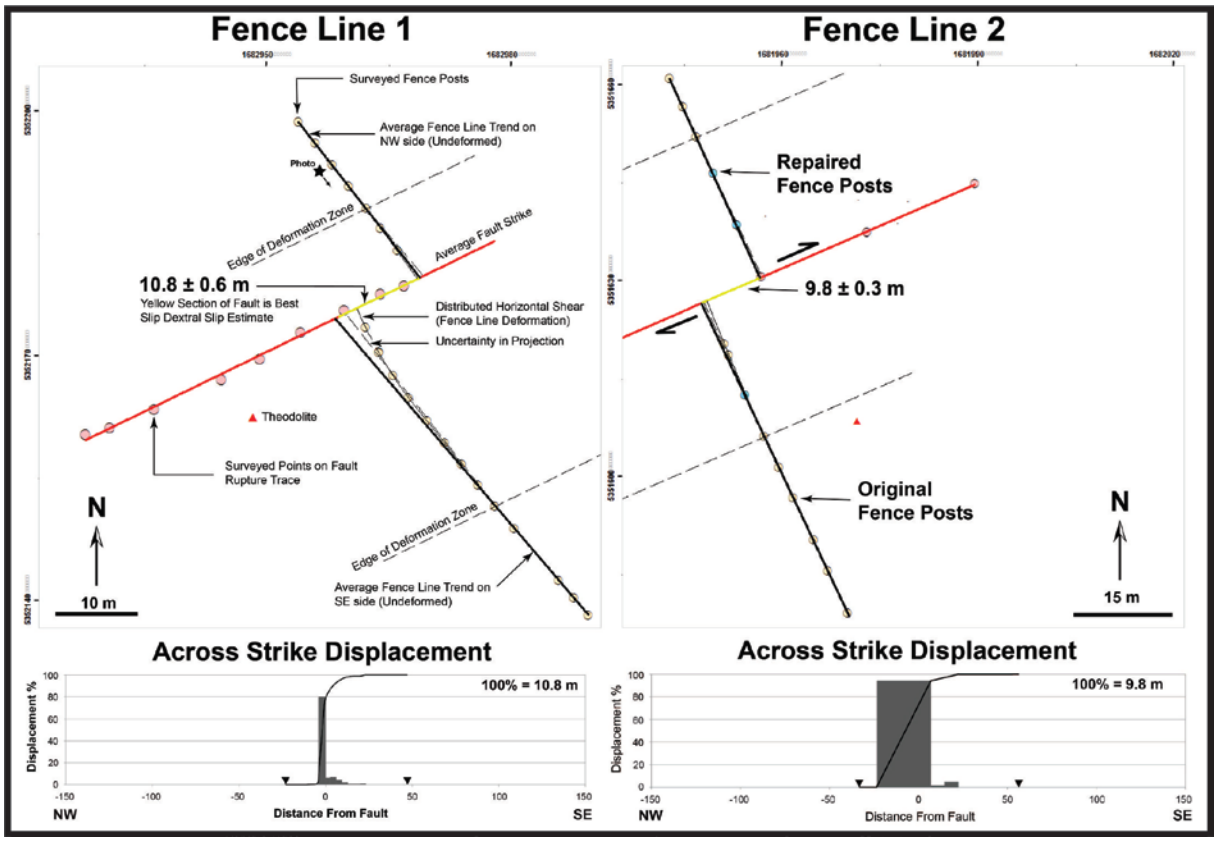

Figure A2.17 Examples of fence line displacements along the Kekerengu Fault near Bluff Cottage that document both the amount of right-lateral displacement and how that displacement is distributed as a function of distance perpendicular to fault strike (see Kearse et al. [2018] for more detail). See Figure A2.15 for locations. Coordinates are New Zealand Transverse Mercator 2000.

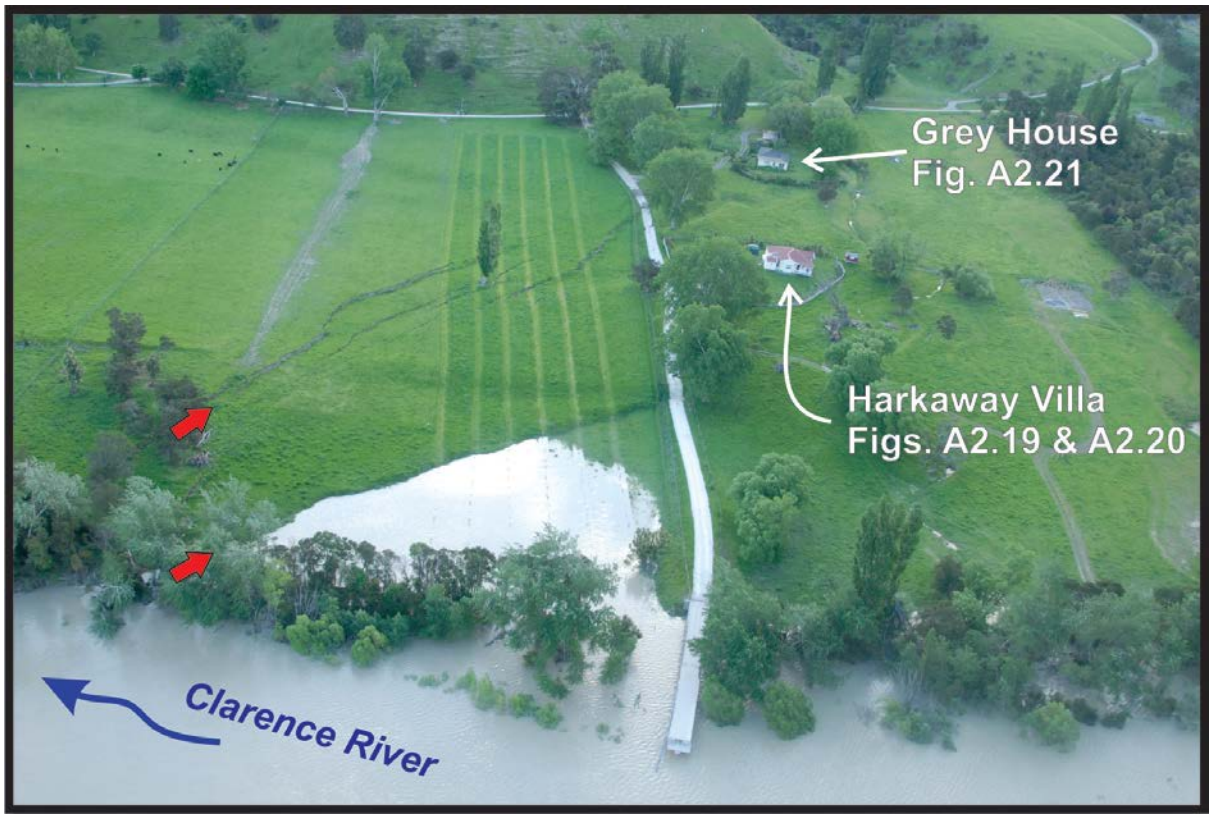

Figure A2.18 Harkaway Villa (Lat: -42.1105, Long: 173.8384), Grey House (Lat: -42.1105, Long: 173.8372) and the Papatea Fault surface rupture; see Figure A2.14 for location. Oblique aerial view looking west, with red arrows denoting position of prominent discrete ruptures in the surface rupture deformation zone of the Papatea Fault. Photo by Will Ries, taken in November 2016.

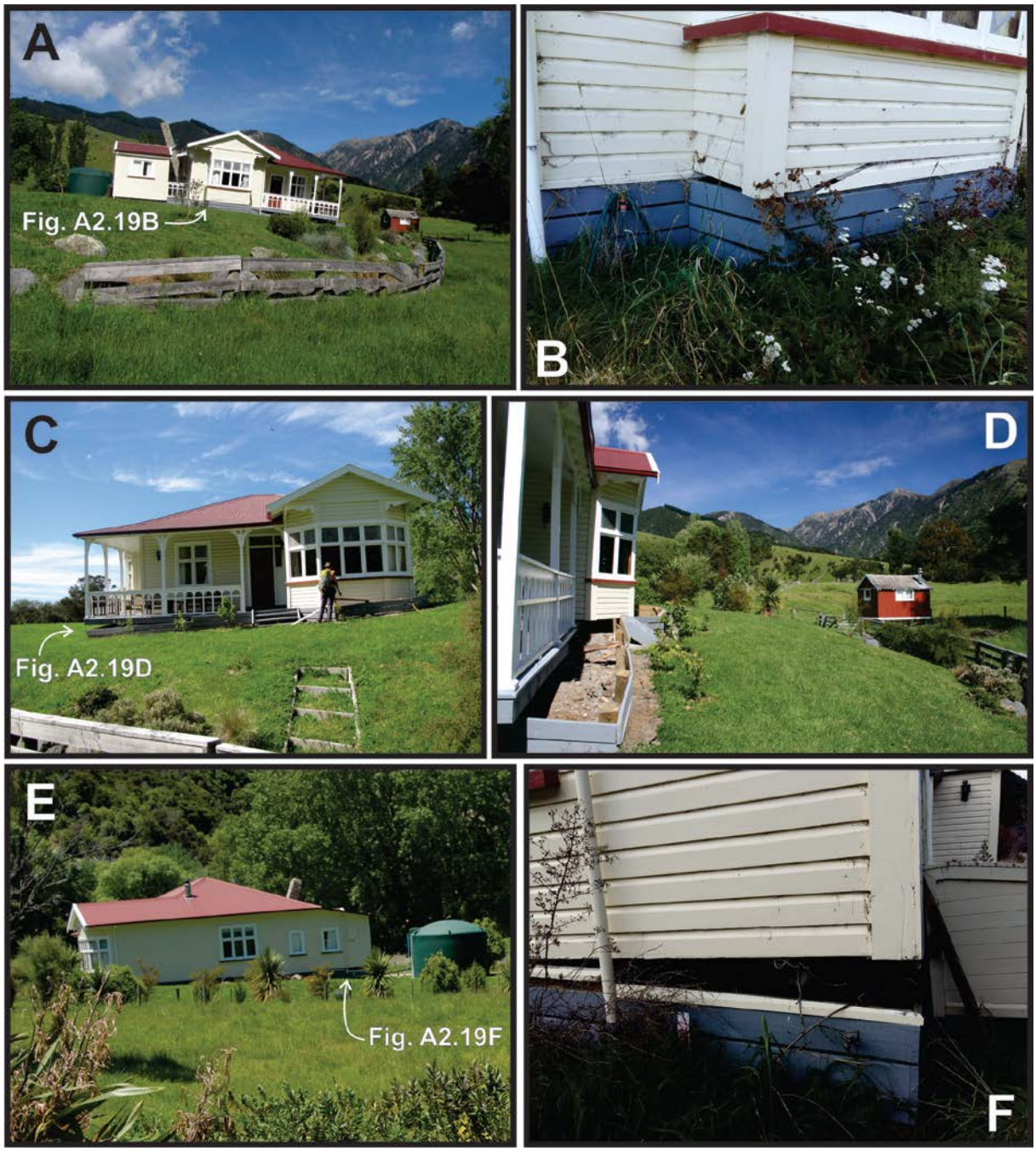

Figure A2.19 Harkaway Villa and Papatea Fault surface rupture. (A) View looking west showing northeast-ward tilt of the villa on the up-thrown (hanging-wall) side of the Papatea Fault. Photo by Julie Rowland, taken in November 2016. (B) View looking northwest showing detail of damage to the east side of the villa. Photo by Julian Garcia-Mayordomo, taken about 18 months after the 2016 Kaikōura earthquake. (C) View looking south of the north side of the villa. Photo by Rob Langridge, taken in November 2016. (D) View looking west of the north side of the villa, showing offset of the foundation piles from the superstructure. Photo by Julie Rowland, taken in November 2016. (E) View looking east of the west side of Harkaway Villa. Photo by Rob Langridge, taken in November 2016. (F) View looking east, showing detail of damage to the west side of the villa. Photo by Julian Garcia-Mayordomo, taken in May 2018.

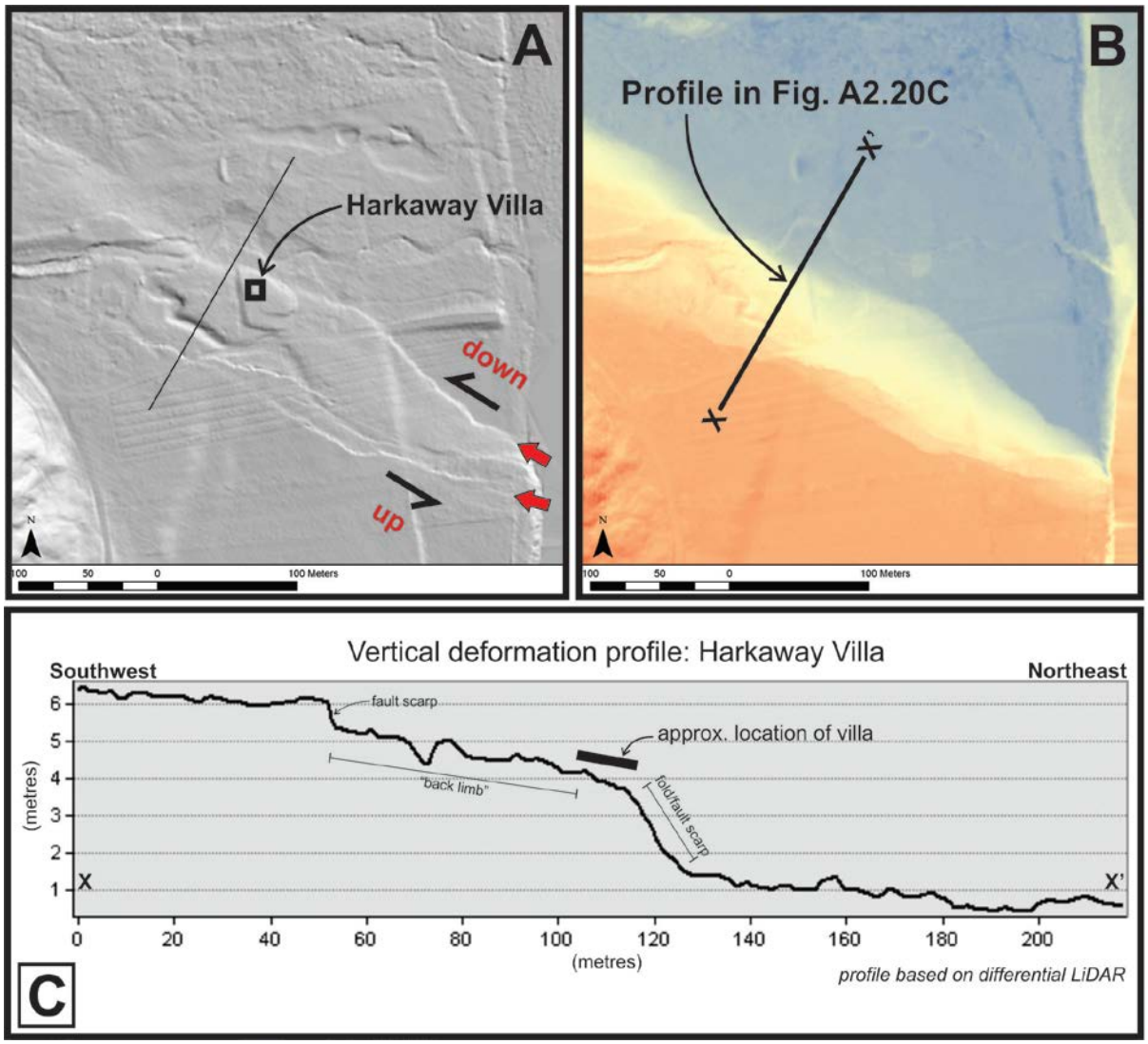

Figure A2.20 Harkaway Villa and Papatea Fault surface rupture. (A) 2016 post-earthquake LiDAR hill shade DEM with black square denoting villa's location and red arrows showing location of prominent discrete ground-surface ruptures. (B) Differential LiDAR DEM with blue colours denoting little vertical change and red colours denoting significant positive vertical change (see C for more detail regarding scale). (C) Vertical deformation profile derived from the differential LiDAR DEM. Vertical exaggeration = 7.5.

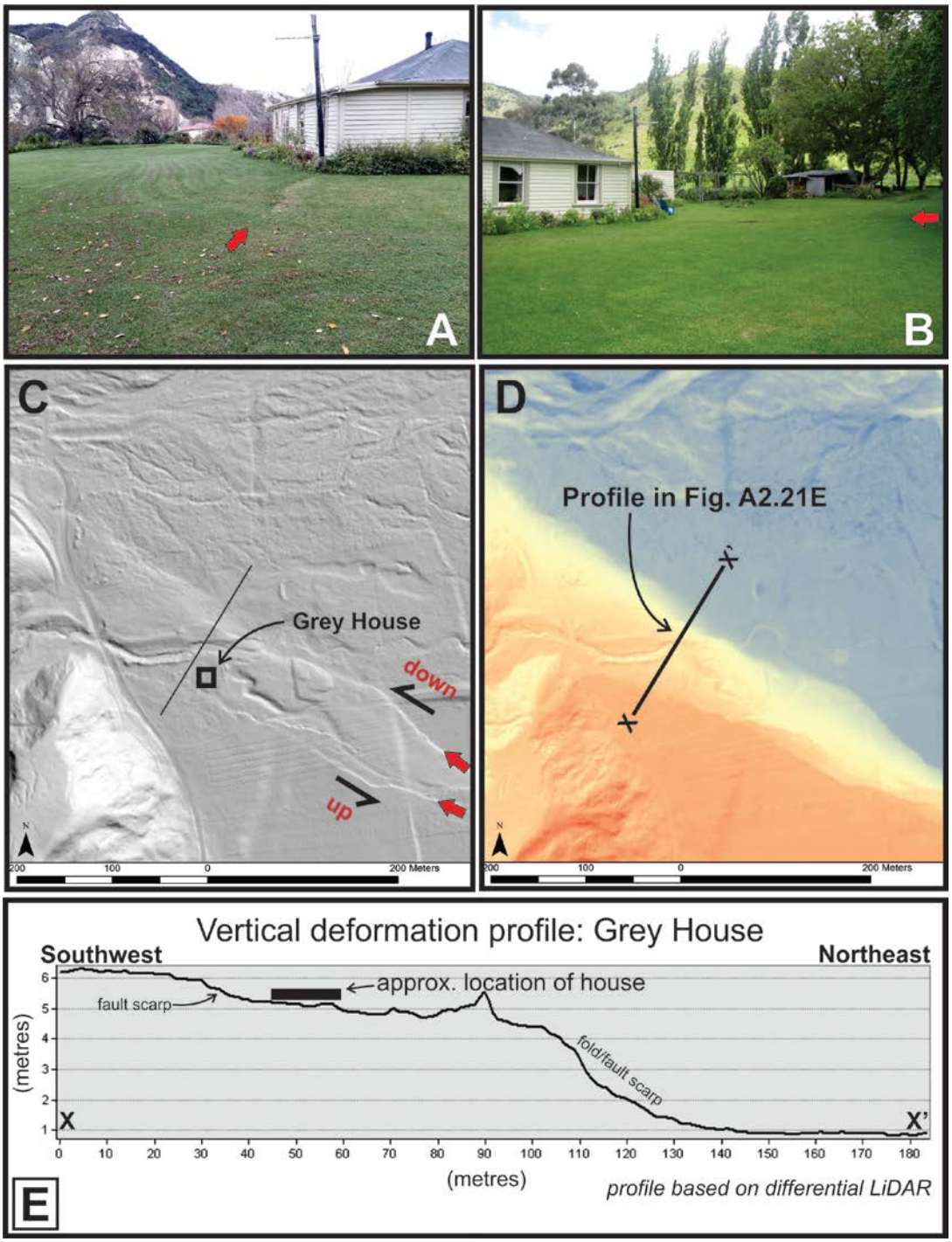

Figure A2.21 Grey House and Papatea Fault surface rupture. (A) View looking east-southeast with red arrow showing location of centimetre-scale discrete rupture that intersects northwest corner of the house. Harkaway Villa (Figures A2.18 and A2.19) is visible in the middle distance. Photo by Julian Garcia-Mayordomo, taken about 18 months after the 2016 Kaikōura earthquake. (B) View looking southwest. Red arrow denotes the location of centimetre-scale discrete rupture that intersects the northwest corner of the house. (C) 2016 post-earthquake LiDAR hill shade DEM with the black square denoting the house's location and red arrows showing the location of prominent discrete ground-surface ruptures. (D) Differential LiDAR DEM with blue colours denoting little vertical change and red colours denoting significant positive vertical change (see E for more detail regarding scale). (E) Vertical deformation profile derived from the differential LiDAR DEM. Vertical exaggeration = 6.4.

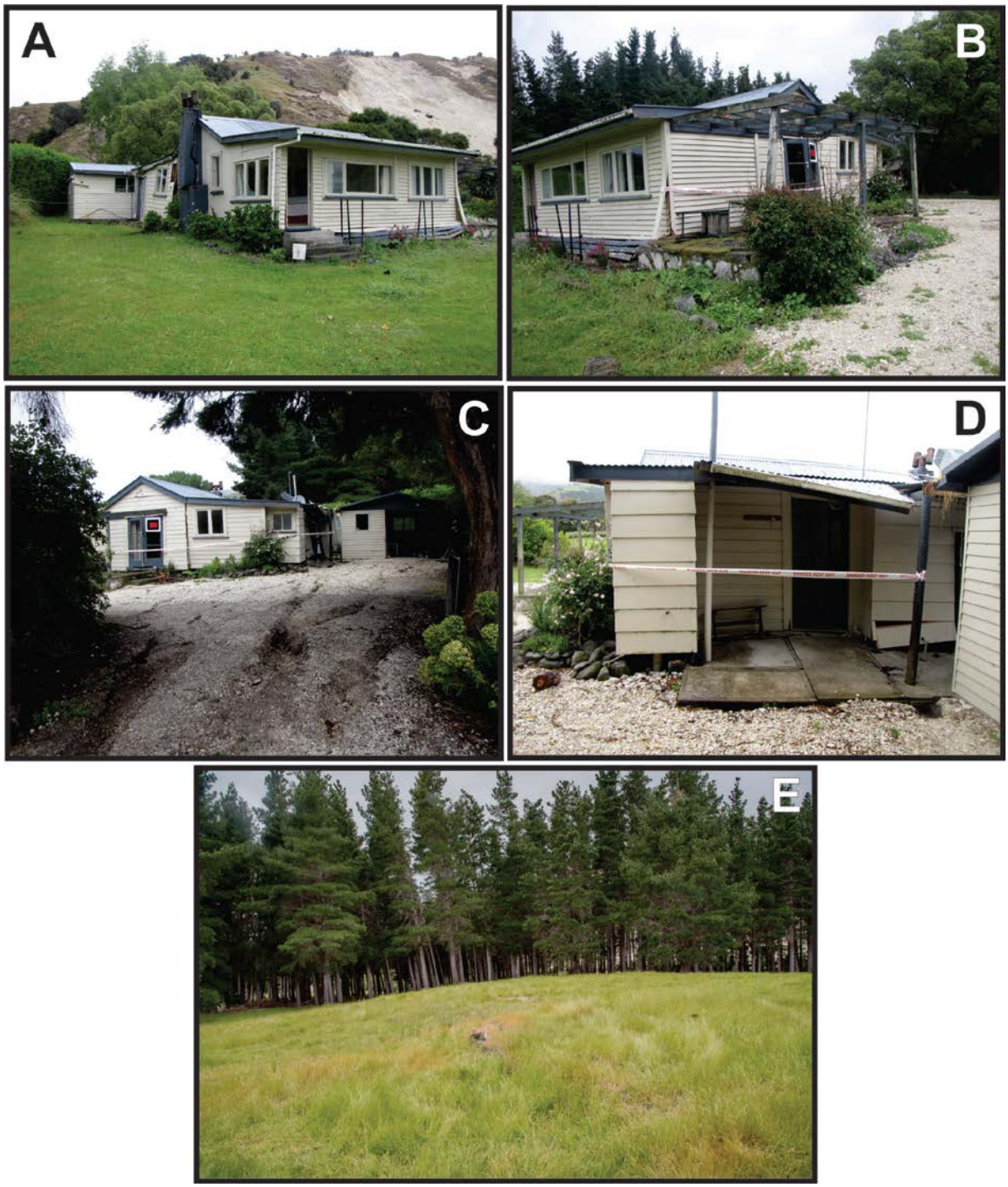

Figure A2.22 Middle Hill Cottage and Papatea Fault surface rupture; see Figure A2.14 for location (Lat: -42.1536, Long: 173.8667). (A) View looking west. Photo by Rob Langridge, taken in December 2016. (B) View looking south-southwest. Photo by Rob Langridge, taken in December 2016. (C) View looking southeast along the strike of extensional fissures located in the crestal region of the primary fold/ fault scarp that extend toward, and intersect, the cottage. Photo by Rob Langridge, taken in December 2016. (D) View looking northeast. Photo by Rob Langridge, taken in December 2016. (E) View from the cottage looking south-southeast along-strike of the Papatea Fault's surface rupture deformation zone. Prior to the 2016 rupture of the Papatea Fault, the ground surface in this photograph was approximately flat and horizontal, and the trunks of the pine trees were all sub-vertical. Photo by Stefano Pucci, taken about a year after the earthquake.

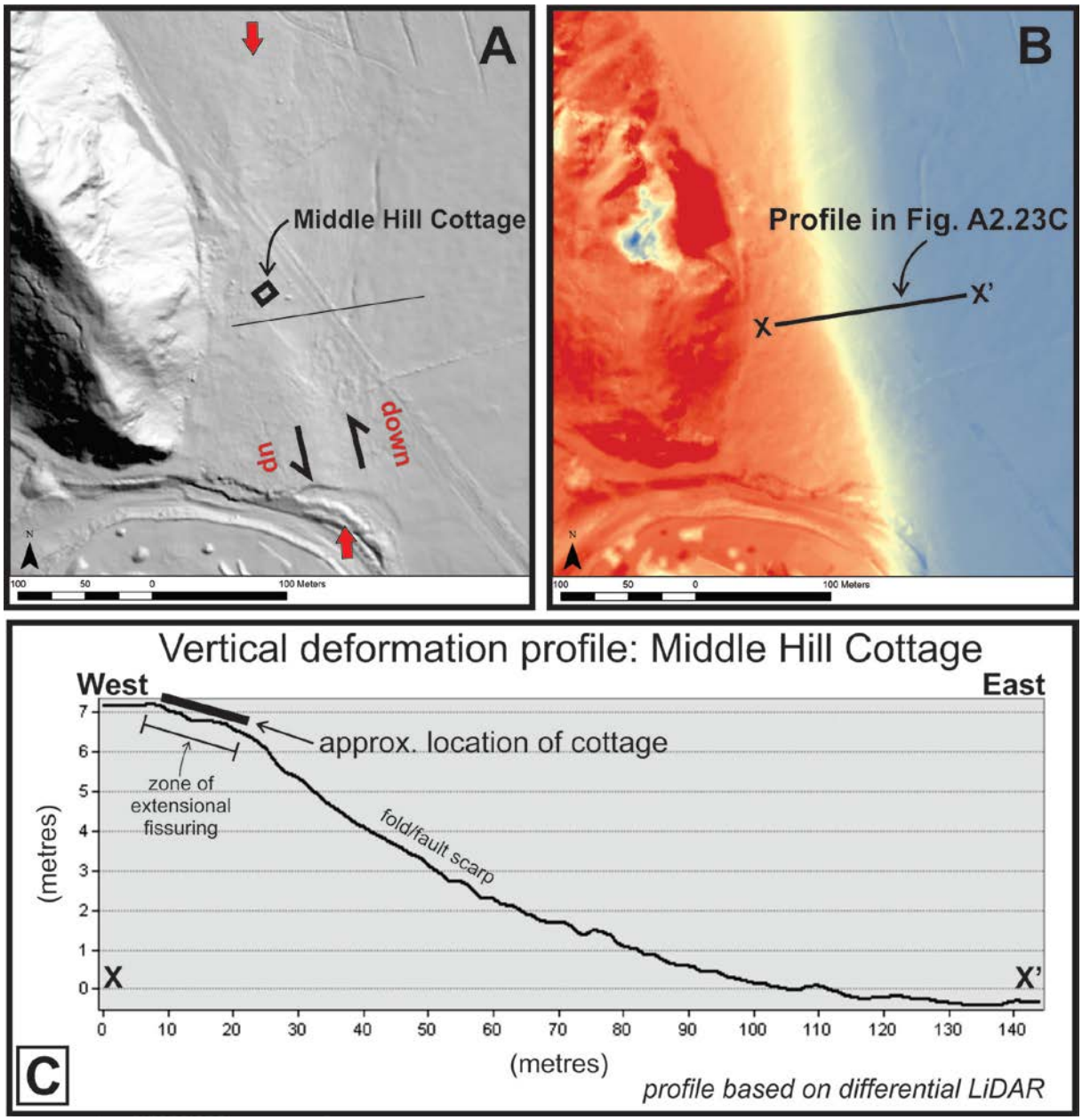

Figure A2.23 Middle Hill Cottage and Papatea Fault surface rupture. (A) 2016 post-earthquake LiDAR hill shade DEM with the black square denoting cottage's location and red arrows showing the location the surface fault rupture scarp. (B) Differential LiDAR DEM with blue colours denoting little vertical change and red colours denoting significant positive vertical change (see C for more detail regarding scale). (C) Vertical deformation profile derived from the differential LiDAR DEM. Vertical exaggeration = 6.1.

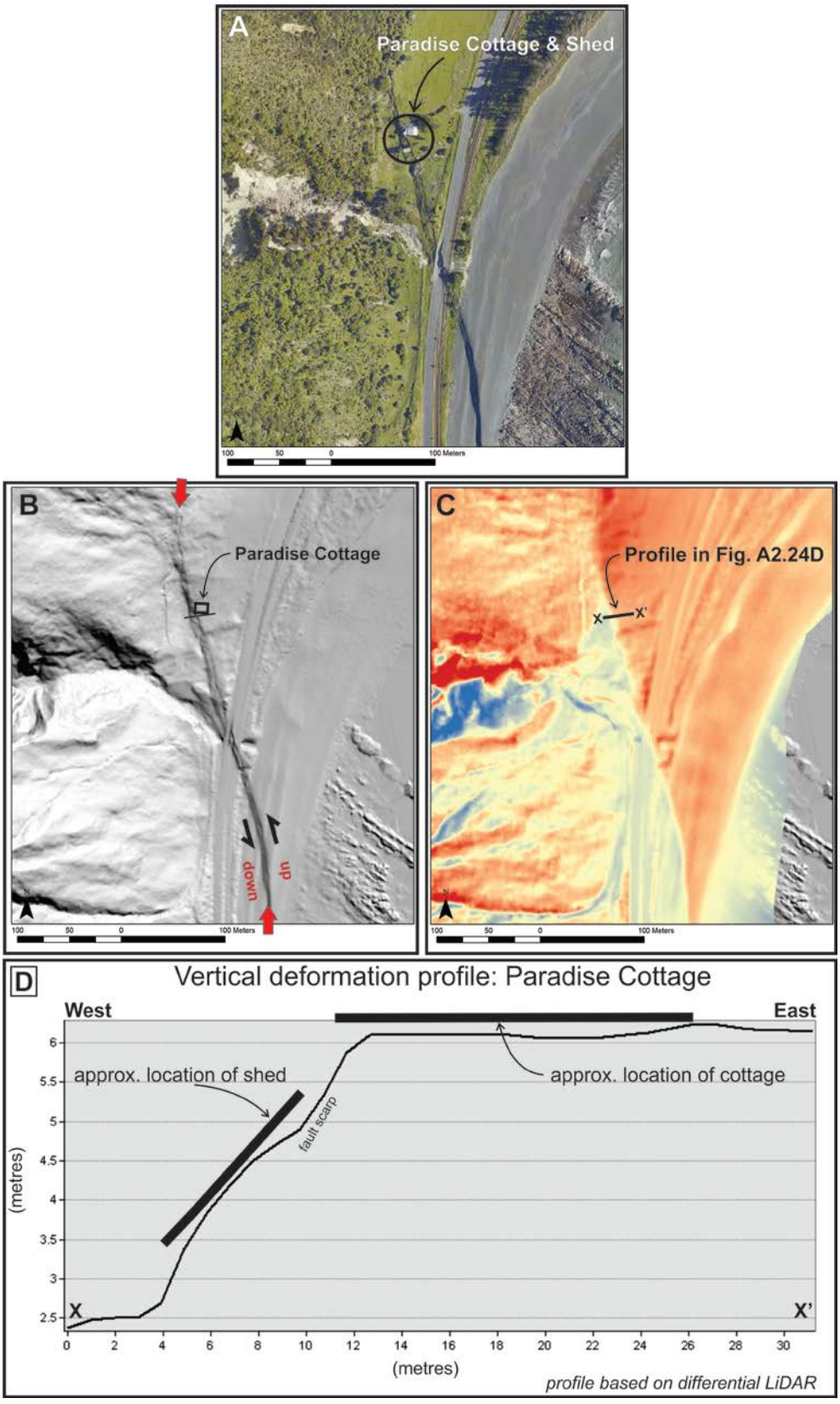

Figure A2.24 Paradise Cottage and Papatea Fault surface rupture; see Figure A2.14 for location (Lat: -42.2010, Long: 173.8753). (A) 2016 post-earthquake vertical aerial orthophotograph. Black circle denotes location of cottage and shed to the south. (B) 2016 post-earthquake LiDAR hill shade DEM showing location of cottage (black square) and prominent discrete ground-surface ruptures (red arrows). (C) Differential LiDAR DEM with blue colours denoting little vertical change and red colours denoting significant positive vertical change (see D for more detail regarding scale). (D) Vertical deformation profile derived from differential LiDAR DEM located half-way between the cottage and the shed. Vertical exaggeration = 3.3.

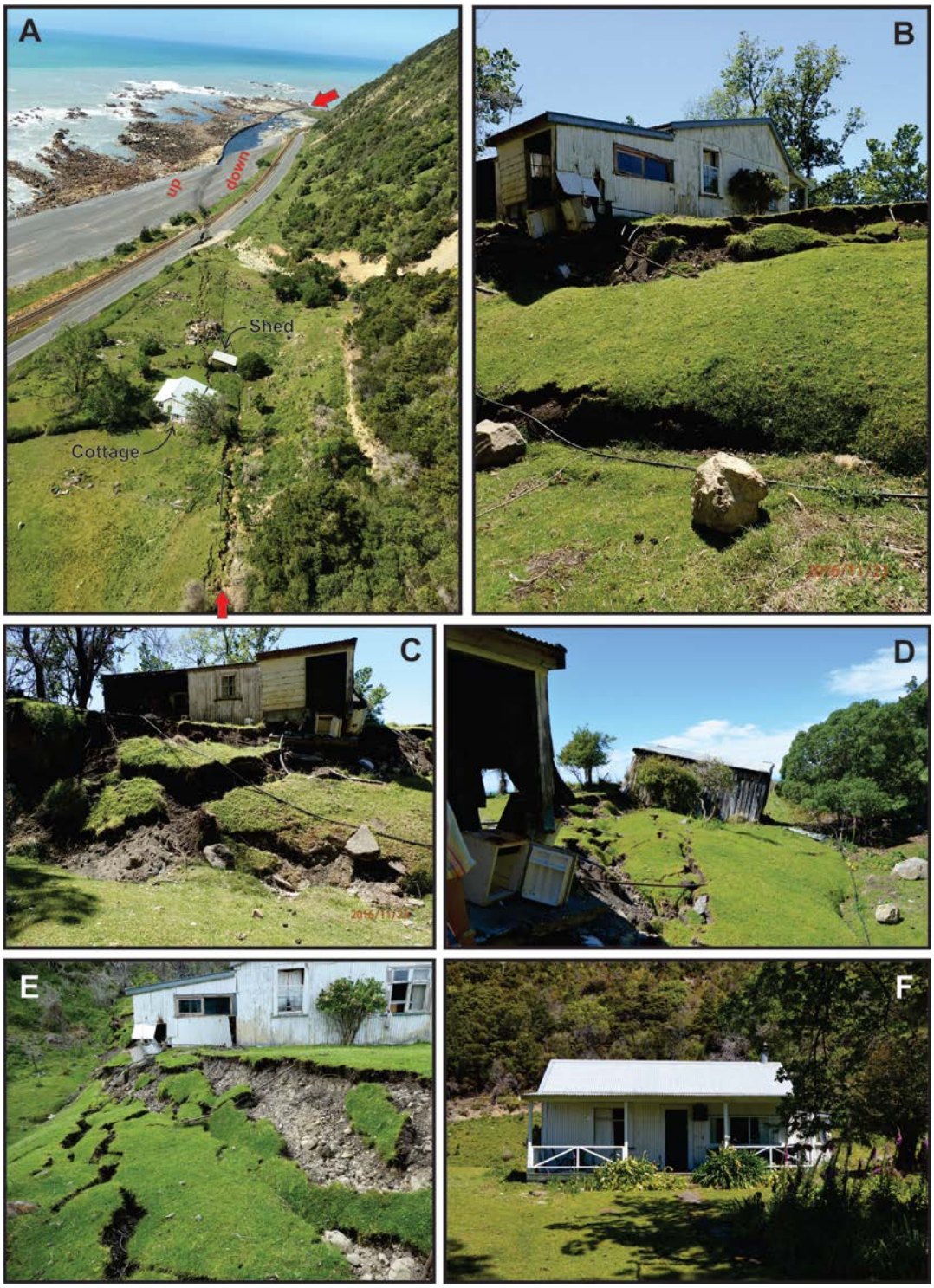

Figure A2.25 Paradise Cottage and Papatea Fault surface rupture; see Figure A2.14 for location. (A) Oblique aerial view looking south-southeast along the strike of the western strand of the Papatea Fault. Red arrows denote the position of prominent discrete rupture. Photo by Will Ries, taken in November 2016. (B) View looking northeast. Photo by Alex Hatem, taken in November 2016. (C) View looking east. Photo by Alex Hatem, taken in November 2016. (D) View looking south-southeast towards the shed. Photo by Robert Zinke, taken in November 2016. (E) View looking north-northwest along-strike of the surface fault rupture. Photo by Tim Little, taken in November 2016. (F) View looking east towards the front side of the cottage. The front of the cottage appears to be little damaged compared with the significant damage behind it. Photo by Robert Zinke, taken in November 2016.

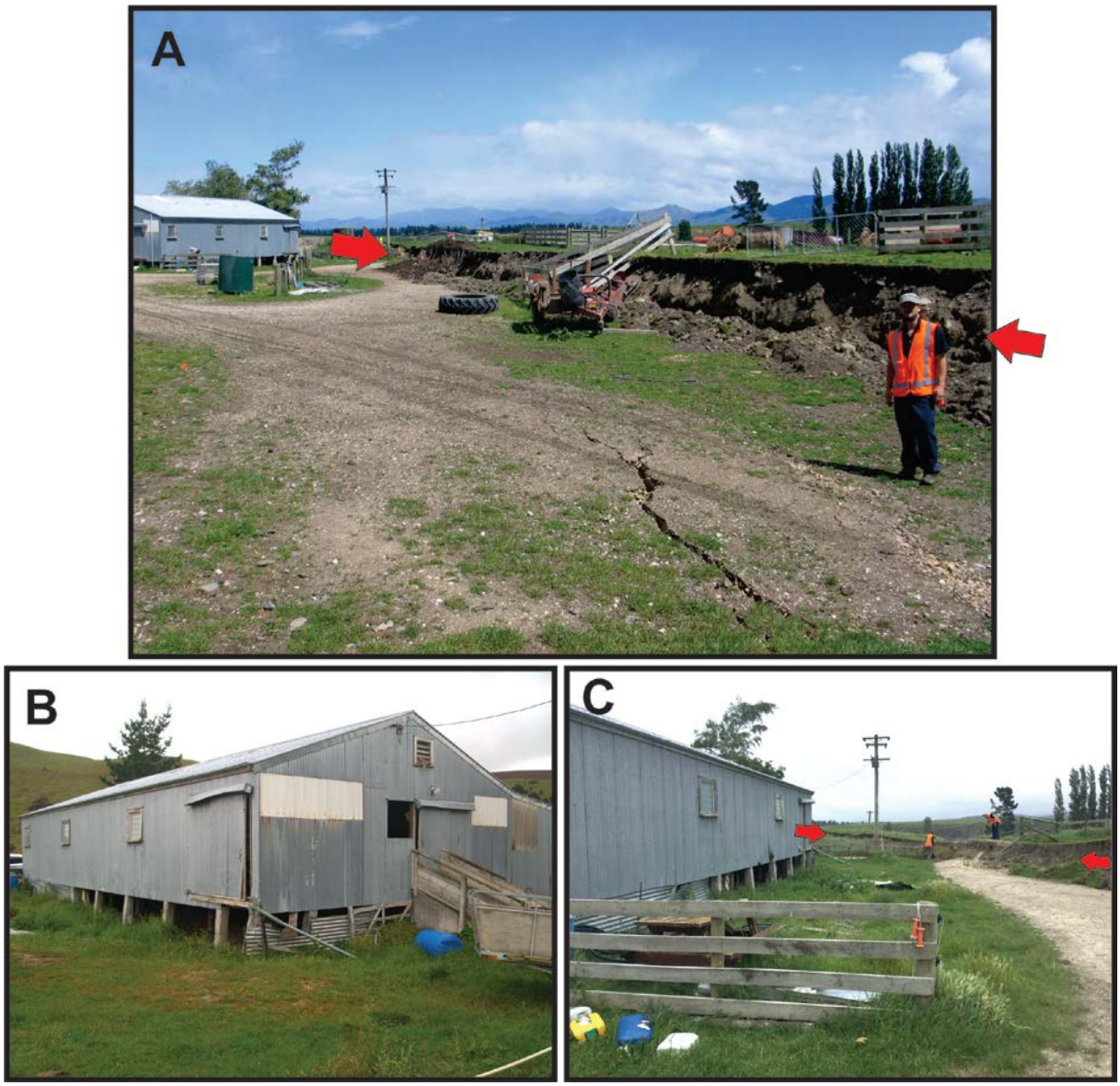

Figure A2.26 Glenbourne Woolshed and The Humps Fault surface rupture; see Figures A2.14 and A2.27 for location (Lat: -42.6152, Long: 173.1058). (A) View looking southwest along the fault rupture towards the woolshed. Note distributed centimetre-scale cracking in the foreground (in front of the high-vis geologist), adjacent to the main trace (red arrow, and behind the high-vis geologist). The distributed centimetre-scale cracking persists along-strike for many tens of metres. Photo by Jarg Pettinga, taken in November 2016. (B) View looking south at the woolshed (main fault scarp is behind the camera). Tilt and rotation of the shallow-seated concrete piles is the only recognisable damage. Photo by Clark Fenton, taken in December 2016. (C) View looking southwest along the side of the woolshed and towards the main fault scarp at this site. Photo by Tim Stahl, taken in November 2016.

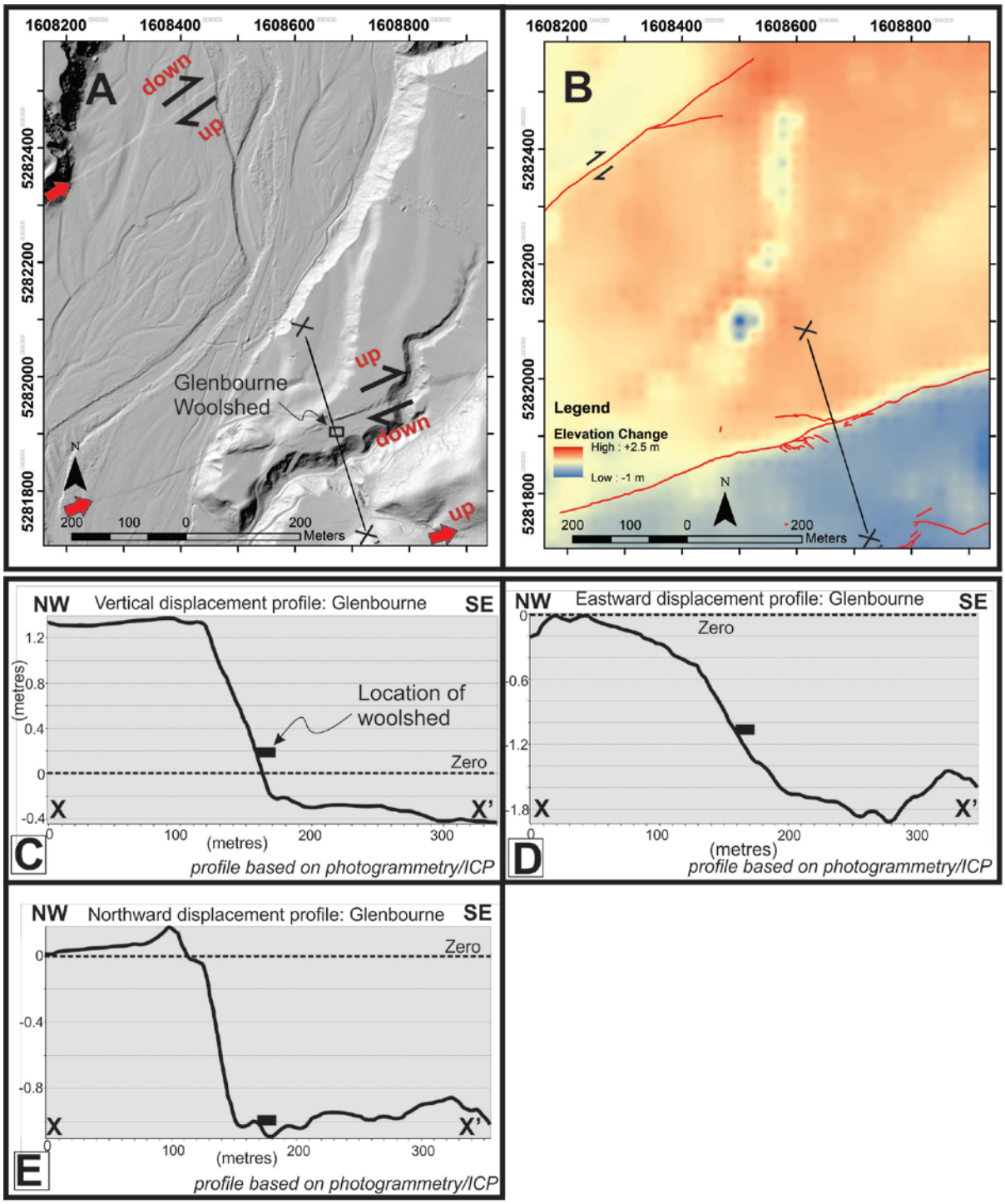

Figure A2.27 Glenbourne Woolshed and The Humps Fault surface rupture. (A) LiDAR hill shade DEM showing location of the woolshed and two prominent discrete fault traces (red arrows), one of which is within ~5 m of the woolshed (see Figure A2.26A, C). (B) Raster of vertical displacements in the same area as (A), using ICP method outlined in the text. (C), (D) and (E) are the vertical, eastward and northward displacement profiles from X to X' on the top two images. The location of the woolshed is shown on each profile. Note that, while relative motions were mapped in the field, the absolute sense of displacement is more complex, with the down-thrown side of the fault moving southwest-ward and the up-thrown side of the fault remaining relatively stable, except in the vertical direction. Y-axis exaggeration in (C) and (D) = 85. Y-axis exaggeration in (E) = 130.

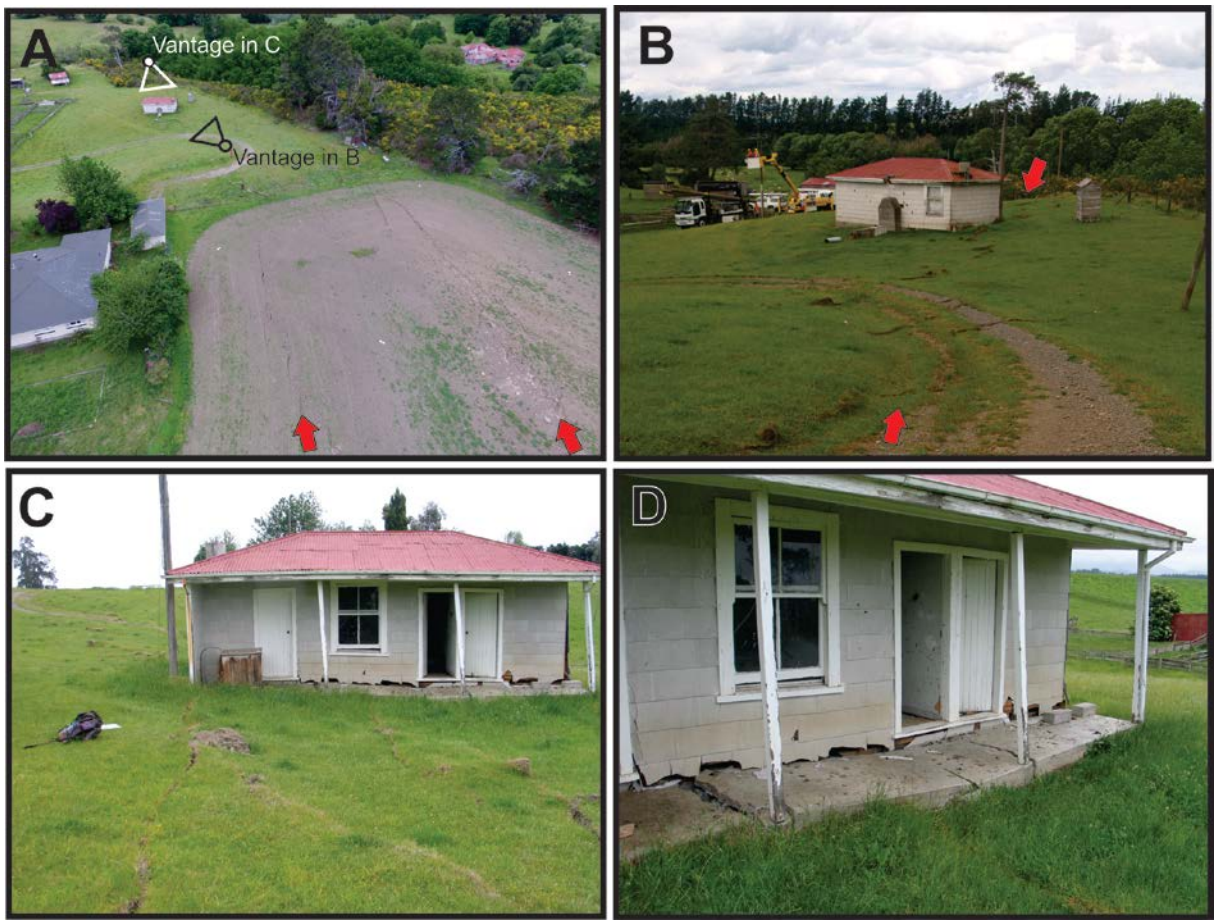

Figure A2.28 Hillview Cottage and The Humps Fault surface rupture; see Figures A2.14 and A2.29 for location (Lat: -42.6287, Long: 173.0154). (A) Oblique aerial view looking east toward the cottage along discrete dextral-normal surface fault ruptures (red arrows). Photo courtesy of Sam McColl, taken from a drone in November 2016. (B) View looking northeast. At this location, the cottage is impacted by decimetre-scale discrete fault rupture (in this case Riedel shears) and centimetres to decimetres of distributed deformation between the shears. Note the collapsed chimney. Photo by Clark Fenton, taken in November 2016. (C, D) Details of damage to the cottage caused by decimetre-scale surface fault rupture. Photos by Jarg Pettinga, taken in November 2016.

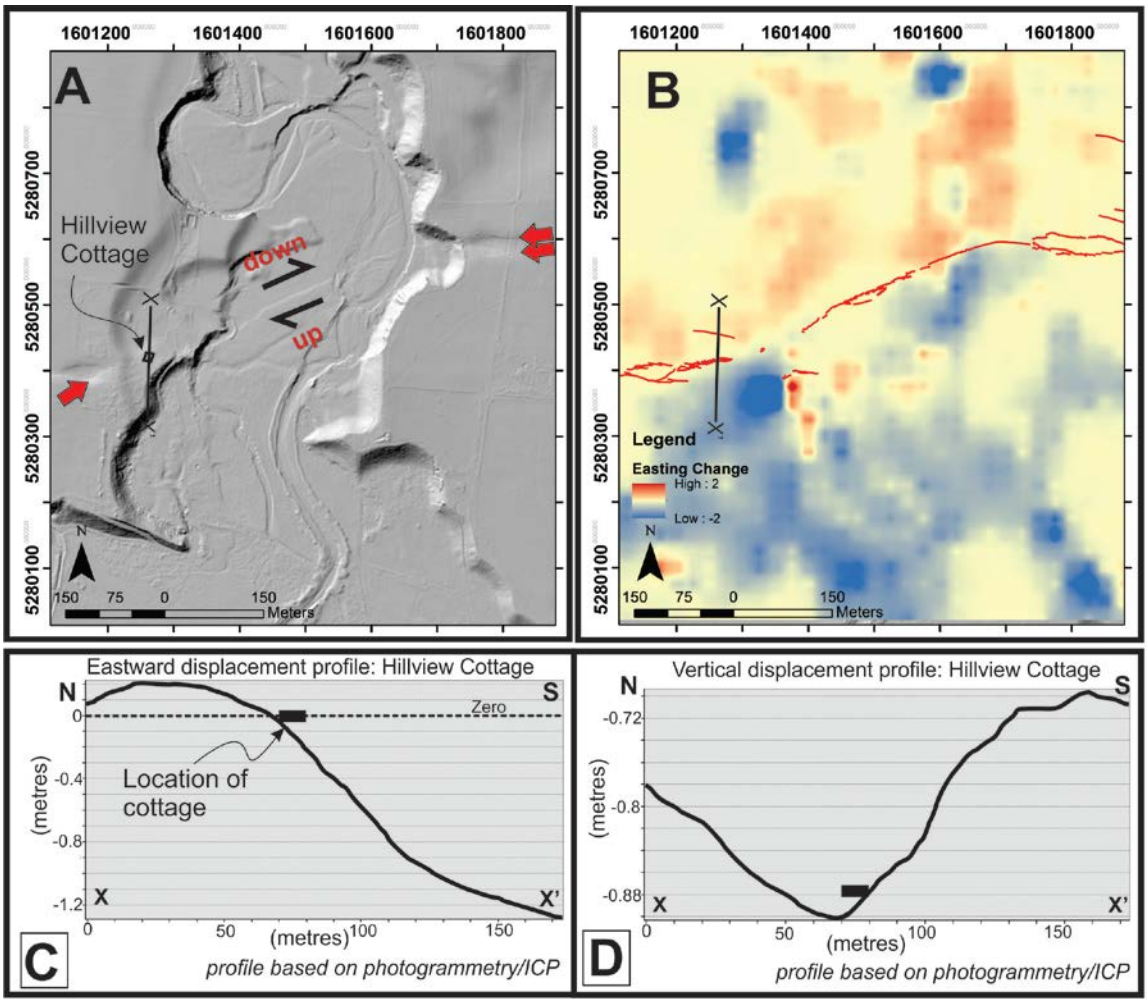

Figure A2.29 Hillview Cottage and The Humps Fault surface rupture. (A) LiDAR hill shade DEM showing location of the cottage within a relatively narrow fault rupture deformation zone (red arrows). (B) Raster of displacement in the east direction (positive is east, negative is west) calculated using ICP method described in text. Some anomalies and artefacts of the grid exist within the dataset, but the overall pattern is one of predominantly dextral displacement. West of the cottage is a small pull-apart, while the 100-m-scale fault geometry is that of a restraining bend. (C, D) The eastward and vertical deformation profiles from X to X', respectively. Y-axis exaggeration in (C) = 60. Y-axis exaggeration in (D) = 385.

A2.5 Discussion

Characterising the hazards associated with surface fault rupture and developing design strategies to mitigate those hazards have been the focus of several publications by JD Bray (e.g. Bray 2001, 2009; Bray and Kelson 2006). In these, he consistently highlights four principal means for mitigating the hazard posed by ground-surface fault rupture:

- land-use planning
- engineering geology
- geotechnical engineering, and
- structural engineering.

Depending on fault rupture characteristics and site conditions, he advocates several potentially effective design measures that include establishing non-arbitrary setback distances; constructing earth fills to partially absorb and distribute underlying rupture; isolating foundations from underlying ground movement (e.g. through the use of slip layers); and designing strong, ductile foundations that resist imposed earth pressures.

Observations of building response in recent New Zealand ground-surface fault rupture earthquake are supportive of Bray's recommendations. Those houses with lightly reinforced concrete slab foundations would have benefited from having foundations that were stronger and more ductile and/or able to isolate underlying fault rupture from the overlying house. Buildings less damaged by surface rupture deformation were those that had foundations that were strong enough to resist imposed strains or isolated ground deformation (wholly or partly) from the superstructure. From the perspective of post-event reinstatement, buildings that performed best also had the capacity to tilt and rotate as a rigid body, thereby limiting the amount of internal deformation/damage. For buildings that could be subjected to tilting due to surface rupture deformation, design measures that not only limit damage, but also facilitate re-levelling are advantageous.

In a large earthquake, surface fault rupture deformation places additional demands on structures, compared to similar structures exposed only to strong ground shaking. Based on the building damage examples presented in this Appendix, some pertinent observations can be made regarding the performance of New Zealand residential structures when subjected to surface fault rupture deformation of varying levels of strain and amounts of displacement.

1. Single-storey, regular-shaped, timber-framed residential structures with light roofs and of modest dimensions (floor area of ≤~200 m^2) subjected to low/moderate surface fault rupture deformation (i.e. shear strains ≤10^{-2} and discrete displacements of decimetre-scale or less) do not appear to pose a collapse hazard.
2. At those levels of deformation, the prospects of damage control and repairability (and therefore post-event functionality) appear to be improved for such residential structures if the cladding contributes to the robustness to the superstructure (e.g. plywood, timber weatherboard) and is not brittle.
3. This favourable behaviour is enhanced if building systems moderate the direct transmission of ground deformation into the superstructure (either by decoupling or by other means) and allow for re-levelling of the structure post-event. For additional discussion regarding the mitigation of surface fault rupture hazard via the decoupling of ground deformation from the superstructure, see, for example, Lazarte et al. (1994), Murbach et al. (1999), Bray (2001, 2009), Bray and Kelson (2006), Van Dissen et al. (2011) and Oettle and Bray (2013).
4. For residential structures with the above-mentioned attributes, non-collapse performance can be achieved at even higher levels of strain (~10^0) and larger discrete displacements (metre-scale) in a predominantly horizontal displacement setting (i.e. strike-slip) if the superstructure decouples from (is isolated from) the underlying ground deformation. Our New Zealand dataset does not contain examples of the performance of residential structures subjected to such large surface fault rupture strains and displacements in a predominantly vertical displacement setting. In a horizontal displacement setting, the decoupled superstructure still rests on (and is supported by) the ground. This may not be the case in a predominantly vertical displacement setting where there is the possibility that fault rupture will leave a significant portion of the decoupled superstructure un-supported and this may lead, if not to collapse, then at least to significant tilting and angular distortions. In addition, in a reverse/thrust vertical displacement setting, there is the potential for a 'bulldozer zone' to develop at the base of the scarp where fault displacement forces the scarp to thrust horizontally across the ground surface, and this too can severely impact structures (Kelson et al. 2001).

In New Zealand, the primary document providing guidance with regards to the mitigation of surface fault rupture hazard is the Ministry for the Environment (MfE) report titled 'Planning for development of land on or close to active faults: A guideline to assist resource management planners in New Zealand' (Kerr et al. 2003; see also Van Dissen et al. 2006). In this guidance document, with its life-safety focus, a distinction is made between single-storey timber-framed residential structures (Building Importance Category 2a structures – i.e. BIC 2a structures) and other normal structures (BIC 2b structures), with more permissive resource consent categories applied to the former. The non-collapse performance of single-storey timber- framed structures when subjected to surface fault rupture in the 2010 Darfield and 2016 Kaikōura earthquakes strongly supports this distinction. In addition, the MfE document makes a distinction between *well-defined* (i.e. concentrated) deformation and *distributed* deformation, with more restrictive resource consent categories applied to the former. Our observations that the severity of damage, in general, increases with both increasing total displacement and increasing strain supports this distinction.

The MfE guidance document also recommends that the siting and construction of a BIC 2a structure (i.e. single-storey timber-framed house) in a greenfield setting within a distributed deformation zone of an active fault with a recurrence interval ≤3500 years be considered a *Discretionary* activity. However, given the life-safety focus of the MfE guidance document, and the non-collapse performance of BIC 2a structures – especially when subjected to distributed lower-strain surface fault rupture deformation, consideration could be given to adopting a more permissive resource consent category such as *Controlled*. Nevertheless, we must stress that consideration of more permissive resource consent categories is only germane from a life-safety perspective. From a damage-control perspective, or a post-event-functionality perspective, application of more permissive resource consent categories will, in general, run counter to those objectives.

A2.6 Conclusions

About two dozen buildings, typically single-storey timber-framed houses, barns and woolsheds with regular shaped floor plans and lightweight roofing materials, have been directly impacted by surface fault rupture in recent New Zealand earthquakes. The amount and style of surface rupture deformation varied considerably, ranging from decimetre-scale distributed folding with estimated shear strains in the order of $\leq 10^{-2}$, to metre-scale discrete rupture with estimated shear strains up to 10^{0}. While the severity of damage generally increased with both increasing total displacement and increasing strain, none of these buildings collapsed. From a life-safety standpoint, all of these buildings performed well and provide insight into construction styles that could best be employed to facilitate non-collapse performance resulting from surface fault rupture and, in certain instances, post-event functionality.

A2.7 Appendix 2 References

Anderson H, Webb T. 1989. The rupture process of the 1987 Edgecumbe earthquake, New Zealand. *New Zealand Journal of Geology and Geophysics*. 32(1):43–52. doi:10.1080/00288306.1989.10421387.

Bastin SH, Ogden M, Wotherspoon LM, van Ballegooy S, Green RA, Stringer M. 2018. Geomorphological influences on the distribution of liquefaction in the Wairau Plains, New Zealand, following the 2016 Kaikōura earthquake. *Bulletin of the Seismological Society of America*. 108(3B):1683–1694. doi:10.1785/0120170248.

Beanland S, Berryman KR, Blick GH. 1989. Geological investigations of the 1987 Edgecumbe earthquake, New Zealand. *New Zealand Journal of Geology and Geophysics*. 32(1):73–91. doi:10.1080/00288306.1989.10421390.

Beavan J, Samsonov S, Motagh M, Wallace L, Ellis S, Palmer N. 2010. The Darfield (Canterbury) earthquake: geodetic observations and preliminary source model. *Bulletin of the New Zealand Society for Earthquake Engineering*. 43(4):228–235. doi:10.5459/bnzsee.43.4.228-235.

Bradley BA, Razafindrakoto HNT, Nazer MA. 2017. Strong ground motion observations of engineering interest from the 14 November 2016 M_W 7.8 Kaikōura, New Zealand earthquake. *Bulletin of the New Zealand Society for Earthquake Engineering*. 50(2):85–93. doi:10.5459/bnzsee.50.2.85-93.

Bray JD. 2001. Developing mitigation measures for the hazards associated with earthquake surface fault rupture. In: *Proceedings of the Workshop on Seismic Fault-Induced Failures, Tokyo, Japan, 11–12 January 2001*. Tokyo (JP): Japan Society for the Promotion of Science. p. 55–79.

Bray JD. 2009. Designing buildings to accommodate earthquake surface fault rupture. In: Goodno B, editor. *Improving the seismic performance of existing buildings and other structures*. 2009 Dec 9–11; San Francisco, California. Reston (VA): American Society of Civil Engineers. p. 1269–1280.

Bray JD, Kelson KI. 2006. Observations of surface fault rupture from the 1906 earthquake in the context of current practice. *Earthquake Spectra*. 22(2):69–89. doi:10.1193/1.2181487.

Clark KJ, Nissen E, Howarth JD, Hamling I, Mountjoy J, Ries W, Jones K, Goldstien S, Cochran U, Villamor P, et al. 2017. Highly variable coastal deformation in the 2016 MW7.8 Kaikōura earthquake reflects rupture complexity along a transpressional plate boundary. *Earth and Planetary Science Letters*. 474:334–344. doi:10.1016/j.epsl.2017.06.048.

Cubrinovski M, Bray JD, de la Torre C, Olsen MJ, Bradley BA, Chiaro G, Stocks E, Wotherspoon L. 2017. Liquefaction effects and associated damages observed at the Wellington CentrePort from the 2016 Kaikoura earthquake. *Bulletin of the New Zealand Society for Earthquake Engineering*. 50(2):152–173. doi:10.5459/bnzsee.50.2.152-173.

Dellow S, Massey C, Cox S, Archibald G, Begg J, Bruce Z, Carey J, Davidson J, Della Pasqua F, Glassey P, et al. 2017. Landslides caused by the Mw7.8 Kaikōura earthquake and the immediate response. *Bulletin of the New Zealand Society for Earthquake Engineering*. 50(2):106–116. doi:10.5459/bnzsee.50.2.106-116.

Downes GL, Dowrick DJ. 2014. Atlas of isoseismal maps of New Zealand earthquakes: 1843–2003. 2nd ed. (revised). Lower Hutt (NZ): GNS Science. 1 DVD. (GNS Science monograph; 25).

Duffy B, Quigley M, Barrell DJA, Van Dissen R, Stahl T, Leprince S, McInnes C, Bilderback E. 2013. Fault kinematics and surface deformation across a releasing bend during the 2010 MW 7.1 Darfield, New Zealand, earthquake revealed by differential LiDAR and cadastral surveying. *GSA Bulletin*. 125(3–4):420–431. doi:10.1130/b30753.1.

Forsyth PJ, Barrell DJA, Jongens R. 2008. Geology of the Christchurch area [map]. Lower Hutt (NZ): GNS Science. 1 folded map + 67 p., scale 1:250,000. (GNS Science 1:250,000 geological map; 16).

Gledhill KR, Ristau J, Reyners ME, Fry B, Holden C. 2010. The Darfield (Canterbury) earthquake of September 2010: preliminary seismological report. *Bulletin of the New Zealand Society for Earthquake Engineering*. 43(4):215–221. doi:10.5459/bnzsee.43.4.215-221.

Hamling IJ, Hreinsdóttir S, Clark K, Elliott J, Liang C, Fielding E, Litchfield N, Villamor P, Wallace L, Wright TJ, et al. 2017. Complex multifault rupture during the 2016 Mw 7.8 Kaikōura earthquake, New Zealand. *Science*. 356(6334):eaam7194. doi:10.1126/science.aam7194.

Holden C, Beavan RJ, Fry B, Reyners ME, Ristau J, Van Dissen RJ, Villamor P, Quigley M. 2011. Preliminary source model of the M_w 7.1 Darfield earthquake from geological, geodetic and seismic data. In: *Ninth Pacific Conference on Earthquake Engineering: building an earthquake resilient society, April 14–16, 2011, University of Auckland, Auckland, New Zealand*. Auckland (NZ): 9PCEE. Paper 164.

Holden C, Kaiser AE, Van Dissen RJ, Jury R. 2013. Sources, ground motion and structural response characteristics in Wellington of the 2013 Cook Strait earthquakes. *Bulletin of the New Zealand Society for Earthquake Engineering*. 46(4):188–195. doi:10.5459/bnzsee.46.4.188-195.

Hornblow S, Quigley M, Nicol A, Van Dissen RJ, Wang N. 2014. Paleoseismology of the 2010 M_w 7.1 Darfield (Canterbury) earthquake source, Greendale Fault, New Zealand. *Tectonophysics*. 637:178–190. doi:10.1016/j.tecto.2014.10.004.

Kaiser A, Balfour N, Fry B, Holden C, Litchfield N, Gerstenberger M, D'Anastasio E, Horspool N, McVerry G, Ristau J, et al. 2017. The 2016 Kaikōura, New Zealand, earthquake: preliminary seismological report. *Seismological Research Letters*. 88(3):727–739. doi:10.1785/0220170018.

Kearse J, Little TA, Van Dissen RJ, Barnes PM, Langridge R, Mountjoy J, Ries W, Villamor P, Clark KJ, Benson A, et al. 2018. Onshore to offshore ground-surface and seabed rupture of the Jordan–Kekerengu–Needles fault network during the 2016 Mw 7.8 Kaikōura earthquake, New Zealand. *Bulletin of the Seismological Society of America*. 108(3B):1573–1595. doi:10.1785/0120170304.

Kelson KI, Kang K-H, Page WD, Lee C-T, Cluff LS. 2001. Representative styles of deformation along the Chelungpu Fault from the 1999 Chi-Chi (Taiwan) Earthquake: geomorphic characteristics and responses of man-made structures. *Bulletin of the Seismological Society of America*. 91(5):930–952. doi:10.1785/0120000741.

Kerr J, Nathan S, Van Dissen R, Webb P, Brunsdon D, King A. 2003. Planning for development of land on or close to active faults: a guideline to assist resource management planners in New Zealand. Wellington (NZ): Ministry for the Environment. 67 p.

Langridge RM, Ries WF, Litchfield NJ, Villamor P, Van Dissen RJ, Barrell DJA, Rattenbury MS, Heron DW, Haubrock S, Townsend DB, et al. 2016. The New Zealand Active Faults Database. *New Zealand Journal of Geology and Geophysics*. 59(1):86–96. doi:10.1080/00288306.2015.1112818.

Langridge RM, Rowland J, Villamor P, Mountjoy J, Townsend DB, Nissen E, Madugo C, Ries WF, Gasston C, Canva A, et al. 2018. Coseismic rupture and preliminary slip estimates for the Papatea Fault and its role in the 2016 Mw 7.8 Kaikōura, New Zealand, earthquake. *Bulletin of the Seismological Society of America*. 108(3B):1596–1622. doi:10.1785/0120170336.

Lazarte CA, Bray JD, Johnson AM, Lemmer RE. 1994. Surface breakage of the 1992 Landers earthquake and its effects on structures. *Bulletin of the Seismological Society of America*. 84(3):547–561.

Litchfield NJ, Villamor P, Van Dissen RJ, Nicol A, Barnes PM, Barrell DJA, Pettinga JR, Langridge RM, Little TA, Mountjoy JJ, et al. 2018. Surface rupture of multiple crustal faults in the 2016 M_W 7.8 Kaikōura, New Zealand, earthquake. *Bulletin of the Seismological Society of America*. 108(3B):1496–1520. doi:10.1785/0120170300.

Massey C, Townsend D, Rathje E, Allstadt KE, Lukovic B, Kaneko Y, Bradley B, Wartman J, Jibson RW, Petley DN, et al. 2018. Landslides triggered by the 14 November 2016 Mw 7.8 Kaikōura earthquake, New Zealand. *Bulletin of the Seismological Society of America*. 108(3B):1630–1648. doi:10.1785/0120170305.

Murbach D, Rockwell TK, Bray JD. 1999. The relationship of foundation deformation to surface and near-surface faulting resulting from the 1992 Landers earthquake. *Earthquake Spectra*. 15(1):121–144. doi:10.1193/1.1586032.

Nairn IA, Beanland S. 1989. Geological setting of the 1987 Edgecumbe earthquake, New Zealand. *New Zealand Journal of Geology and Geophysics*. 32(1):1–13. doi:10.1080/00288306.1989.10421383.

Nicol A, Khajavi N, Pettinga JR, Fenton C, Stahl T, Bannister S, Pedley K, Hyland-Brook N, Bushell T, Hamling I, et al. 2018. Preliminary geometry, displacement, and kinematics of fault ruptures in the epicentral region of the 2016 Mw 7.8 Kaikōura, New Zealand, earthquake. *Bulletin of the Seismological Society of America*. 108(3B):1521–1539. doi:10.1785/0120170329.

Nissen E, Krishnan AK, Arrowsmith JR, Saripalli S. 2012. Three-dimensional surface displacements and rotations from differencing pre- and post-earthquake LiDAR point clouds. *Geophysical Research Letters*. 39(16):L16301. doi:10.1029/2012gl052460.

Oettle NK, Bray JD. 2013. Geotechnical mitigation strategies for earthquake surface fault rupture. *Journal of Geotechnical and Geoenvironmental Engineering*. 139(11):1864–1874. doi:10.1061/(ASCE)GT.1943-5606.0000933.

Pender MJ, Robertson TW. 1987. Edgecombe earthquake: reconnaissance report. *Bulletin of the New Zealand Society for Earthquake Engineering*. 20(3):201–249. doi:10.5459/bnzsee.20.3.201-249.

Power WL, Clark KJ, King DN, Borrero J, Howarth JD, Lane EM, Goring D, Goff J, Chagué-Goff C, Williams J, et al. 2017. Tsunami runup and tide-gauge observations from the 14 November 2016 M7.8 Kaikoura earthquake, New Zealand. *Pure and Applied Geophysics*. 174(7):2457–2473. doi:10.1007/s00024-017-1566-2.

Quigley M, Van Dissen RJ, Litchfield NJ, Villamor P, Duffy B, Barrell DJA, Furlong K, Stahl T, Bilderback E, Noble D. 2012. Surface rupture during the 2010 M_w 7.1 Darfield (Canterbury) earthquake: implications for fault rupture dynamics and seismic-hazard analysis. *Geology*. 40(1):55–58. doi:10.1130/g32528.1.

Quigley M, Van Dissen RJ, Villamor P, Litchfield NJ, Barrell DJA, Furlong K, Stahl T, Duffy B, Bilderback E, Noble D, et al. 2010. Surface rupture of the Greendale Fault during the Darfield (Canterbury) Earthquake, New Zealand: initial findings. *Bulletin of the New Zealand Society for Earthquake Engineering*. 43(4):236–242. doi:10.5459/bnzsee.43.4.236-242.

Stirling M, Litchfield N, Villamor P, Van Dissen RJ, Nicol A, Pettinga J, Barnes P, Langridge R, Little T, Barrell DJA, et al. 2017. The Mw7.8 Kaikōura earthquake: surface fault rupture and seismic hazard context. *Bulletin of the New Zealand Society for Earthquake Engineering*. 50(2):73–84. doi:10.5459/bnzsee.50.2.73-84.

Stringer ME, Bastin S, McGann CR, Cappellaro C, El Kortbawi M, McMahon R, Wotherspoon LM, Green RA, Aricheta J, Davis R, et al. 2017. Geotechnical aspects of the 2016 Kaikōura earthquake on the South Island of New Zealand. *Bulletin of the New Zealand Society for Earthquake Engineering*. 50(2):117–141. doi:10.5459/bnzsee.50.2.117-141.

Van Dissen RJ, Barrell DJA, Litchfield NJ, Villamor P, Quigley M, King AB, Furlong K, Begg JG, Townsend DB, Mackenzie H, et al. 2011. Surface rupture displacement on the Greendale Fault during the M_w 7.1 Darfield (Canterbury) Earthquake, New Zealand, and its impact on man-made structures. In: *Proceedings of the Ninth Pacific Conference on Earthquake Engineering: building an earthquake resilient society*. 2011 Apr 14–16; Auckland, New Zealand. Auckland (NZ): 9PCEE. Paper 186.

Van Dissen RJ, Heron DW, Becker JS, King AB, Kerr JE. 2006. Mitigating active fault surface rupture hazard in New Zealand: development of national guidelines, and assessment of their implementation. In. *100th anniversary earthquake conference, April 18–22, 2006, San Francisco, California: proceedings*. Oakland (CA): Earthquake Engineering Research Institute. Paper 633.

Van Dissen RJ, Stahl T, King A, Pettinga JR, Fenton C, Little TA, Litchfield NJ, Stirling MW, Langridge RM, Nicol A, et al. 2019. Impacts of surface fault rupture on residential structures during the 2016 Mw 7.8 Kaikōura earthquake, New Zealand. *Bulletin of the New Zealand Society for Earthquake Engineering*. 52(1):1–22. doi:10.5459/bnzsee.52.1.1-22.

APPENDIX 3 EXAMPLES OF RESOURCE CONSENT CATEGORY TABLES

Tables A3.1 and A3.2 present examples of relationships between Resource Consent Category, Building Importance Category, fault Recurrence Interval Class, and Fault Complexity for both previously developed and greenfield sites along the Wellington, Ohariu, Shepherds Gully, Moonshine and Terawhiti faults. These examples are modified from the MfE Active Fault Guidelines based on recommendations made for a similar fault mapping study for the Kāpiti Coast District Council (Van Dissen and Heron 2003).

Table A3.1 Example of relationships between Resource Consent Category, Building Importance Category, fault Recurrence Interval Class and Fault Complexity for developed and/or already subdivided sites, based on the MfE Active Fault Guidelines (Kerr et al. 2003).

Developed and/or Already Subdivided Sites					
WELLINGTON FAULT (based on fault Recurrence Interval Class I, ≤2000 years)					
Building Importance Category	**1**	**2a**	**2b**	**3**	**4**
Fault Complexity	**Resource Consent Category**				
Well-defined and well-defined extended	Permitted	*Non-Complying*	*Non-Complying*	*Non-Complying*	Non-Complying
Distributed and uncertain constrained	Permitted	*Discretionary*	*Non-Complying*	*Non-Complying*	Non-Complying
Uncertain poorly-constrained	Permitted	*Discretionary*	*Non-Complying*	*Non-Complying*	Non-Complying
OHARIU FAULT (based on fault Recurrence Interval Class II, >2000 years to ≤3500 years)					
Building Importance Category	**1**	**2a**	**2b**	**3**	**4**
Fault Complexity	**Resource Consent Category**				
Well-defined and well-defined extended	Permitted	Permitted*	*Non-Complying*	*Non-Complying*	Prohibited
Distributed and uncertain constrained	Permitted	Permitted	*Discretionary*	*Non-Complying*	Non-Complying
Uncertain poorly-constrained	Permitted	Permitted	*Discretionary*	*Non-Complying*	Non-Complying
SHEPHERDS GULLY FAULT (based on fault Recurrence Interval Class III, >3500 years to ≤5000 years)					
Building Importance Category	**1**	**2a**	**2b**	**3**	**4**
Fault Complexity	**Resource Consent Category**				
Well-defined and well-defined extended	Permitted	Permitted*	Permitted*	*Non-Complying*	Non-Complying
Distributed and uncertain constrained	Permitted	Permitted	Permitted	*Discretionary*	Non-Complying
Uncertain poorly-constrained	Permitted	Permitted	Permitted	*Discretionary*	Non-Complying

Developed and/or Already Subdivided Sites					
MOONSHINE FAULT and TERAWHITI FAULT (based on fault Recurrence Interval Class IV, >5000 years to ≤10,000 years)					
Building Importance Category	**1**	**2a**	**2b**	**3**	**4**
Fault Complexity	**Resource Consent Category**				
Well-defined and well-defined extended	Permitted	Permitted*	Permitted*	Permitted*	Non-Complying
Distributed and uncertain constrained	Permitted	Permitted	Permitted	Permitted	Non-Complying
Uncertain poorly-constrained	Permitted	Permitted	Permitted	Permitted	Non-Complying

Notes:

[#] No well-defined Fault Avoidance Zones have been identified for the Moonshine Fault.

* Indicates that the Resource Consent Category is permitted but could be controlled or discretionary given that the fault location is well-defined.

Italics: The use of italics indicates that the Resource Consent Category of these categories is more flexible. For example, where *discretionary* is indicated, *controlled* may be considered more suitable by Council, or vice versa.

Table A3.2 Example of relationships between Resource Consent Category, Building Importance Category, fault Recurrence Interval Class and Fault Complexity for Greenfield sites, based on the MfE Active Fault Guidelines (Kerr et al. 2003).

Greenfield Sites					
WELLINGTON FAULT (based on fault Recurrence Interval Class I, ≤2000 years)					
Building Importance Category	**1**	**2a**	**2b**	**3**	**4**
Fault Complexity	**Resource Consent Category**				
Well-defined and well-defined extended	Permitted	*Non-Complying*	*Non-Complying*	*Non-Complying*	Prohibited
Distributed and uncertain constrained	Permitted	*Discretionary*	*Non-Complying*	*Non-Complying*	Non-Complying
Uncertain poorly-constrained	Permitted	*Discretionary*	*Non-Complying*	*Non-Complying*	Non-Complying
OHARIU FAULT (based on fault Recurrence Interval Class II, >2000 years to ≤ 3500 years)					
Building Importance Category	**1**	**2a**	**2b**	**3**	**4**
Fault Complexity	**Resource Consent Category**				
Well-defined and well-defined extended	Permitted	*Non-Complying*	*Non-Complying*	*Non-Complying*	Prohibited
Distributed and uncertain constrained	Permitted	*Discretionary*	*Non-Complying*	*Non-Complying*	Non-Complying
Uncertain poorly-constrained	Permitted	*Controlled*	*Discretionary*	*Non-Complying*	Non-Complying

Greenfield Sites					
SHEPHERDS GULLY FAULT (based on fault Recurrence Interval Class III, >3500 years to ≤5000 years)					
Building Importance Category	**1**	**2a**	**2b**	**3**	**4**
Fault Complexity	**Resource Consent Category**				
Well-defined and well-defined extended	Permitted	Permitted*	*Non-Complying*	*Non-Complying*	Non-Complying
Distributed and uncertain constrained	Permitted	Permitted	*Discretionary*	*Discretionary*	Non-Complying
Uncertain poorly-constrained	Permitted	Permitted	*Discretionary*	*Discretionary*	Non-Complying
MOONSHINE FAULT and TERAWHITI FAULT (based on fault Recurrence Interval Class IV, >5000 years to ≤10,000 years)					
Building Importance Category	**1**	**2a**	**2b**	**3**	**4**
Fault Complexity	**Resource Consent Category**				
Well-defined and well-defined extended	Permitted	Permitted*	Permitted*	*Non-complying*	Non-Complying
Distributed and uncertain constrained	Permitted	Permitted	Permitted	*Discretionary*	Non-Complying
Uncertain poorly-constrained	Permitted	Permitted	Permitted	*Discretionary*	Non-Complying

Notes:

[#] No well-defined Fault Avoidance Zones have been identified for the Moonshine Fault.

* Indicates that the Resource Consent Category is permitted but could be controlled or discretionary given that the fault location is well-defined.

Italics: The use of italics indicates that the Resource Consent Category of these categories is more flexible. For example, where *discretionary* is indicated, *controlled* may be considered more suitable by Council, or vice versa.

www.gns.cri.nz

Principal Location

1 Fairway Drive, Avalon
Lower Hutt 5010
PO Box 30368
Lower Hutt 5040
New Zealand
T +64-4-570 1444
F +64-4-570 4600

Other Locations

Dunedin Research Centre
764 Cumberland Street
Private Bag 1930
Dunedin 9054
New Zealand
T +64-3-477 4050
F +64-3-477 5232

Wairakei Research Centre
114 Karetoto Road
Private Bag 2000
Taupo 3352
New Zealand
T +64-7-374 8211
F +64-7-374 8199

National Isotope Centre
30 Gracefield Road
PO Box 30368
Lower Hutt 5040
New Zealand
T +64-4-570 1444
F +64-4-570 4657